APPROVAL SHEET

Title of Dissertation: Self-Powered Glucose Biosensing System

Name of Candidate: Tanmay Abhay Kulkarni
Doctor of Philosophy, 2017

Dissertation and Abstract approved: _____

Professor Gymama Slaughter
Associate Professor
Department of Computer Science
and Electrical Engineering

Date Approved: _____

ABSTRACT

Title of dissertation: Self-powered glucose biosensing system

Name of Candidate: Tanmay Abhay Kulkarni

Dissertation directed by: Professor Gymama Slaughter
Associate professor
Computer Science and Electrical Engineering

In this dissertation, we designed and developed a novel self-powered glucose biosensor (SPGS) system that can simultaneously sense blood glucose and generate bioelectricity to power implantable bioelectronics. We characterize the power generation and biosensing capabilities in the presence of glucose analyte. The system comprises a biofuel cell employing bioelectrodes composed of a compressed network of three-dimensional multi-walled carbon nanotubes (MWCNTs) with immobilized redox enzymes, pyroquinoline quinone glucose dehydrogenase (PQQ-GDH) and bilirubin oxidase (BOD_X) functioning as the anodic and cathodic catalyst, respectively. The overall dimension of the biofuel cell prototype was 5 mm x 5 mm yielding an active surface area of 0.04 cm^2. When operated in 20 mM glucose, the biofuel cell exhibited an open circuit voltage and power density of 552.37 mV and 0.225 mW/cm^2 at 285.46 mV, respectively, with a current density of 1.285 mA/cm^2. Moreover, at physiological glucose concentration (5 mM), the biofuel cell exhibits an open circuit voltage and power density of 391.36 mV and 84.64 $\mu W/cm^2$ at 214.3 mV, respectively, with a current density of 602.5 $\mu A/cm^2$. This micropower harvested by a single glucose biofuel cell is only practical for powering micropower devices and the power produced is linearly correlated with glucose over a dynamic range of 3 - 20 mM glucose. These findings showed that glucose biofuel cells can be further investigated in the development of a self-powered glucose biosensor. To achieve this task, we incorporated a charge pump circuit and a capacitor as the transducer element. By monitoring the capacitor charging

frequencies, which are influenced by the concentration of the glucose analyte in the biofuel cell, a linear dynamic range of 3 - 20 mM glucose is observed. The operational stability of SPGS was monitored over a period of 53 days and was found to be stable with 4.17% (least) and 9.09% (peak) drop in sensor performance under continuous discharge in 20 mM and 3 mM glucose, respectively. Thereby not requiring recalibration during the 53-day period and retaining over 90% of the initial activity compared to the Continuous Glucose Monitors (CGM) that requires calibration every 12 hours. The system was further characterized by testing the performance of the system at various temperature, pH and amidst various interfering and competing chemical species such as uric acid, ascorbic acid, fructose, maltose and galactose. To amplify the system's performance further, a step-up DC converter circuit was interfaced with the charge pump circuit. The output from the charge pump circuit provided a necessary 1.4 V trigger to drive the step-up DC converter circuit. The system exhibited a 3.7-fold increase in sensitivity while powering a digital glucometer device. These results demonstrate that SPGSs can simultaneously generate bioelectricity to power ultra-low powered bioelectronic devices and sense glucose. To the best of our knowledge, practical power was generated to power a glucometer and the sensing characteristics are an improvement over the existing state of art. Such a practical glucose sensing system powered by a single enzymatic glucose biofuel cell overcomes the drawbacks of present glucose monitors by eliminating the battery, device bulkiness and the frequent need for recalibration.

SELF-POWERED GLUCOSE BIOSENSING SYSTEM

By

Tanmay Abhay Kulkarni

Dissertation submitted to the Faculty of the Graduate School

of the University of Maryland in partial fulfillment

of the requirements for the degree of

Doctor of Philosophy

2017

Acknowledgement

I would like to express my deepest appreciation to my advisor Dr. Gymama Slaughter, who has mentored and guided me throughout the course of my doctorate studies. She showed faith in me and my research abilities for, which I am sincerely thankful. She was quick to understand my shortcomings and strove towards helping me overcome them. She always set challenging deadlines for me, which caused me to push myself and in the process have tremendously helped me. She has been a true mentor for me and has guided me to choose my path after doctoral studies. Dr. Gymama Slaughter has played a vital role in my success and I couldn't have asked for a better mentor.

I would also like to thank my parents Mr. Abhay Kulkarni and Mrs. Swapna Kulkarni along with my sister Mrs. Anushri Kulkarni-Desai and my girlfriend Ms. Prarthana Ravishankar for their constant support, love and affection. They were the four pillars to my success. It is difficult being away from my family and yet focus on the studies. Their sacrifice has served to be a strong motivation for me in completing my doctoral studies. Their moral support, listening to me when I discuss my research, supporting me through thick and thin is unmatched. I also thank them for their patience and understanding when I couldn't talk to them or meet with them for a long time. Lastly, to see tears of joy in their eyes after I successfully defended my dissertation gave me a sense of satisfaction and a proud feeling. I would like to dedicate this thesis to my late grandparents, who I know will be proud of me. I am truly blessed to have such a wonderful and loving family.

I would also like to thank my committee members Dr. Morris, Dr. Choa, Dr. Johnson and Dr. Kochunov for their support and valuable feedback. Their questions have helped me gain a broader insight on the intricate details pertaining to my project. I would like to thank my peers their support and our blown-out Q & A session during practice presentations.

I would like to thank and acknowledge the National Science Foundation (NSF) for providing funds to make this project possible.

Lastly, I am grateful towards my family and friends for their support and love.

TABLE OF CONTENTS

LIST OF FIGURES

LIST OF TABLES

Chapter 1: Introduction

Diabetes is one of the most fatal diseases suffered by humans worldwide. According to a 2014 report from the Center for Disease Control (CDC), 29.1 million people or 9.3% of the population suffers from diabetes, in the United States (US) alone and the cost incurred to keep diabetes under control was 245 billion US dollars [1]. It is not diabetes alone, but the complications that arise due to diabetes that makes it the seventh leading cause of death in the US. Some of the complications include; gastroparesis, foot complications, diabetic ketoacidosis, kidney disease, etc [2]. Diabetes is a metabolic disorder caused by abnormal blood glucose levels and is a result of either insufficient hormone insulin produced by the pancreas, or the body cells not responding to the insulin produced. Diabetes is quickly becoming an epidemic mostly due to the unhealthy lifestyles and undue stress faced by many people in their day to day lives. Table I represents normal levels of blood glucose for non-diabetic and diabetic individuals.

Table I. Normal blood glucose levels for non-diabetic and diabetic people

Non-diabetic people		**Diabetic people**	
Test	**Blood glucose (mg/dL)**	**Test**	**Blood glucose(mg/dL)**
Normal	79.2-110	**Pre-meal**	90-130
Fasting	70-100	**Post-meal**	< 180

According to the American Diabetes Association (ADA), diabetes is classified into four major types:

1. Type I: In this type, the body fails to produce enough insulin needed to supply glucose to fuel the cells in the body. This type of diabetes is less common and mostly diagnosed in

young adults and children and accounts for 5% of total diabetes cases [1]. Although there is no definite remedy to cure this type of diabetes, type I diabetes can be kept in check by employing insulin therapy.

2. Type II: In this type, the body is insulin resistant. It is the most common form of diabetes accounting for 90 – 95% of the total diabetes cases [1]. In order to overcome the insulin resistance, the pancreas produces excess insulin. Over a period of time, the pancreas is no longer able to keep up with the excessive insulin production which results in a condition characterized as hyperglycemia.
3. Gestational diabetes: This type of diabetes occurs in pregnant women who have elevated blood sugar levels and occurs during the second or third trimester of their pregnancy. The prevalence of gestational diabetes was as high as 9.2% of the pregnant women according to the CDC report (2014). Women with gestational diabetes have a higher risk of developing type II diabetes in the future [1].
4. Other diabetes: Other forms of diabetes mellitus include congenital diabetes, which is due to genetic defects of insulin secretion; cystic fibrosis-related diabetes, steroid diabetes, which is induced by high doses of glucocorticoids; and several forms of monogenic diabetes. These other types of diabetes account for 1 – 5% of the total diabetes cases [1].

Upon being diagnosed with diabetes, the individual is required to monitor and keep his/ her blood glucose level under control by maintaining a nutritious diet and living a stress free and healthy lifestyle.

Currently, invasive technology is available for individuals with diabetes to monitor and maintain normal blood glucose levels. The most common monitor is the finger prick test, which involves pricking the finger using a lancet and extracting the blood drop with a disposable glucose test strip,

which is then placed in a glucometer (Figure 1A) to measure the blood glucose level. The glucometer uses an amperometric principle of operation for measuring blood glucose level. The disposable test strip consists of a glucose selective enzyme and a capillary system. The capillary system is used to draw in the solution at one end of the strip. The glucose selective enzyme oxidizes the glucose in the blood to produce gluconic acid and release electrons. These electrons are proportional to the glucose concentration. The current is measured using a transimpedance amplifier, which shows variable voltage to varying glucose concentration. External factors like temperature, humidity and altitude affects the rate of enzyme reaction; and hence, the glucose measurement. In addition, the device is very bulky and, at times, depending on different batches of the test strips, the glucometer requires recalibration. The blood glucose reading can drift by as large as 4 mmol/dL or 72 mg/dL, which can prove to be fatal. Therefore, close monitoring of the blood glucose levels may involve pricking the finger multiple times a day, which may prove painful and tedious.

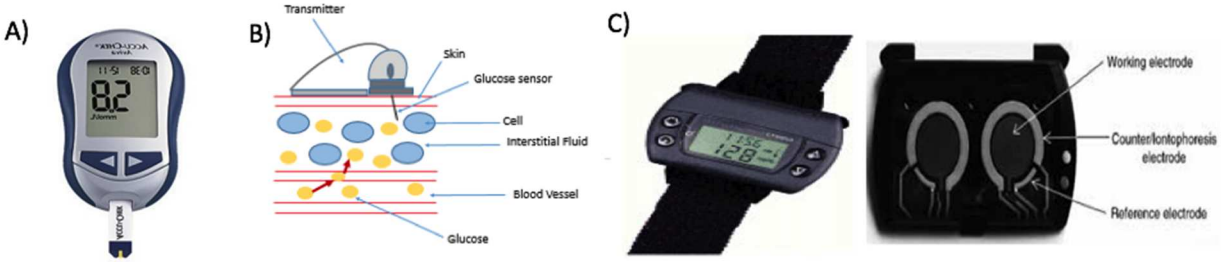

Figure 1. Current technologies to monitor the blood glucose levels. A) A glucometer (image courtesy:imedicalapps.com). B) CGM device C) A GlucoWatch G2 Biographer designed by Cygnus Inc (image courtesy: fda.gov).

In order to minimize the high frequency of finger prick test, researchers have developed a continuous glucose monitoring (CGM) device (Figure 1B), which is another invasive technique to monitor blood glucose level. This device consists of a disposable strip that acts as a sensor implanted under the skin with a non-implantable potentiostat circuit and transmitter outside of the

body. The biosensor is 10 mm in length and is implanted in the subcutaneous tissue. This biosensor consists of a glucose selective enzyme which reacts electrochemically with the interstitial fluid to oxidize glucose and release electrons. The generated current, which is proportional to the glucose concentration, is transmitted via a transmitter attached to the skin externally. The transmitter sends a signal every five minutes to the receiver, which displays the blood glucose levels at the user end device. This device is powered by an external power source such as a battery, thereby rendering the device bulky. The CGM device often requires recalibration every 12 hours after the first day, and recalibrating 3 – 4 times a day improves the device accuracy. The sensor can last up to 7 days, after which it must be replaced. Although CGMs minimize the need for finger pricking, it does not eliminate its need entirely.

Several attempts have been made to design a noninvasive glucose monitoring device [3 - 5]. Of all the attempts, the only device that was approved by the U.S. Food and Drug Administration (FDA) was the "GlucoWatch G2 Biographer," which was designed by Cygnus Inc. (Figure 1C). GlucoWatch G2 Biographer assembly comprises a biosensor, iontopherosis electrodes, hydrogel discs and an adhesive to hold the watch secured to the skin. It uses a single AAA battery to power the watch. It works on the principle of iontophoretic current and the glucose sample is obtained through a reverse iontophoresis process in which a very small current is passed through the skin. The extracted glucose is stored in the hydrogel discs which consists of a glucose oxidase enzyme that converts the glucose to gluconic acid and hydrogen peroxide. The hydrogen peroxide reacts with the platinum biosensor to generate a current that is proportional to the glucose in the system and is read by the Biographer. The corresponding glucose reading is displayed on an LCD screen after being processed. However, a Biographer requires at least a 2 hour warm up period after which it is calibrated using traditional glucose measuring technique. This device can display glucose

reading up to 6 times per hour over a 13-hour period. However, due to the inconsistencies in the measurement of glucose levels caused by perspiration, this device was short lived in the market. Both Medtronic's Minimed Paradigm RTS and the Dexcom system CGM devices have a bulky receiver, often making them cumbersome to carry. Also, one must calibrate the receiver for accurate blood glucose measurements which takes nearly 2 hours and demonstrates a maximum lifetime of just one week. Although these devices show promising results, the quest to maintain normal blood glucose levels and improve the quality of lives for individuals with diabetes remains a challenge. It is imperative that there is a closed loop system that would be minimally invasive, flexible and easy to use. Our proposed SPGS system uses employs a transducer element and electrochemical conversion of glucose to generate electrical power and sense glucose. The electrochemical conversion of glucose to gluconolactone and electrons is achieved via the use of a glucose selective enzyme. The SPGS system eliminates the need for a potentiostat circuit, and integrates a capacitor as a transducer element, in which varying glucose concentration is converted into a corresponding charge and discharge frequency. This SPGS system would eliminate the need to conduct a finger prick test, or use batteries, and will continuously measure the blood glucose level. The long-term goal will be to potentially implant the SPGS system in the body to acquire real-time glucose data without the need for an external power source, unlike a CGM device or the GlucoWatch, which requires a battery in order to operate. Here we develop a self-powered biosensing microsystem consisting of two major components viz. a sensing unit and a powering unit to sense glucose and supply power to a small portable electronic device. Currently, a glucose sensing circuit powered by a single enzymatic glucose biofuel cell cease to exist as the power produced by a single biofuel cell is insufficient to drive the sensing circuit. However, stacking multiple biofuel cells in series to amplify the electrical power has been demonstrated by various

research groups at the expense of making the overall system bulky. Here the proposed system uses a mediatorless, biocompatible single enzymatic glucose biofuel cell as a power source to drive the sensing circuit. The use of enzymes overcome the drawback of non-enzymatic glucose sensors reported earlier by eliminating the need for metal catalysts to oxidize the glucose fuel. The novel design of our biofuel cell system enables us to achieve higher electrical power density than those previously reported. Moreover, the use of amplification circuits reduces the overall dimension of the system to enable simultaneous glucose sensing and powering of a microelectronic device, thereby making the system truly novel.

Chapter 2: Glucose biosensor

A glucose biosensor is a device that senses the concentration of glucose in a complex mixture. A blood glucose sensor measures the concentration of glucose in the blood by breaking down the glucose molecules to produce electrons with the help of glucose selective enzymes. These electrons reduce Flavin adenine dinucleotide (FAD), a redox cofactor in an enzyme to $FADH_2$. On complete oxidation of glucose, the current generated correlates to the glucose concentration. Thus, the biorecognition enzyme element is immobilized on a transducer, which in turn transduces the chemical signal into an electrical signal that can be read by a read-out circuit. Since the enzymes act as catalysts, they are not consumed in the oxidation reaction of glucose, making them reusable. Also, the enzymes provide an alternate route for the glucose oxidation reaction with a lower activation energy, thereby allowing the reaction to be thermodynamically favorable. The biosensor mainly consists of the active region that is modified with the enzyme for the detection of the chemical constituent of interest. A transducer converts the chemical signal into an electrical signal that is processed using a signal processing unit into a readable form [6 - 8]. The active region can incorporate biorecognition elements, such as receptors, enzymes, antibodies, nucleic acids, microorganisms and lectins [9 - 10]. The chemical constituent of interest in this study is the glucose analyte, and it is detected commonly via amperometric detection principle. When the immobilized glucose selective enzyme comes in contact with the glucose analyte, it oxidizes glucose to generate electrons. These electrons contribute to the generation of current, which is proportional to the concentration of glucose analyte.

The commonly represented transducer classes include electrochemical, optical, thermometric, piezoelectric, and magnetic. Electrochemical transducers are preferred over other types of transducers mainly due to their higher sensitivity, ease of maintenance and cost-effectiveness.

Electrochemical sensors may be subdivided into potentiometric, amperometric, or conductometric types [11 - 13]. Enzymatic amperometric glucose biosensors are the most commonly available commercially because they are cheap, clean and easily renewable, and have been widely studied over the last few decades, and are preferred over abiotic glucose biosensors. Amperometric biosensors monitor current generated when there is a direct or mediated electron transfer between the active region of the enzyme and the substrate [14, 15].

Commonly used glucose selective enzymes at anode are hexokinase, glucose oxidase (GOx) or glucose-1-dehydrogenase (GDH) [16, 17]. The hexokinase assay is the reference method for glucose measurement using a spectrophotometry technique in many clinical laboratories [18]. Glucose biosensors used for detecting the blood glucose levels are usually based on the two enzyme families, GOx and GDH. These enzymes differ in formation of byproducts, redox potentials, cofactors and glucose selectivity [19]. GOx is the most commonly used enzyme for biosensors; it has a relatively higher selectivity for glucose. GOx is easy renewable, cheap, and has a higher tolerance for pH and temperature than many other enzymes, allowing easy manufacturing and storage of the glucose sensors [19, 20].

In 1975, Clark's technology was used to design the first commercially successful glucose biosensor by the Yellow Springs Instrument Company analyzer (Model 23A YSI analyzer) for the direct measurement of glucose based on the amperometric detection of hydrogen peroxide. This analyzer was short-lived because of its high cost due to the expensive platinum electrode. The first-generation glucose biosensors used natural oxygen substrate and detected the hydrogen peroxide. Measurements of peroxide was preferred in the case of the miniaturized devices [21]. However, they required a high operation potential for high selectivity, soon making them unfit for monitoring glucose. Several unwanted components in complex mixture interfered with the detection of

glucose. As a result, extensive research has been performed in the late 1980s to limit the interference of such components like ascorbic acid, uric acid, and certain drugs in complex mixtures. The shortcomings were overcome due to the development of mediated glucose biosensors, which are also known as second-generation glucose sensors. Non-physiological electron acceptors, called redox mediators, assisted in the electron transfer from the enzyme to the surface of the working electrode [22]. A variety of electron mediators, such as ferrocene, ferricyanide, quinines, tetrathialfulvalene (TTF), tetracyanoquinodimethane (TCNQ), thionine, methylene blue, and methyl viologen were used to improve the sensitivity and performance of the sensor [23 -26]. Some of the important features of a good mediator are that their passive reaction with oxygen, stability in both the oxidized and reduced forms, independent of pH, showing reversible electron transfer kinetics, and reacting rapidly with the enzyme [26]. Ferrocenes were extensively studied as electron mediators between both GOx and Glucose-1-Dehydrogenase dependent Pyrroloquinoline Quinone (GDH-PQQ) and the electrodes and showed promising results [23, 27 - 29].

2.1 Different generations of glucose sensors

During the 1980s, various methods were developed to improve sensor performance. This included the introduction of commercial screen-printed strips for glucose monitoring and the use of modified electrodes and tailored membranes [23, 30 - 33]. The first electrochemical blood glucose monitor for self-monitoring of diabetic patients was introduced in 1987 by Medisense Inc., which used GDH-PQQ and a ferrocene derivative [31]. Over a period of time, different generations of glucose biosensors have been introduced, each with a purpose to improve the standard of living of individuals with diabetes. The first generation of the glucose biosensor relies heavily on

coenzymes and oxygen, resulting in the generation and detection of hydrogen peroxide. The biocatalytic reaction involves the reduction of the flavin group (FAD) in the enzyme by reacting with glucose to produce the reduced form of the enzyme ($FADH_2$) followed by re-oxidation of the flavin by molecular oxygen to regenerate the oxidized form of the enzyme GOx (FAD) [24].

$$GOx(FAD) + Glucose \rightarrow GOx(FADH_2) + Gluconolactone \quad \text{..... (1)}$$

$$GOx(FADH_2) + O_2 \rightarrow GOx(FAD) + H_2O_2 \quad \text{..... (2)}$$

Peroxide formation measurements are commonly performed with Platinum electrode at a moderate anodic potential of +0.6 V (vs Ag/AgCl). The amperometric measurements of hydrogen peroxide is performed at higher potential at which some other species including ascorbic acid, uric acid, etc are also reduced. Similarly, oxygen-based devices rely heavily on oxygen for electron acceptor and often succumbs to errors due to fluctuations in oxygen tensions and the stoichiometric limitations of oxygen. This limitation was overcome by designing an oxygen-rich carbon paste enzyme electrode. Also, glucose dehydrogenase is independent of oxygen cofactor and could be an effective substitution for glucose oxidase.

The second generation of glucose sensors were designed using a mediator that facilitates the flow of electrons between the active site of the enzyme and the substrate. Since there exists a thick protein layer surrounding the active FAD site on the enzyme, the direct transfer of electrons is nearly impossible. The use of artificial mediators helped to achieve direct electron transfer (DET) as follows:

$$Glucose + GO_{x_{(ox)}} \rightarrow gluconic\ acid + GOx_{(red)} \quad \text{..... (3)}$$

$$GO_{x_{(red)}} + 2M_{(ox)} \rightarrow GOx_{(ox)} + 2M_{(red)} + 2H^{+} \quad \text{..... (4)}$$

$$2M_{(red)} \rightarrow 2M_{(ox)} + 2e^{-} \quad \text{..... (5)}$$

$M_{(ox)}$ and $M_{(red)}$ are oxidized and reduced forms of mediator, respectively. Re-oxidation of reduced form at the electrode gives a current signal which is proportional to glucose concentration. Various glucose biosensors are based on the use of ferrocene or ferricyanide mediators. To facilitate better direct electron transfer, various methods have been employed, which include enzyme wiring of GOx by electron-conducting redox hydrogels, the chemical modification of GOx with electron-relay groups and the application of nanomaterial as electrical connectors [34 - 37]. With the advent of nanotechnology, various nanomaterials like palladium nanoparticles and carbon nanotubes are used as the connector between the active sites of the enzyme and the substrate.

The third-generation of glucose biosensors are reagentless and based on direct transfer between the enzyme and the electrode without mediators, thus disregarding potential problems of high toxicity. Although glucose oxidase is used commonly to oxidize glucose, there are very few instances of DET using GOx enzyme. The electrode design must ensure that the distance between the active site and the electrode must be as small as possible. One technique for creating third-generation amperometric glucose biosensors is to use conducting organic salt electrodes based on charge-transfer complexes such as tetrathiafulvalene-tetracyanoquinodimethane (TTF-TCNQ) [38, 39]. The third-generation glucose biosensors paved way to the development of implantable, needle-type devices for continuous in vivo monitoring of blood glucose. Although significant progress has been done, more optimization is required for efficient transfer of electrons between active region and substrate.

2.2 Continuous glucose monitoring (CGM) devices

Before the development of *in vivo* glucose monitoring devices, continuous ex vivo monitoring of blood glucose was employed [40]. CGM devices offer an improved control of diabetes by providing real-time data of an internal insulin release system. Currently, a continuous subcutaneous glucose monitor is commonly used. However, CGM devices that measure the blood glucose directly are more prone to surface contamination of the electrode by proteins and coagulation factors and enhance the risk of thromboembolism. This cleared the path for subcutaneously implantable needle-type electrodes measuring glucose concentrations in interstitial fluid [41 - 46]. Shichiri et al. was the first to demonstrate the needle-type enzyme electrode for subcutaneous implantation in 1982 [25]. The first commercial needle-type glucose biosensor was marketed by Minimed (Sylmar, CA, USA). However, it failed to provide real-time data [46]. Following that, several FDA approved CGM devices by manufacturers such as Medtronic and Dexcom are most commonly used. These devices displayed real-time glucose concentrations every one to five minutes. The disposable sensor can be used for three to seven days [47]. Continuous subcutaneous glucose monitoring can also be achieved without direct contact between the interstitial fluid and transducer by using microdialysis principle [48, 49], which was employed by GlucoDay (Menarini, Florence, Italy) and SCGM (Roche, Mannheim, Germany). This approach was advantageous over the invasive needle type sensor in terms of both precision and accuracy, and lower drift signal [50]. Along with accuracy and precision, some of the other essential features possessed by these devices should include biocompatibility, calibration, long-term stability, specificity, linearity, and miniaturization. The accuracy of these innovative devices was lower than that of traditional glucose biosensors. However, these devices use a potentiostat circuit which

consist of three electrode assembly viz. a working electrode, a reference electrode and a counter electrode. The current at the counter electrode is adjusted such that the voltage at the working electrode remains stable with respect to the reference electrode. The potentiostat measures the potential difference between the working and the reference electrode and based on the potential, it applies the current through the counter electrode and measures the current as an iR voltage drop over a series resistor as illustrated in Figure 2.

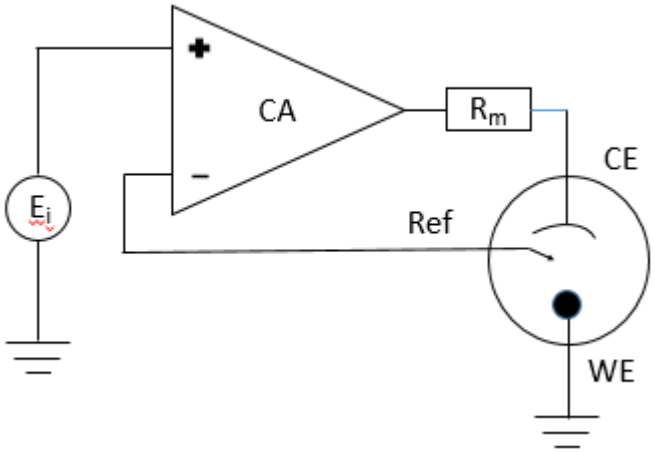

Figure 2. A schematic of potentiostat circuit

Non-invasive glucose monitoring systems have been developed by incorporating optical or transdermal approaches [51, 52]. The principle of optical glucose sensors involves using the physical properties of light in the interstitial fluid or the anterior chamber of the eye. These approaches include polarimetry [53], Raman spectroscopy [54], infrared absorption spectroscopy [55], photo acoustics [56], and optical coherence tomography [57]. The GlucoWatch Biographer, manufactured by Cygnus, Inc. (Redwood City, CA, USA), was the first transdermal glucose sensor approved by the US FDA. This watch-like device was based on transdermal extraction of interstitial fluid by reverse iontophoresis but had a long warm up time, resulting in false alarms,

skin irritation, sweating and consistent inaccuracy. As a result, the Biographer was withdrawn in 2008 from the consumer market. Despite tremendous efforts, a reliable non-invasive glucose measuring method is still not available.

Point of care (POC) glucose testing consists of a test strip inserted into the meter followed by a small drop of capillary blood obtained from the fingertip with a lancing device applied to the test strip. The measurement results are displayed as plasma glucose equivalents using a conversion factor [58]. Introduction of ExacTech in 1987 opened the doors to the portable glucose biosensor device. Eventually the market was flooded with different glucose sensor devices. According to the 2010 issue of the Diabetes Forecast Resource Guide, there are 56 different POC glucose sensors from 18 different companies. However, over 90% of the market is occupied by products manufactured by four major companies, including Abbott, Bayer, LifeScan, and Roche. Most of the meters are plasma-blood calibrated. The measurement requires a 0.3- to 1.5-μL drop of blood and yielded results within 10 seconds. Currently, many POC devices can be directly connected to laboratory information systems via proprietary data management systems. An effective glucose biosensor should be easy to handle, require minimal amounts of blood, and should perform rapid measurements. Suboptimal measurement quality can lead to significant inaccuracies and increased patient morbidity and mortality.

Glucose biosensing is a very vast field with rapid improvement in the development of glucose sensing devices from time to time. Some of the important features possessed by the glucose biosensors include precision, sensitivity and stability along with minimal invasive nature of the sensor. Glucose sensing not only helps diabetes patients monitor their blood glucose levels but can also be used in the food industry to monitor the glucose content of various food materials. With the proliferation of the diabetes disease and more impetus being given to its treatment, novel

glucose biosensor technologies including POC devices, CGMS, and noninvasive glucose monitoring systems, have been developed. However, the currently available devices in the market used to monitor the blood glucose level has a couple of drawbacks. A glucometer needs a finger prick test every time blood glucose needs to be monitored which is painful and tedious. The CGM devices measures the interstitial blood glucose. Moreover, recalibration is an issue and it relies on conventional blood glucose monitoring method for calibration. Thus, it does not eliminate the need for finger prick test. The Biographer GlucoWatch also measures the interstitial blood glucose level, however it does not provide an accurate glucose measurement. All the above devices run on batteries which makes these glucose monitors bulky in size. Glucose biosensors are constantly evolving as per the demand and there is a need for a self-powered glucose biosensing microsystem which will eliminate the dependence on glucometers and CGM devices, thereby improving the standard of living of people suffering from diabetes. With the additional benefit of eliminating the need for batteries as the power source by relying on natural and clean glucose as fuel.

Chapter 3: Electrochemical power sources

Batteries have been used as a source of power for couple of decades and are finding applications in almost every part of our lives. Batteries come with a limited amount of stored chemical energy and need to be recharged or replaced once all the chemical energy is utilized. The electrochemical conversion of this stored chemical energy into power forms the working principle of a battery. Batteries mainly consists of an anode and a cathode and an electrolyte separating both electrodes. The electrolyte can be in either a solid or a liquid state as shown in Figure 3.

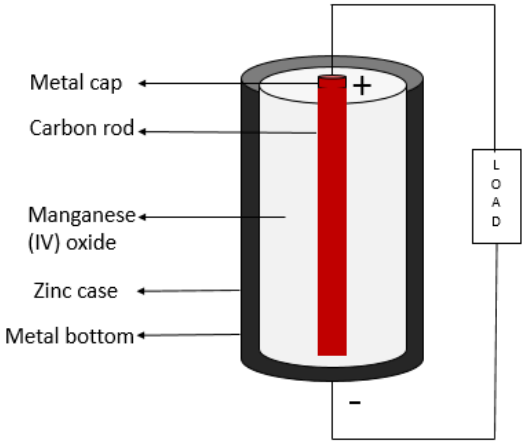

Figure 3. An illustration of battery

The outer zinc casing in this illustration serves as the anode and is oxidized, thereby consumed according to the following reaction:

$$Zn\,(s) \rightarrow Zn^{2+}(aq) + 2e^{-} \quad \ldots\ldots (6)$$

On the other hand, the cathode comprising of a paste of manganese dioxide and ammonium chloride is reduced according to the following reaction:

$$2MnO_2(s) + 2e^- + NH_4Cl\ (aq) \rightarrow Mn_2O_3\ (s) + 2NH_3(aq) + H_2O\ (l) + 2Cl^- \ldots\ldots\ldots\ldots (7)$$

Thus, the overall cell reaction is as follows:

$$\mathrm{Zn}(s) + 2MnO_2(s) + 2NH_4Cl\ (aq) \rightarrow Mn_2O_3(s) + \mathrm{Zn}(NH_3)_2\mathrm{Cl}_2\ (aq) + \mathrm{H_2O}(l) \ldots\ldots (8)$$

The positive ions flow towards the positive terminal through the electrolyte, and the electrons flow towards the terminal through the external circuit. The active masses are continuously consumed as the power is generated. Since the active mass supply is limited, the battery will eventually run out once the active mass is completely depleted. In order to overcome this limited supply of chemical energy, lithium ion (Li-ion) batteries were invented. These batteries are rechargeable and commonly consist of metal oxide as the positive electrode, a negative electrode carbon rod and lithium salt in organic solvent as the electrolyte. The redox reactions are reversible depending on the current flow direction, thereby making these batteries rechargeable. The following reversible redox reactions occur in a Li-ion battery:

$$At\ anode: xLiC_6 \leftrightarrow xLi^+ + xe^- + xC_6 \ldots\ldots\ldots\ldots (9)$$

$$At\ cathode: Li_{1-x}CoO_2 + xLi^+ + xe^- \leftrightarrow LiCoO_2 \ldots\ldots\ldots\ldots (10)$$

$$The\ overall\ cell\ reaction: \mathrm{LiC_6} + \mathrm{CoO} \leftrightarrow \mathrm{C_6} + \mathrm{LiCoO_2} \ldots\ldots\ldots\ldots (11)$$

The battery is recharged by supplying an external voltage higher than that produced by the battery while discharging. This process causes the electron to flow from the cathode to anode. However, the chemical energy which is used as a source of power in these batteries is often toxic and eco-destructive. These prompted researchers to come up with an eco-friendly and renewable source of

fuel, leading to a cleaner environment. Following the invention of the gas batteries by Grove [59], Neidrach and Grubb at General Electric introduced the first conventional fuel cell for NASA [60]. This simple and efficient fuel cell is the hydrogen fuel cell, which uses hydrogen gas as the fuel as shown in Figure 4.

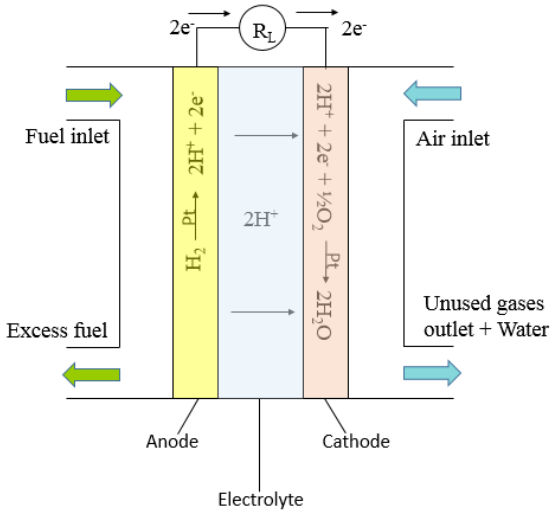

Figure 4. A Hydrogen fuel cell

The cell consists of a noble metal electrocatalyst (i.e., platinum), which is used to oxidize hydrogen and reduce oxygen. In a hydrogen fuel cell, hydrogen is oxidized by the platinum electrocatalyst to produce protons and electrons, which travels through the electrolyte and the external circuitry, respectively. The flow of electrons results in the generation of electricity. At the cathode, the electrons recombine with oxygen in the presence of protons, thereby resulting in the reduction of oxygen to produce water as the by-product. Most fuel cells employ hydrogen fuel because the platinum electrocatalyst utilized is very efficient in oxidizing hydrogen. However, its large-scale application as a power source is limited because platinum is very expensive and nonrenewable. In addition, a hydrogen fuel cell requires continuous supply of hydrogen fuel to generate electrical power by the oxidation of hydrogen, and is also susceptible to carbon contamination, which further

complicates the oxidation process due to carbon monoxide poisoning of the electrocatalyst. The high cost of this noble metal electrocatalyst coupled with the production of hydrogen and electrocatalyst poisoning results in an unsustainability of hydrogen fuel cells as an ideal power source for implantable bioelectronic devices.

The idea of energy conversion from organic fuel sources comes from the very basic reaction of photosynthesis. In photosynthesis, light energy is trapped by chlorophyll to generate Adenosine Triphosphate (ATP) and at the same time a hydrolysis reaction takes place that releases electrons. These electrons further react with the carrier molecule Nicotinamide Adenine Dinucleotide Phosphate (NADPH) and reduces it from the oxidized state $NADPH^{+}$ to NADPH. In this environmentally friendly energy conversion reaction, the light energy is converted into chemical energy by plants and microorganisms [61]. This stored chemical energy can then be further utilized as a fuel source for other purposes. Thus, the fundamental sugar producing reaction in photosynthesis involves the utilization of atmospheric carbon dioxide and light dependent products, ATP and NADPH, to produce sugar and release oxygen back into the environment:

$$6CO_2 + 12H_2O \rightarrow C_6H_{12}O_6 + 6O_2 \quad \text{..... (12)}$$

$$C_6H_{12}O_6 + 6H_2O \rightarrow 6CO_2 + 24H^+ + 24e^- \quad \text{..... (13)}$$

Furthermore, one molecule of glucose upon complete oxidation to CO_2 during the aerobic metabolic pathway generates 24 electrons to produce electrical energy. The large amount of glucose produced by the above reaction can serve as a fuel in glucose biofuel cells. The motivation behind extensive research in glucose biofuel cell technology is attributed to the search for an alternative sustainable 'green' fuel source that is cost-effective and can meet the increasing global

energy demands and recent advancements in bioelectronics. Since glucose is an essential energy source in many living organisms, glucose biofuel cells have found application in powering implantable bioelectronic devices used to diagnose and treat a variety of conditions ranging from metabolic disorders to neurological disorders. Conventional fuel cell assembly consists of an anode, a cathode and an electrolyte and relies on the conversion of chemical energy, into electrical energy. Two types of reactions occur in a fuel cell: oxidation and reduction reaction also known as redox reaction. The oxidation reaction occurs at the interface of the anode and electrolyte; whereas the reduction reaction occurs at the interface of the cathode and electrolyte. Oxidation of fuel releases electrons, which travel through an external circuitry towards the cathode, thus producing electricity. Glucose biofuel cell is a subclass of conventional fuel cells, wherein glucose is utilized as the fuel in the presence of oxygen and is then oxidized to form gluconolactone and release electrons at high voltages, enabling oxygen to be reduced to produce bioelectricity. The experimental set up for such energy generation is shown in Figure 5.

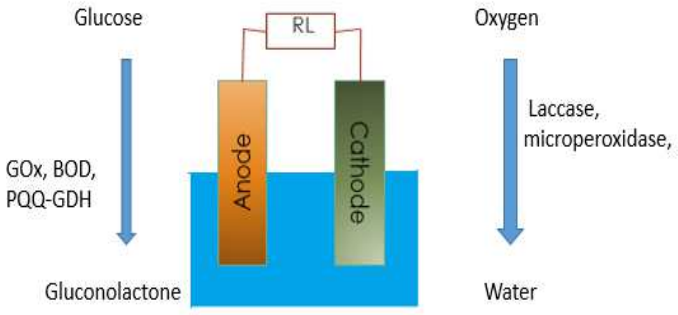

Figure 5. An enzymatic glucose biofuel cell

Although glucose biofuel cells are classified as electrochemical power sources, they are different from batteries and can be differentiated based on the anodic catalysts used for the oxidation of the fuel. A battery is a closed loop system consisting of internal stored chemical energy that needs to be recharged or replaced once all the chemical energy is utilized. On the other hand, a fuel cell is

an open loop system consisting of a cathode, an anode and the electrolyte-containing fuel that produces power as long as there is a continuous supply of fuel. Instead of relying on precious metal catalysts to oxidize the glucose fuel, which forms the basis of operation of non-enzymatic glucose fuel cells, the enzymatic glucose biofuel cell uses naturally occurring enzymes derived from living organisms making it a cheap, renewable and clean source of power. These glucose biofuel cells consist of an anode, a cathode and an electrolyte containing glucose fuel. The electrodes are modified with enzymes which act as a catalyst to initiate the redox reaction. The anode is modified by a glucose selective enzyme which oxidizes the glucose fuel to form gluconolactone with the release of electrons and protons. These protons and electrons travel towards cathode, through the electrolyte external circuit respectively. At cathode, oxygen is reduced by an oxygen reducing enzyme in the presence of the electrons and protons to form water. The flow of electrons results in current generation, thus, power is generated. The redox reaction occurs at the interface of the electrolytes and bioelectrodes and are as follows:

$$At\ anode: Glucose \xrightarrow{glucose\ selective\ enzyme} Gluconic\ acid + 2H^+ + 2e^- \quad \ldots\ldots\ldots\ldots\ldots\ldots (14)$$

$$At\ cathode: O_2 + 4H^+ + 4e^- \xrightarrow{oxygen\ reducing\ enyzemes} 2H_2O \quad \ldots\ldots\ldots\ldots\ldots\ldots\ldots\ldots (15)$$

The above reaction mechanism does not produce any poisonous byproducts, which is the case in non-enzymatic glucose fuel cells. Therefore, a major advantage of glucose biofuel cells over conventional fuel cells is that they employ renewable enzymes that are environmentally friendly. Thereby, making enzymatic glucose biofuel cells a 'green' alternative to convention fuel cells for generating power with high conversion efficiency at ambient temperatures and pH conditions. An enzymatic glucose biofuel cell can be a good alternative to a battery that powers pacemaker

circuits, which currently run on a Li-ion battery for 6 - 10 years and need to be replaced from time to time. [62].

The most promising and challenging application for glucose biofuel cell is its integration into implantable bioelectronics. Therefore, dependable power harvesting technologies are required for sustaining implantable bioelectronics operation *in vivo* for the lifetime of the patient without the need of continuous battery replacements [63]. Advances in implantable bioelectronics such as cardio-stimulators, drug delivery, and glucose biosensors make feasible the concept of using glucose biofuel cells to power low-powered biomedical devices [60, 64, 65]. It is shown that conceptually a biofuel cell can harvest electrical power from cerebrospinal fluid when implanted within the subarachnoid space as illustrated in Figure 6. This integration has the potential to restore proper function to damaged organs without the need for an external power supply.

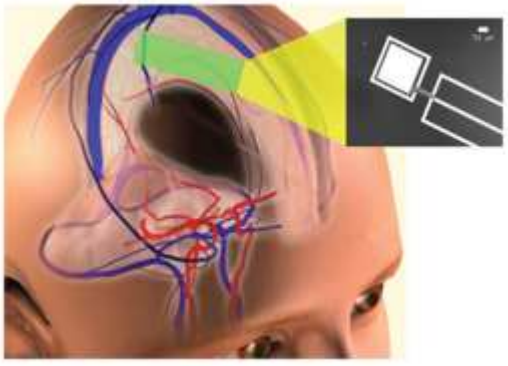

Figure 6. Conceptual schematic of energy harvesting from cerebrospinal fluid by an implantable glucose fuel cell. The inset illustrates a micrograph of one prototype, showing the metal layers of the anode (central electrode) and cathode contact (outer ring) patterned on a silicon wafer. (Rapoport et al. 2012)

Although conventional fuel cells and batteries remain the power source currently employed for powering electronic devices, they are known to be cost inefficient, contain harmful chemicals, and have limited supply of stored chemical energy. Biofuel cells, on the other hand, have been

researched extensively to overcome some of these disadvantages by utilizing naturally occurring enzymes to catalyze the redox reactions at the interface of the bioelectrodes and electrolyte solution to generate power in the presence of the analyte/ fuel. The impetus has been given to the design of power sources that employ naturally and readily-available catalysts, cost-effective and environment friendly source of fuel, thereby resulting in the development of an enzymatic glucose biofuel cell. Currently, high performance glucose biofuel cells mostly employ carbon nanotubes (CNTs) as the electrode material due to their high surface area mediated electron transfer. Buckypaper, which comprise of 3D multi-walled carbon nanotubes (MWCNTs), is a popular electrode substrate material. It consists of an aggregated chain of carbon nanotubes, making it conductive throughout, and along with its multi-dimensional structure which increases the active surface area. The development of these nanostructured electrode materials has been shown to greatly improve the electroactive area for enzyme immobilization [66 - 68]. Several reports also demonstrated the transition from *in vitro* to *in vivo* characterization of enzymatic glucose biofuel cells [64, 69 - 73]. Katz pioneered the implantation of glucose biofuel cells by implanting a glucose biofuel cell in snail as shown in Figure 7.

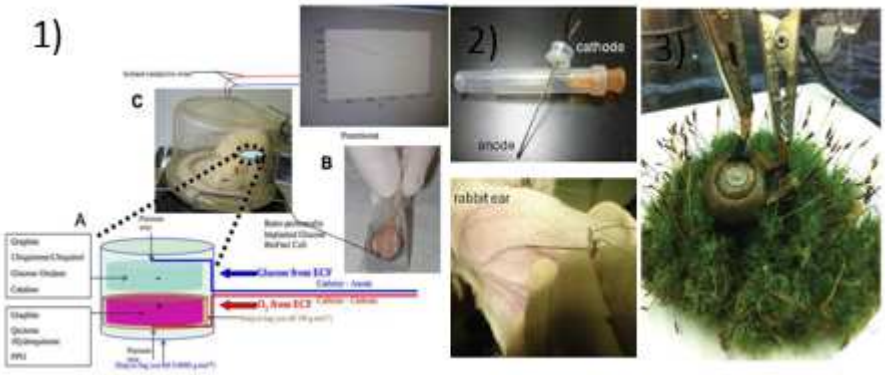

Figure 7. Bioimplantations of glucose biofuel cell in animals. (1) Schematic diagram of the principle, preparation, implantation and operation of an implantable "Quinone-Ubiquinone Glucose BioFuel Cell" (2) Photographs of an assembled biofuel cell for power generation from a rabbit vein. (3) Photograph of a snail with implanted biocatalytic electrodes.

The assembly produced a power density of 30 μW/cm² with an open circuit voltage of 530 mV and a current density of 170 μA/cm². While size is an important constraint to be considered while fabricating a biofuel cell, knowing the power specifications is equally important. A pacemaker device needs a minimum power of 10 μW for its proper functioning. The electrical parameters produced by a single biofuel cell didn't fulfill these necessary requirements. The open circuit voltage and the short circuit current density can be improved by stacking two or more biofuel cells in series or in parallel depending on the application [71]. Figure 8 illustrates two glucose biofuel cells connected in series using two lobsters each implanted with a biofuel.

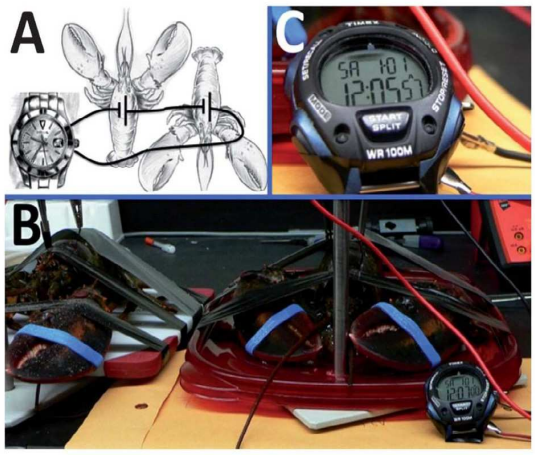

Figure 8. Series combination of Glucose biofuel cell as a source of power. A) Pictorial representation of two biofuel cells connected in series. B) Experimental set up of implanted glucose biofuel cell C) A stopwatch powered by glucose biofuel cell implanted inside the lobster. (MacVittie et al., 2013).

This arrangement resulted in an enhanced potential of 1.2 V as opposed to 0.54 V for a single cell. Katz et al. implemented a pacemaker circuit using a single glucose biofuel cell and boost convertors consisting of a charge pump and a DC-DC converter to generate the 3 V to drive the

pacemaker circuit [74]. In this work, the charge pump assembly was used to excite the input voltage (0.3 – 0.5 V) to 2 V and the DC-DC converter was used to amplify the 2 V supply to result in a stable 3 V power supply used to drive the pacemaker circuit. Thus, a single implanted biofuel cell inside a lobster exhibited an open circuit voltage of 0.47 V and a short circuit current density of 0.83 mA/cm^2 and delivered sufficient energy to power the cardiac pacemaker circuit. In addition, Southcott et al. [71, 73] connected an implantable biofuel cell operating under conditions mimicking the blood circulatory system, to a charge pump and a DC-DC converter circuit to amplify and stabilize the power produced by the single biofuel cell to power a pacemaker circuit. Satisfactory operation of the pacemaker circuit was observed (Figure 9).

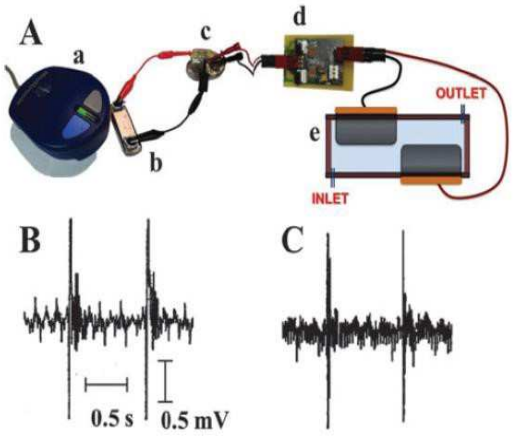

Figure 9. Glucose biofuel cell powering a pacemaker circuit. (A) Experimental setup depicting (a) a sensor, (b) an implantable loop recorder, (c) a pacemaker, (d) the charge pump–DC–DC interface circuit, and (e) the biofuel flow cell (B) Registered pulses generated by the pacemaker when it is powered by the standard battery. C) Registered pulses generated by the pacemaker when it is powered by the biofuel cell (Southcott et al., 2013).

With the overarching goal of replacing external power sources, these enzymatic glucose biofuel cells can serve as micro-power generators for micro-/nanosize implantable bioelectronic devices [63] such as cardiac pacemakers and implantable biosensors for monitoring physiological state [75]. The advantage of using this chemical approach to harvest energy is that the fuel source,

glucose is continuously replenished in living organisms [76]. In 2015, Falk et al. reported a wireless self-powered bioelectronic device, which employed a self-sustained carbohydrate and oxygen sensitive biofuel cell system. The self-sustained wireless system consists of a micropotentiostat for biosensing, an energy harvesting module for amplifying the input voltage, a radio transmitter for data transmission and separate sensing bioelectrodes for carbohydrate and oxygen sensing. The enzymatic biofuel cell was operated in a carbohydrate and oxygen-containing buffer and was shown to supply sufficient drive strength (at least 44 μA and 0.57 V) to power the wireless units interfaced to it. Bench-top prototype was demonstrated using various concentrations of the carbohydrates and oxygen to wirelessly monitor real-time changes in analyte concentrations, using the enzymatic biofuel cell as the power supply. Desmaele et al. [77] fabricated a multilevel membraneless enzymatic glucose biofuel cell using thin polyester films as flexible electrode substrates. The overall setup comprised of four anodes and cathodes having an individual geometric surface area of 25 mm^2 and a thickness of 425 μm. The parallel arrangement resulted in a maximum power of 12.5 μW and the voltage booster circuit produced an output voltage of 3.1 V, which is sufficient for powering the wireless sensor circuit and transmitting temperature measurements to a remote desktop.

The development of implantable glucose biofuel cells from well-established biological materials for the generation of electrical power have a much higher chance of being biocompatible, and surviving long term implantation in living organisms. The energy converted from glucose in the body using glucose biofuel cells finds potential application in powering bioelectronic devices and portable electronic devices, such as cardiac pacemakers, neurophysiological monitors, etc. Since glucose is abundant in the body, the glucose biofuel cell will continuously generate electricity as long as there is a continuous supply of glucose with the assumption that the enzymes do not lose

its activity over time. Thus, numerous efforts have been made to develop lightweight glucose biofuel cells that can power ultra-low power devices over a long period of time without the need for surgical replacements.

Realizing the importance of enzymatic glucose biofuel cell as a power source, scientists began employing these biofuel cells to power glucose sensors which gave rise to a self-powering glucose sensing system (SPGS). SPGS system comprising of GO_x anode and a Pt/C cathode was reported by Liu et al. [78]. This SPGS exhibited a linear dynamic range of 2-30 mM *in vitro* at relatively low O_2 concentrations. When operating in 30 mM glucose, an open circuit voltage of 480 mV and short circuit current of 19 nA was achieved. The power output was observed to be stable over a period of 60 days of continuous operation at 37 °C in 30 mM glucose. In addition, Pinyou et al. [79] reported a miniaturized glucose biofuel cell based on screen printed electrode modified with glucose dehydrogenase and bilirubin oxidase. The power generated from the oxidation of fuel is used to power an electrolyser and transduced into an optical read-out. An open circuit voltage of 567 mV and a maximum power of 6.8 $\mu W/cm^2$ was achieved. The power generated by the biofuel cell is proportional to the concentration of glucose, and a linear dynamic range of 0.1 mM to 1 mM was reported. The power generated by this miniaturized biofuel cell was utilized by the electrolyser that detected the glucose concentration dependent dye spectrophotometrically led to the development of a self-powered glucose biosensor with a dynamic range of 0.1–0.6 mM. Yoshino et al. [80] also reported a free-standing enzyme/mediator/electrode consisting of polyvinylimidazole-[Os(bipyridine) 2 Cl] (PVI[Os(bpy) 2 Cl]) composites and glucose oxidase inside a 1 mm x 1 mm film of carbon nanotubes wound on one of the lead of a light emitting diode (LED) device to serve as the anode. An air breathing cathode (carbon fabric) composed of bilirubin oxidase was employed as the cathode and connected to the other lead of the LED. The assembled

biofuel cell served as a self-powered glucose monitor inside a grape, where the blinking of the LED is inversely proportional to the power of the biofuel cell. The presence of glucose/ sugar in the fruit resulted in the blinking of the LED (Figure 10) and this has potential applications in blood glucose monitoring, if the exact concentration of glucose/ sugar can be deduced.

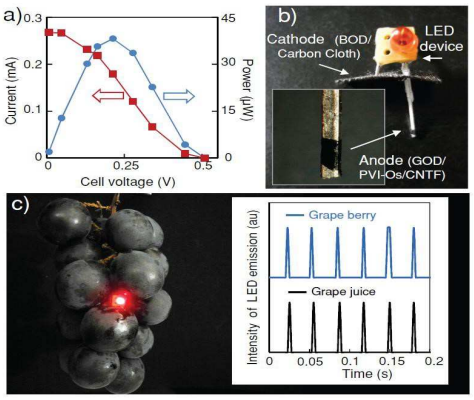

Figure 10. Glucose biofuel cell implantation in fruit. a) Performance of a biofuel cell composed of an anode of GOD/PVI-[Os(bby) 2 Cl]/CNTF film (20 μ m thickness) and a cathode of BOD-modifi ed carbon cloth (1 cm × 1 cm), b) Photograph of the LED-based self-powered sugar indicator, c) Biofuel cell implanted in a grape and the time course of LED emission (inset) (Yoshino et al., 2013).

Falk et al. [81, 82] reported the development of a miniaturized biofuel cell as a power source for a glucose sensing contact lenses by harvesting the biochemical energy stored in ascorbate, which is naturally present in tears. The anode was constructed from 3-D nanostructured gold electrodes (gold nanowires and gold nanoparticles conductive complex) and cathode employed myrothecium verrucaria bilirubin oxidase. The biofuel cell was operated in human lachrymal liquid and an open circuit voltage of 0.54 V, a maximal power density of 3.1 μW/ cm^2 at cell voltage of 0.25 V was reported. A stable current density of 0.55 μA/cm^2 at a cell voltage of 0.4 V was observed for 6 h of continuous operation. Although the biofuel cell was not directly used to power glucose

biosensing contact lenses, it provides a proof-concept that the reported findings that electrical power can be generated from an ascorbate/O_2 biofuel cell and used as power source for glucose-sensing contact lenses for continuous monitoring of blood glucose. Although enzymatic glucose biofuel cells are still plagued by low power densities and short lifetimes, a considerable amount of research in biofuel cells development has been conducted in the field since 1911 to enable the realization of enzymatic biofuel cells as power sources for implantable bioelectronic devices, thus decreasing our reliance on batteries. Additionally, the enzymatic glucose biofuel cells low power production has been overcome by using various power amplification circuits as previously described. Thereby, the advantages of these glucose biofuel cells over conventional fuel cells and batteries have made them a popular choice of power source.

The above works cited report different instances where glucose biofuel cells were used as a glucose biosensor because the power characteristics correlated well to glucose concentrations, thereby resulting in the capability to sense glucose. In some cases, the glucose biofuel cell was used to power a separate glucose biosensor. However, there have been no reports of developing a system comprising of the enzymatic glucose biofuel cell with a transducer to convert the power generated into an electrical signal (frequency) that correlates to the concentration of glucose, while powering an electronic device simultaneously. Such a system would eliminate the use of external power sources currently available for glucometer and CGM devices and eliminate the need for potentiostat circuits. The sensing device would then be truly self-sufficient, wherein it converts the chemical energy stored in glucose within the body to generate power as well as sense glucose concentration via the monitoring of the charge cycle of the trancing element. In this work, we fabricate an enzymatic glucose biofuel cell, which is used as a power source to drive the charge pump circuit and the step-up DC convertor amplification circuits to generate practical electrical

power. The capacitor interfaced with the charge pump is used to sense glucose by monitoring the charge cycle across it whereas, the step-up DC convertor circuit is used to condition the triggering signal from the charge pump to produces a steady DC output to drive glucometer device.

In the following chapters, we describe the fabrication and characterization of enzymatic glucose biofuel cell as a power source. Chapter 4 explores palladium nanowires and carbon nanotubes as the electrode substrate materials to improve the surface area for enzyme immobilization. We further characterized the biofuel cell system in various glucose concentration and monitored its operational stability overtime.

Chapter 5 focusses on the development of the self-powered glucose sensing (SPGS) system comprising a glucose sensing circuit (charge pump and a capacitor). The performance of the sensing circuit was evaluated in various glucose concentration by monitoring the change in frequency of charge cycle across the capacitor. Optimal pH and temperature conditions for the glucose sensing circuit was determined. The stability profile of the glucose sensing circuit was studied to determine the duration over which our sensor can operate without recalibration.

Chapter 6, focuses on the demonstration of simultaneous glucose sensing and powering of a glucometer device. The sensor key parameters such as sensitivity, selectivity, dynamic range, response time were determined. Lastly, we also determined whether the powering of glucometer device has any adverse effect on the glucose sensing.

Chapter 7 concludes the research conducted by discussing the important findings and significance of the results achieved. We further suggest ways to improve the performance of our system to ultimately design and develop a closed loop system consisting of biofuel cell, sensing and powering unit capable of transferring sensed data wirelessly.

Chapter 4: The development of an enzymatic glucose biofuel cell

The most commonly used glucose selective enzymes in the fabrication of an enzymatic glucose biofuel cell bioanode are glucose oxidase and glucose dehydrogenase. Whereas, laccase and bilirubin oxidase are commonly used as the oxygen reducing enzyme in the construction of the biocathode. Apart from the enzyme, it is important to achieve a direct electron transfer between the active site of the enzyme and the current collector in order to achieve higher current output. In order to achieve that, the substrates need to be electrically conductive as well as possess a high surface area for enzyme immobilization. The enzymes being highly selective eliminates the possibility of cross-reaction in the presence of other analytes, thereby enhancing the sensitivity, selectivity, stability and efficiency of the enzymatic glucose biofuel cell. Moreover, these enzymatic glucose biofuel cells can produce power as long as there is a continuous supply of fuel. Due to their cost-effective and clean nature, they have become a popular choice as a power source and may potentially replace batteries, which we have come to heavily rely on. This chapter describes various fabrication techniques employed in our lab to fabricate an enzymatic glucose biofuel cell.

4.1 Fabrication of palladium nanowire array for biofuel cell application

Nanowires and nanotubes have been used extensively to improve the active surface area for enzyme immobilization. Platinum (Pt) metal served this purpose in the early days; however, Pt is a costly and nonrenewable metal in addition to being poisonous [83], thereby resulting in a short cell life. To improve the active surface area for enzyme immobilization, we employ palladium (Pd) nanowire metal array. Although Pd has been demonstrated to exhibit a high degree of selectivity for glucose in non-enzymatic amperometric glucose sensing under high pH (0.1 M NaOH)

conditions [84], there are no reports of Pd being used in non-enzymatic glucose-based biofuel cell application due to the large overpotential of Pd. The Pd nanowire array electrodes realized from the anodized aluminum oxide (AAO) template electrodeposition method [85, 86] exhibit a large surface area, which results in an increased number of adsorption sites for the immobilization of glucose oxidase. This further enables the electron generated during the biocatalysis to be directly transferred to the Pd electrode from the active center of glucose oxidase, thereby compensating for the large overpotential of the bare Pd electrode.

4.1.1 Experimental methods

Anodic aluminum oxide (AAO) has a porous structure which helps trap Pd in its pores and eventually form nanowires. A thin film of Au (100 Å) was sputtered onto one side of the AAO (3 x 3 mm^2) templates to provide an electrical conduction path for the electrodeposition of the Pd nanowires by exposing the pores of the AAO template to the underlying Au film. Silver epoxy was used to glue the Au side of AAO onto an Aluminum (4 x 10 mm^2) sheet to create an electrical connection. The Al-AAO template served as the working electrode in a three-electrode electrochemical cell setup with a platinum wire and a $Ag/AgCl_{(sat)}$ electrode as the counter and reference electrodes, respectively in a water jacketed electrochemical cell. The Al-AAO template was immersed in the electrodeposition solution containing 1 g/L $Pd(NH_3)_4Cl_2$ (99.99%) and 10 g/L NH_4Cl (99.99%) for ~15 min prior to electrochemically depositing Pd from the aqueous solution at a pH of 8. The electrodeposition was conducted at − 600 mV versus Ag/AgCl at a temperature of 30 °C for 2 h using BASi potentiostat/galvanostat EC Epsilon. After electrodeposition, the substrate was rinsed in deionized water and the AAO template was etched away in 2 M NaOH for

6 min at room temperature with mild agitation. The resulting free standing Pd nanowire array electrodes (Figure 11) were then rinsed three times with ethanol followed by deionized water.

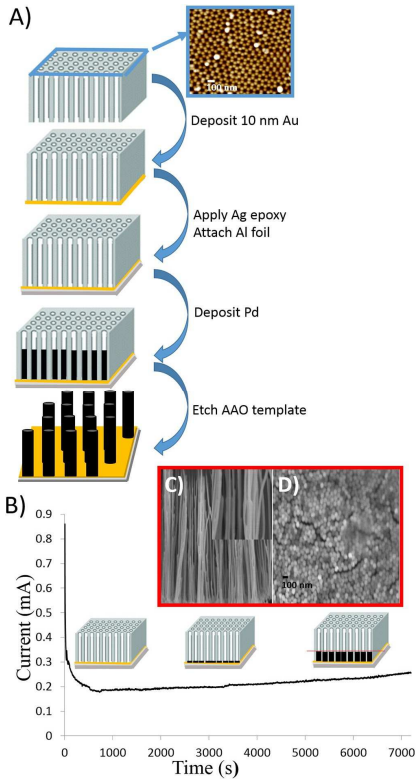

Figure 11. A) Schematic representation of the electrodeposition of Pd nanowire using AAO template. Top right: AFM top-view micrograph of the AAO template with pore diameter ranging from 62 to 70 nm. B) Current transient curve for the electrochemical deposition of the Pdinto the AAO template. C) SEM cross-sectional view and D) top-view micrographs of free standing Pd nanowires after etching away the AAO template in 2 mM NaOH.

4.1.2 Functionalization of Pd Nanowire bioelectrodes

The surface of the as-prepared Pd nanowire bioelectrodes was subsequently functionalized by treatment with γ-APS, 0.1 vol% in ethanol at 40 °C for 30 min in order to introduce silane surface functionalities as previously reported [87]. After silanization, the Pd nanowire array bioelectrodes were rinsed by sequential washing for 1 min in an ethanol, and then in ethanol/water mixture (1:1,

v/v). Finally, the γ-APS-coated Pd nanowire array bioelectrodes were cured at 110 °C for 20 min in a convection oven, incubated in 6% glutaraldehyde at room temperature for 30 min. The surfaces of the Pd nanowires were thoroughly rinsed and placed in 0.1 M phosphate buffer (pH 7). This was followed by a derivatization step to create a continuous path of covalent bonding between the Pd nanowire bioelectrode surfaces and the biocatalysts.

4.1.3 Enzyme immobilization

The biocatalyst immobilizations were achieved by incubating the γAPS-aldehyde functionalized Pd nanowire bioelectrodes in the appropriate enzyme solution (bioanode: 1 mg/ml glucose oxidase and 0.5 mg/ml catalase or biocathode: 1 mg/ml laccase in 0.05 M phosphate buffer with 0.15 M NaCl ((PBS), pH 7) for 30 min. The surfaces were thoroughly rinsed in PBS and incubated for an additional 30 min in HEPES buffer containing 0.2 M EDC and 0.05 M PEG-NHS solution at room temperature in the dark. Finally, the electrodes were rinsed thoroughly in buffer.

The immobilized enzyme bioanode and biocathode surface were encapsulated with HEMA-based hydrogel membrane to enhance the lifetime of immobilized enzymes. The HEMA-based hydrogel was chosen because it allows efficient diffusion of glucose into the Pd nanowire matrix. The monomer mixture comprised of HEMA, PEGMA and TEGDA in a mole ratio of 80:10:10. DMPA, 4 wt%, photoinitiator was then completely dissolved in the mixture and 5 μL of the monomer mixture and was solvent casted onto the Pd nanowire bioelectrodes. UV irradiation (2.3 W/cm^2, 366 nm, UVP Model CX-2000) was performed for 20 min to polymerize the methacrylates. The PEGMA monomer was added to the hydrogel formulation to provide for long-term stabilization of membrane-immobilized biocatalysts. This establishes PEG chains, set pendant to the polymer

network, in the form of network supported polymer brushes. PEG chains are well-known to stabilize proteins, preventing their denaturation and promoting long-term bioactivity [87].

4.1.4 Results and discussion:

Electrochemical characterizations were conducted on BASi potentiostat/galvanostats EC Epsilon at 37 °C. The electrochemical experiments were performed in a conventional three-electrode cell with the exception of the biofuel cell characterizations. The $Ag/AgCl_{(sat)}$ and Pt wire were used as the reference and counter electrode, respectively. Various glucose concentrations were investigated. The working buffer solution was 0.1 M phosphate buffer saline unless otherwise indicated. All potentials referenced in the present work are measured against $Ag/AgCl_{(sat)}$ reference electrode. The anodes were characterized using potentiostatic polarization curves generated by applying a series of potentials to the anode while measuring the resulting steady-state current density as a function of time. Cyclic voltammetry was conducted with scan rates of 20 mV s^{-1} under air, unless otherwise indicated. Cyclic voltammetry measurements were performed in 5 mM glucose to compare and evaluate the electrocatalytic activity of the nonenzymatic and enzymatic bioanodes in a classical three-electrode arrangement containing the reference electrode $Ag/AgCl(KCl_{sat})$ and a counter Pt electrode. In principle, the combination of glucose oxidase and Pd nanowire arrays leads to the development of a glucose oxidase bioanode that can oxidize glucose, enhance the bioanode conductivity and facilitate the electron transfer of the biocatalyst without the use of a mediator [88].

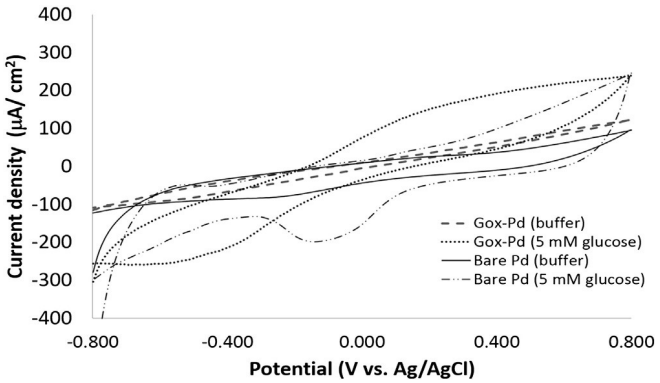

Figure 12. Cyclic voltammograms of the bare Pd and GOx-Pd bioanodes measured in air-saturated 0.1 M PBS and air-saturated 5 mM glucose under physiologic conditions (pH 7 and 37 °C). Scan rate: 20 mV s^{-1}.

Figure 12 represents the cyclic voltammograms (CVs) of the GOx-Pd and bare Pd bioanodes measured in air-saturated 0.1 M PBS and air-saturated glucose 5 mM with a scan rate of 20 mV/s. The CV profile in phosphate buffer saline for both bioanodes was nearly featureless. In the presence of 5 mM glucose, an increase in the electrocatalytic current for the bare Pd nanowires was observed in the potential range of 0.3 to 0.8 V, which suggests that the oxidation of glucose and the cathodic peak at −0.14 V are attributed to the reduction of the palladium oxide formed at higher potential during the forward scan [84]. Surface confined redox processes associated with the presence of glucose oxidase were apparent in the CV of the GOx-Pd nanowires in the presence of 5 mM glucose. The anodic current increased, suggesting catalytic activity towards glucose.

Additional CVs were performed with the enzymatic bioanode in different glucose concentration to evaluate the electrocatalytic activity of the GOx-Pd bioanode. Figure 13A represents the CVs of the GOx-Pd bioanode measured in air-saturated 0.1 M PBS and glucose: 1 mM, 5 mM and 10 mM. In the presence of increasing glucose concentration, the shape of the CVs changes considerably. In the presence of glucose, an onset potential was observed at ca. −0.3 V vs. Ag/AgCl for glucose oxidation, thereby suggesting that this redox system exhibits an increase in the

electrocatalytic current as a function of glucose concentration, and thus corresponds to glucose oxidation. The electrocatalytic current generated in the presence of 5 mM glucose in air-saturated PBS, oxygen purged PBS and nitrogen-purged PBS under physiologic conditions (pH 7 and 37 °C) is shown in Figure 13B. A large anodic and cathodic currents were observed in the presence of oxygen because oxygen accepts electrons from glucose oxidase, while such large current was not observed in nitrogen-purged PBS containing 5 mM glucose and 5 mM glucose in air-saturated PBS. These results reveal that GOx-Pd nanowires exhibit electron transfer activity without the use of mediators. Thus, the GOx-Pd nanowire bioanode is well suited for use in a single compartment enzymatic glucose biofuel cells.

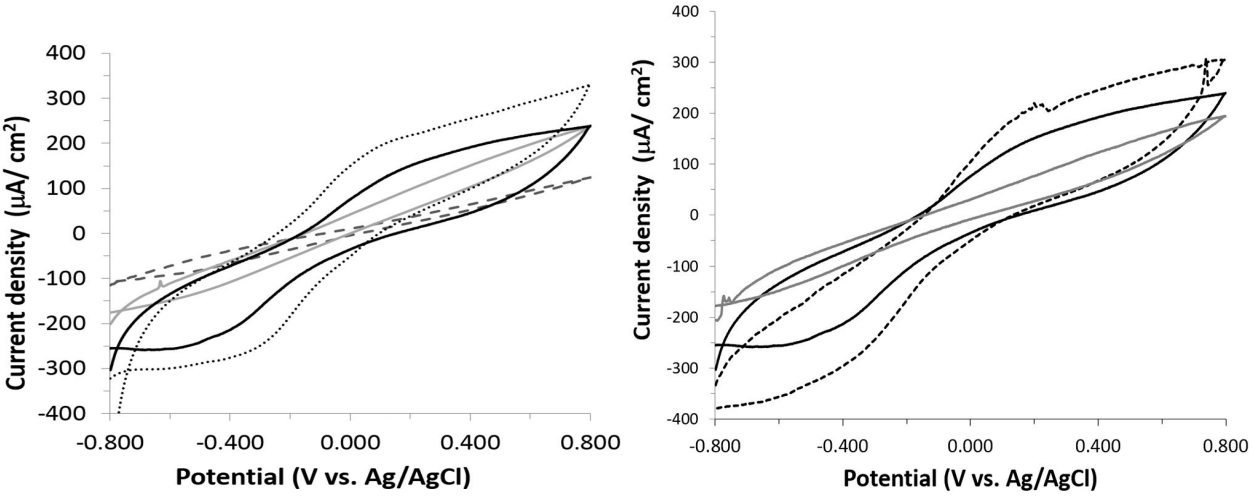

Figure 13. A) Cyclic voltammograms of the GOx-Pd bioanode measured in air-saturated 0.1 M PBS (dashed line) and air-saturated glucose: 1 mM (gray line), 5 mM (black line) and 20 mM (dotted line) under physiologic conditions (pH 7 and 37 °C). Scan rate: 20 mV s^{-1}. B) Cyclic voltammograms of theGOx-Pd bioanode measured in the presence of 5 mM glucose in air-saturated PBS (black line), oxygen-purged PBS (dash line) and nitrogenpurged PBS (gray line) under physiologic conditions (pH 7 and 37 °C). Scan rate: 20 mV s^{-1}.

The biofuel cell characterizations were carried out in phosphate buffer saline (pH 7). The polarization curves for the biofuel cell were obtained from the use of a series of external loads (1

KΩ to 1 MΩ). The bioanode and biocathode were constructed using Pd nanowires and positioned 20 mm apart in the single compartment cell. The glucose oxidase selectively catalyzes glucose oxidation in the presence of oxygen and laccase catalyzes oxygen reduction reaction at the cathode, thereby enabling the use of a single compartment design for testing. All current densities were calculated using geometrical area of the bioelectrodes. As demonstrated above, the higher current density generated by the GOx-Pd bioanode makes it promising as a bioanode in glucose/O_2 biofuel cells. The GOx-catalase-Pd bioanode and the laccase-Pd biocathode were assembled into a single compartment biofuel cell using glucose prepared in PBS as the electrolyte (Figure 14).

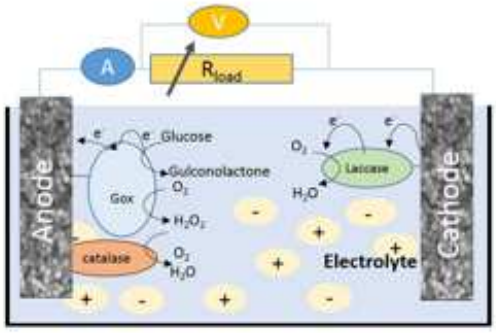

Figure 14. Schematic representation of the glucose biofuel cell structure

The open-circuit voltage (V_{oc}) of the biofuel cell constructed using bare Pd nanowires was 13.4 mV, this makes the bare Pd nanowires impractical for improving V_{oc} of the biofuel cell and maximizing the power generated. Here, we developed a glucose/O_2 biofuel cell using the GOx-Pd bioanode which exhibits a more favorable improvement of V_{oc} of the biofuel cell. Figure 11 shows the I–V and power characteristics of the glucose biofuel cell at different external loads (1 kΩ to 1 MΩ) in 1 mM, 5 mM and 10 mM glucose solution saturated with air.

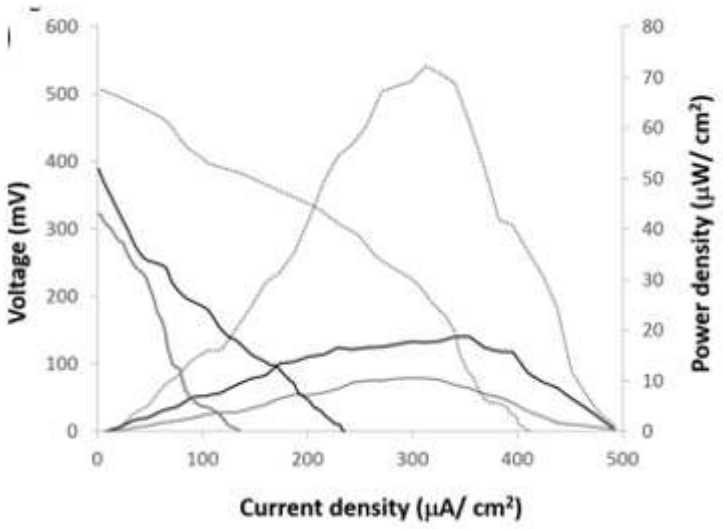

Figure 15. I–V and power density curves of the glucose biofuel cell at different external loads in1 mM (gray line), 5 mM (black line) and 10 mM (dotted line) glucose in PBS (pH 7 and 37 °C) saturated with air.

The open-circuit voltage of the fuel cell was 322, 389 and 506 mV for 1 mM, 5 mM and 10 mM glucose, respectively. The power of the cell at different loads obtained with various glucose concentrations is shown in the Figure 15. The maximum power densities were 10.5 μW/cm^2 at 0.20 V (1 mM glucose), 18.8 μW/cm^2 at 0.17 V (5 mM glucose), and 72.2 μW/cm^2 at 0.25 V (10 mM glucose). The results observed here follow the trends of the bioanode for the oxidation of glucose when tested separately in a three-electrode cell setup for CV characterization. The short-circuit current densities were 136 μA/cm^2, 233 μA/cm^2, and 411 μA/cm^2, for 1 mM, 5 mM and 10 mM glucose, respectively. These values compare well with those recently reported for other glucose biofuel cells based on immobilized enzymes [89-91]. The cell performance operating in 5 mM glucose under O_2-saturated condition exhibited an overall stable current density profile, wherein the current density dropped by 21% over a period of five weeks in 5 mM glucose. This stability could be attributed to the large electroactive surface area afforded by the Pd nanowire array

electrodes and the fast electron transfer between the enzymes and electrodes. There is clearly an enhanced cell performance as the concentration of the glucose fuel increases. These results lead to the conclusion that GOx-Pd nanowire bioelectrode is a very attractive platform for biofuel cells because no mediators are used. Although this platform serves the purpose, it has some shortcomings. Apart from the biocompatibility issue of Palladium metal, it is a rare-earth metal and expensive. Moreover, the glucose oxidase enzyme produces poisonous hydrogen peroxide which is cytotoxic and a product of oxidative stress [92] that affects the cell stability and longevity unless treated with catalase or decomposed at higher potentials.

4.2 Glucose biofuel cell as a glucose biosensor

Another enzyme immobilization technique which is independent of any metals as well as the glucose oxidase is immobilizing glucose dehydrogenase on a dense mesh network multi-walled carbon nanotubes (MWCNTs) [93]. The MWCNTs (Buckypaper) are approximately 50,000 times thinner than human hair filament. It has an inbuilt three-dimensional structure which enables improved surface area for immobilization of enzymes. Buckypaper is highly porous and electrically conductive (105.82 $mho.cm^{-1}$) [94]. Previously, glucose oxidase (GOx) was a popular choice of glucose selective enzyme due to its high selectivity towards glucose fuel. It is derived from Aspergillus Niger which remains a common source for GOx. However, glucose oxidase produces harmful cytotoxic hydrogen peroxide, which affects the cell stability and longevity. Reduction in pH is observed sometimes during oxidation of glucose which hinders the enzyme performance [95]. This enzyme is not useful in the case of third-generation glucose sensors as it is unable to transfer electrons directly to the conventional electrodes. To improve the direct electron transfer, polymers, artificial cofactor derivatives and thienoviologens are commonly used, which at times affects the selectivity of the glucose sensor. Due to its ineffectiveness as a third-generation

glucose sensor along with production of toxic hydrogen peroxide, we employ pyroquinoline quinone glucose dehydrogenase (PQQ-GDH). PQQ-GDH does not produce hydrogen peroxide as a byproduct, thereby making it a favored glucose selective enzyme for bio-implantation application in developing the SPGS system.

4.2.1 Experimental methods

1 cm x 0.2 cm strips of metallic type buckypaper were used as the electrode material because of the high surface area for enzyme loading afforded by the mesh network of carbon nanotubes [66, 72, 96). Initially the electrodes were rinsed in 2-proponal to remove any impurities present on the surface of the buckypaper as a result of the manufacturing process. In order for the polyaromatic pyrenyl group of the PBSE, a heterobifunctional cross-linker, to interact with the MWCNTs via π–π stacking [97] as seen in Figure 16A, the electrodes were immediately incubated with 10 mM PBSE, in DMSO with moderate shaking for 1 h in the dark. Following the incubation period, the electrodes were subsequently rinsed with DMSO and 100 mM phosphate buffer solution (pH 7) to remove any loosely bound PBSE and any traces of DMSO on the electrodes, respectively. The bioelectrodes were prepared by immobilizing anodic and cathodic enzymes, PQQ-GDH and laccase on a separate PBSE-functionalized electrode. The bioanode was prepared by incubating the PBSE-functionalized electrodes in a solution of PQQ-GDH in 10 mM PBS containing 1 mM $CaCl_2$ (pH 7). Whereas, the biocathode was prepared by incubating the PBSE functionalized electrodes in the solution of laccase in 10 mM PBS (pH 7). The immobilization reactions were conducted at room temperature with moderate shaking at room temperature for a period of 1 h. The amino functional groups from the enzymes react with the carboxyl functional group from the PBSE (Figure 16A) by breaking the double bond between the carbon and oxygen atom. The π

electrons present in the π bond moves towards the oxygen atom making it formally negative charged. In addition, the nitrogen atom reacts with the carbon atom to donate an electron making it formally positive. These formally positive and negative states result in the formation of an intermediate product that is unstable (Figure 16B). As a result, the π electron returns to form a double bond and releases the R′–O group along with one hydrogen atom. This reaction enables the nitrogen atom to become electrically neutral and, hence, stable. Overall, this reaction results in the formation of a peptide (amide) bond (–CO–NH–) between the amino and carboxyl functional groups [98], thereby resulting in the enzyme-modified electrodes as shown in Figure 16C.

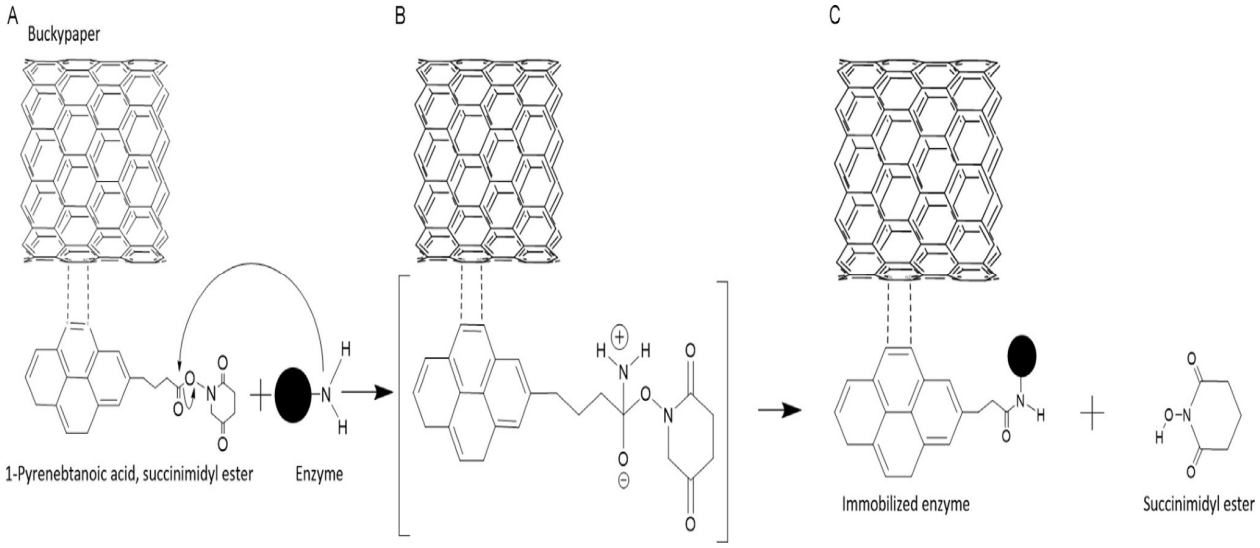

Figure 16. Enzyme immobilization scheme. (A) PBSE interact with the buckypaper via π–π stacking and amino functional group on the enzyme reacts with the carboxyl functional group on the PBSE to form a peptide bond. (B) Formation of the unstable intermediate product. (C) Immobilized enzyme along with the byproduct.

Furthermore, the bioelectrodes were additionally coated with 2 µL of a 10-fold diluted 5 wt% Nafion® solution and left to dry in a desiccator for 15 min. The resulting bioelectrodes exhibited an active surface area of 0.08 cm^2 and a volume of 0.024 cm^3. The bioanode was stored in 100 mM

PBS (pH 7) and the biocathode was stored in 100 mM PBS (pH 6) in the refrigerator when not in use.

4.2.2 Glucose biofuel cell measurements

Figure 17 provides a depiction of the experimental setup of the glucose biofuel cell consisting of bioanode and biocathode previously described by using glucose analyte and oxygen in an air-saturated environment as fuel and oxidant, where the load represents external variable load resistor.

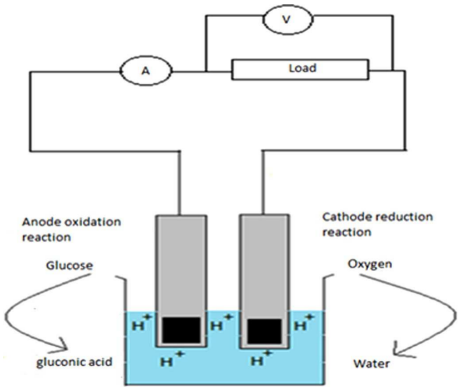

Figure 17. Illustration of the experimental setup for the glucose biofuel cell consisting of a cathode, an anode and an electrolyte containing glucose fuel and the redox reactions that occur within the glucose biofuel cell.

At the bioanode, PQQ-GDH oxidizes glucose to produce gluconolactone by releasing electrons and positive ions. The electrons travel through the external circuitry, thus producing current, and the positive ions travel through the electrolyte containing the glucose fuel and recombine at biocathode, where laccase reduces oxygen to water. The glucose biofuel cell was characterized in the presence of various concentrations of glucose analyte. The current and voltage values were monitored across and in series with the load resistor respectively at 37 °C and pH 7.

4.2.3 Results and discussions

The bioelectrodes display a huge advantage of providing a dense network of MWCNTs for electrically wiring large amounts of enzymes. The electrocatalytic activity of the bioanode and biocathode using cyclic voltammetry (CV) affirmed the direct electron transfer between the active center of the bioelectrodes and the MWCNTs.

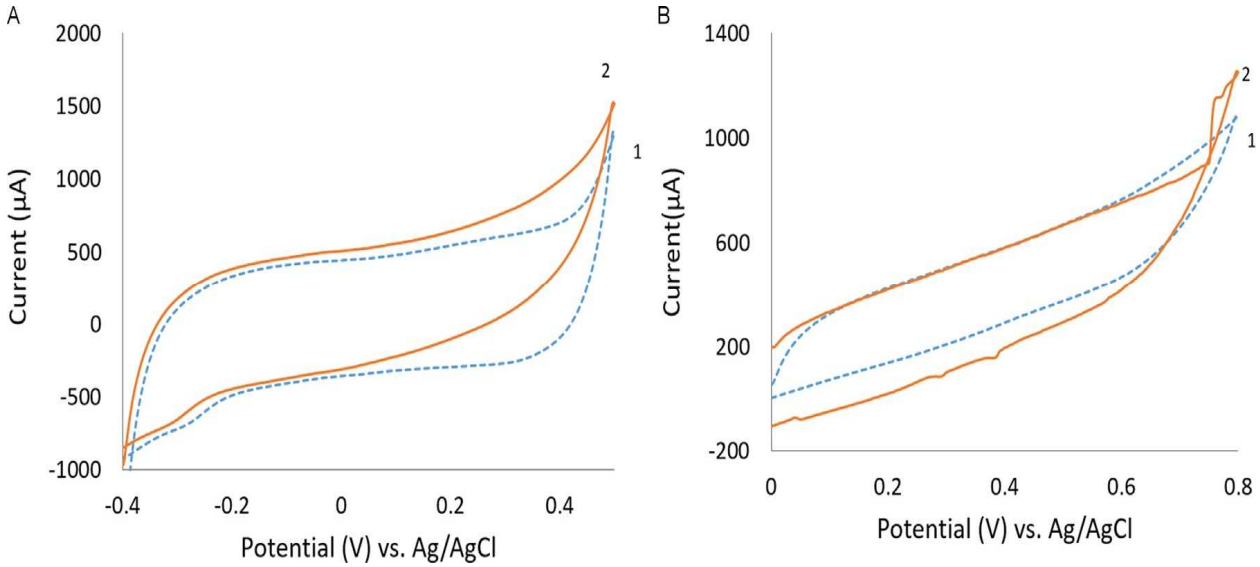

Figure 18. Cyclic voltammogram of (A) bioanode in the absence of glucose pH 7 (blue) and presence of 20 mM glucose (orange). (B) Biocathode in 100 mM phosphate buffer (pH 6) saturated with N_2 (blue) and in the presence of O_2 (orange). All CVs were performed at 37 °C.

The CV experiments were performed at 37 °C at a scan rate of 20 mV s^{-1} (Figure 18). The catalytic electrooxidation of 20 mM glucose was detected at an onset voltage of 190 mV vs Ag/AgCl (Figure 18A), whereas the reduction of oxygen due to the laccase modified biocathode exhibited an onset voltage of 380 mV vs Ag/AgCl (Figure 18B). The open circuit voltage of the glucose biofuel cell operating in 20 mM glucose was 530 mV, which is very similar to the potential difference at which glucose oxidation and oxygen reduction start to occur in the cyclic voltammograms under the air-saturated environment. These results are comparable or superior to those previously reported using

GO_X or PQQ-GDH [99, 100]. The high open circuit voltage could be attributed to the fact that the oxidation of glucose by PQQ-GDH does not produce hydrogen peroxide in contrast to GO_X or mixture of various enzymes [101 - 105]. The production of hydrogen peroxide as a byproduct in glucose oxidation reaction leads to the denaturing of the enzyme. Thus, bioanode based on PQQ-GDH enhances the bioanode performance.

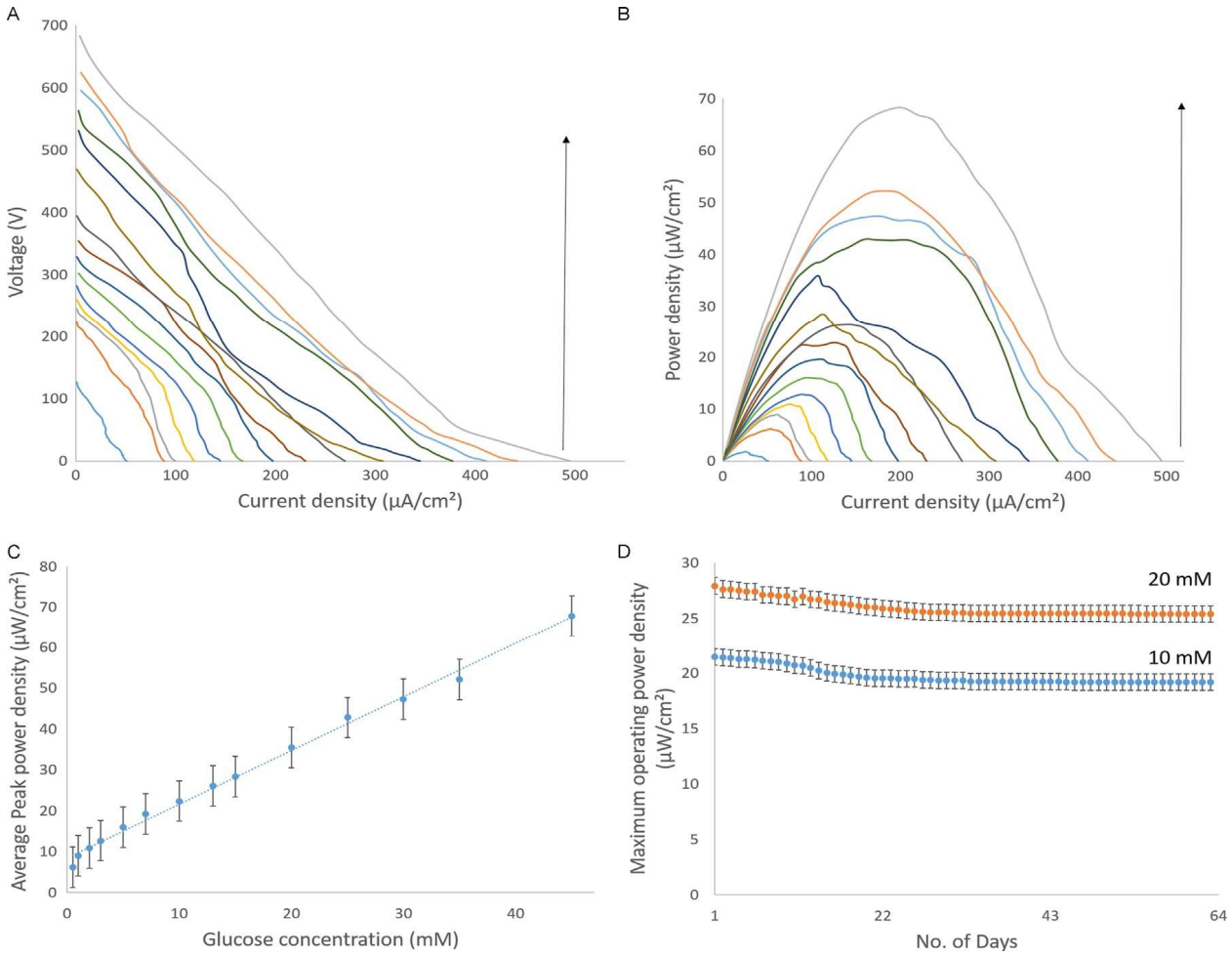

Figure 19. Glucose biofuel cell characterization. (A) Polarization curve and (B) corresponding power curves of glucose biofuel cell at varying glucose concentrations in 0.1 M PBS (37 °C, pH 7). (C) Calibration curve of glucose biofuel cell response to glucose analyte (error bars indicated the RSD). (D) 30-day stability profile in the presence of 10 mM and 20 mM glucose (37 °C, pH 7).

Furthermore, the glucose biofuel cell was characterized in vitro at various standard glucose solutions by measuring the voltage and the current values at varying resistances. The current and power densities were calculated using the geometrical surface area of the bioanode. Figure 19A depicts the polarization of the cell, wherein the open circuit voltage and the short circuit current increased with increasing glucose concentrations due to the availability of more glucose molecules. The maximum cell parameters were obtained in the presence of 45 mM glucose in air-saturated environment (37 °C, pH 7) with an open circuit voltage, short circuit current and power density of 681.8 mV, 39.6 mA, and 67.86 mW/cm^2 at a cell voltage of 335 mV, respectively. This compares favorably to those previously published glucose biofuel cells employing GOx and PQQ-GDH [68, 91, 106 - 109]. At physiological glucose concentration (5 mM glucose at 37 °C, pH 7), the cell exhibits an open circuit voltage of 302.1 mV, a maximum power density of 15.98 mW/cm^2 at a cell voltage of 166.3 mV (Figure 19B). Triplicate testing of the cell parameters to various glucose concentrations yielded a dynamic linear range of 0.5–45 mM glucose with the following regression equation (n = 14, $r^2 = 0.995$):

$$Cell\ response\ \left(\mu\frac{W}{cm^2}\right) = 1.3128\ [glucose](mM) + 8.4841\ \left(\mu\frac{W}{cm^2}\right) \quad (16)$$

As illustrated in Figure 19C, the biofuel cell performance (power density) significantly increased upon increasing the glucose analyte concentration from 0.1 mM to 45 mM. The biofuel cell stability was further investigated separately in 10 mM and 20 mM glucose solutions under constant load discharge by applying a load resistance of 90 and 84 kΩ for 1 h each day over a period of 63 days. Figure 19D shows the successive 1 h constant load discharge curve acquired during the 63 day periods. A 2% and 3% drop in power density was observed after 1 week of operation in 10

mM and 20 mM glucose, respectively. The overall drop in power density after 63 days of operation in 10 mM and 20 mM glucose at 37 °C and pH 7, was 10.61% and 9.11%, respectively. This slight drop in power density is attributed to the use of PQQ-GDH and nafion, which provided a hydrophobic surface and improved the durability of the bioelectrodes [67], thus, improving the biofuel cell stability. The peak power density produced by the biofuel cell was higher than that reported [110], which was stable for 1 week. Nevertheless, more than 90% of the glucose biofuel cell activity was maintained after the 63 days of operation in air-saturated 10 mM and 20 mM glucose, proving the stability of the bioelectrocatalytic ensemble achieved with the compressed MWCNTs, enzymes and nafion coating. The power produced by the above assembly was successfully applied to the charge pump circuit that amplified the voltage to 1.8 V which was enough to power the LED. This work demonstrated successful characterization of an enzymatic glucose biofuel cell employing PQQ-GDH dependent bioanode which oxidized glucose fuel and laccase dependent biocathode which reduced oxygen. This redox process generated current which was observed to be increasing with glucose concentration due to the availability of more glucose molecules for oxidation at higher glucose concentration. There has been significant research already performed in the field of biofuel cell. After ascertaining the fact that the enzymatic glucose biofuel cells can produce electrical parameters, it was important to explore the stability aspect of the biofuel cell. We successfully demonstrated the operation of an enzymatic glucose biofuel cell over 3 months. This was the longest streak using PQQ-GDH ad laccase enzymes at anode and cathode respectively, which successfully powered an LED, to the best of our knowledge. Further improvement in the stability of the system coupled with higher power densities would eliminate the need for voltage boost circuits and the biofuel cell by itself would be able to power microelectronic devices. Although the thought is far-fetched, significant steps have already been

taken to replace batteries with enzymatic glucose biofuel cells as a power source for bioelectronic devices.

Chapter 5: Self-powered glucose biosensing system

Researchers have been seeking to bridge the gap between glucose monitoring and insulin delivery by developing an artificial pancreas, which would consist of a CGM system, an insulin delivery system and a computer program that adjusts the insulin delivery based on changes in the blood glucose levels. The bridge between the glucose monitoring and insulin delivery systems has been implemented in the early stages and SPGSs have the potential to overcome the shortcomings of glucose monitors based on potentiostatic circuits by continuously and autonomously monitoring blood glucose. This technology uses the amalgamation of glucose biofuel cell and glucose biosensor operation principles. The glucose biofuel cell consists of an anode, a cathode and an electrolyte containing glucose fuel. The oxidation of glucose at anode results in power generation, which can be utilized to meet the need for external power sources, and glucose in the body will be used to simultaneously generate bioelectricity. Blood glucose levels will also be continuously monitored. The power produced by a single biofuel cell is, however, not sufficient to power an implantable bioelectronics device (i.e., glucose biosensor). Although stacked multiple glucose biofuel cells [71] may fulfill the power requirement needed to power a glucose biosensor, it becomes a bulky device overall, thereby defeating the purpose of miniaturized implantable biofuel cell device. To overcome this limitation, a charge pump integrated circuit (IC) is used to amplify the minimum input voltage of 0.3 V, which is easily produced by a single glucose biofuel cell to a voltage range of 1.8–2.2 V. The resulting power has been shown to be enough to power implantable bioelectronic devices [73, 107]. Further amplification to 3 V has been achieved using a DC–DC convertor to enable the powering of pacemaker circuit [77].

5.1 Glucose sensing circuit

Although the power produced by a single glucose biofuel cell has been shown to be incapable of powering any bioelectronic devices, significant work has been done by stacking multiple glucose biofuel cell to enhance the electrical parameters [111, 77] to power low-powered bioelectronic devices. Due to implantation and power constraints, several research groups have implemented a charge pump IC [112] to excite the voltage generated by biofuel cells, however there is still a need to develop SPGS systems with long term stability in order to compete with the existing technology. And significant efforts have been made in the development of SPGSs in past couple of years [113] because they can be considered as an alternative to conventionally-powered sources, specifically for implantable bioelectronics. In this work, we fabricated and characterized a complete SPGS system by exciting the voltage generated from the glucose biofuel cell via a charge pump IC, and the resulting amplified voltage is used to charge the capacitor functioning as a transducer. The combination of charge pump IC and capacitor with the glucose biofuel cell enables the realization of a complete SPGS system that can simultaneously power ultra-low-powered bioelectronics and sense glucose, while eliminating the need for a potentiostat circuit.

5.1.1 Experimental methods:

Here we demonstrate the application of the glucose biofuel cell as a self-powered glucose biosensing system by constructing a power amplifying circuit as seen in Figure 20A and 20B using a printed circuit board, wherein the charge pump IC requires an input voltage of at least 0.25 V. The charge pump IC boosts the voltage generated by the biofuel cell to 1.8 V. The 302.5 mV generated by the glucose biofuel cell operating in 5 mM glucose is sufficient to serve as the input voltage to the charge pump IC, which in turn supplied a continuous burst of power via the 0.1 μF capacitor to power a light emitting diode (LED) as a small portable electronic device.

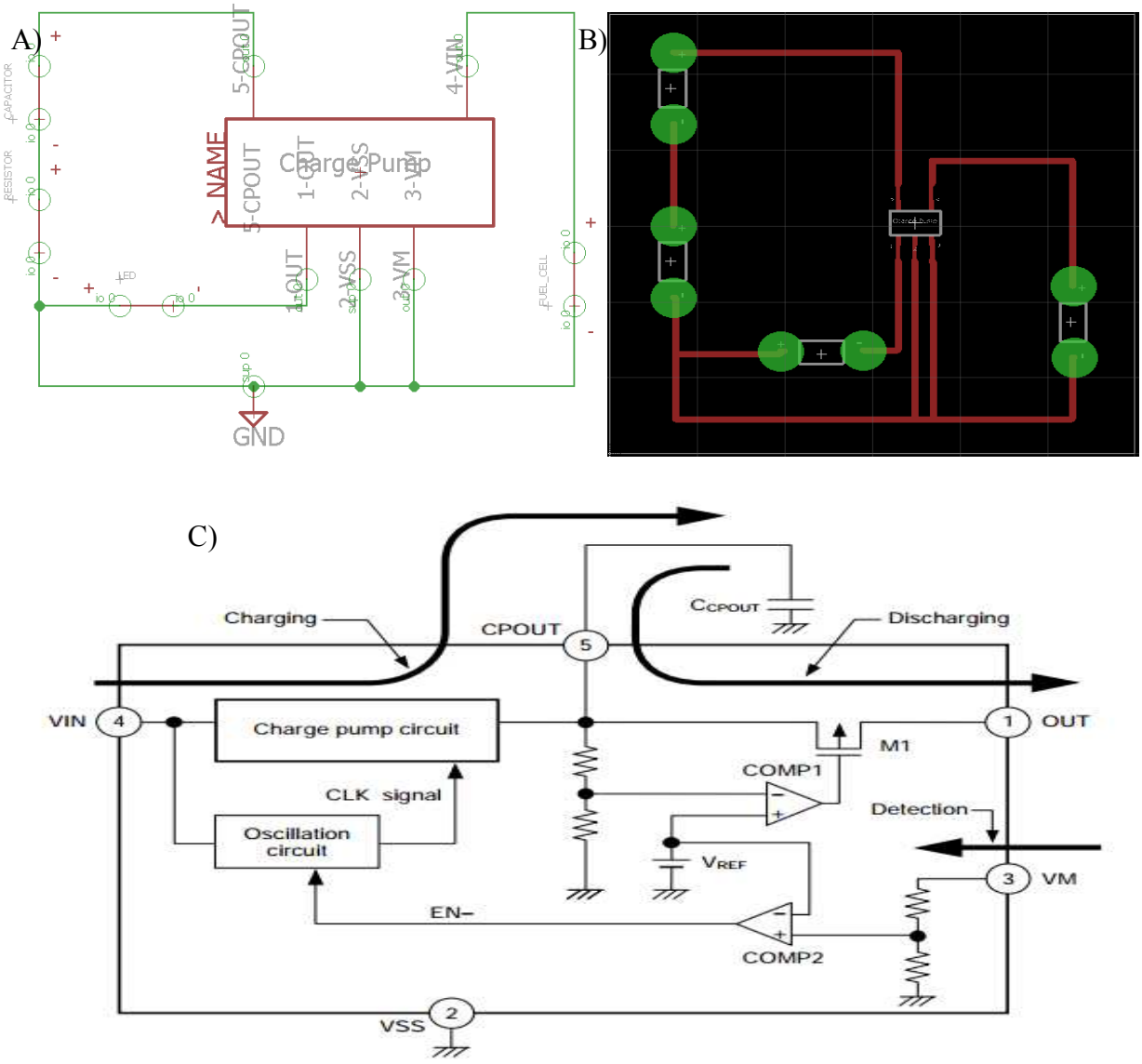

Figure 20. A) Eagle schematic of charge pump circuit. B) Eagle board used to fabricate PCB consisting of 0.1 mF transducer element capacitor and micro-electronic device LED. C) Internal circuit of the charge pump IC with two stage capacitor.

The charge pump circuit is used to amplify the electrical parameters generated by a single biofuel cell. However, stacked glucose biofuel cells have successfully demonstrated the amplification of electrical parameters at the expense of bulky circuit. Charge pump circuit possesses a potential solution to the before-mentioned problem. Internal structure of the s882Z series charge pump IC is shown in Figure 20C. It takes an input power of 0.3 V or higher to trigger the oscillation circuit

which gives a clock signal output that drives the charge pump circuit. Power from V_{IN} pin is converted to step up electric power in the charge pump circuit. This electric power is gradually charged up to the startup capacitor C_{POUT} pin, and its voltage rises gradually. When the C_{POUT} voltage reaches the discharge start voltage (V_{CPOUT1}) which is 1.8 V, the output signal of the comparator (COMP1) changes from high level to low, which enables the discharge control switch M_1. As a result, the stepped up electric power to C_{POUT} is discharged from the OUT pin. When C_{POUT} voltage drops to discharge stop voltage (V_{CPOUT2}), which is 1.2 V, M_1 switches off and the discharge is stopped. When the V_M pin voltage (V_{VM}) reaches or exceeds the shutdown voltage (VOFF), the output signal (EN−) of the comparator (COMP2) changes from low level to high. As a result, the oscillation circuit stops operation and the shutdown state is entered. If V_{VM} does not reach the shutdown voltage, the stepped-up power from the charge pump circuit is recharged to C_{POUT}. Thus, charging and discharging can be observed via the output capacitor and the voltage toggles between 1.8 V and 1.2 V. Thereby enabling the capacitor to be used as a transducer to sense various glucose concentrations, where the frequency of charge and discharge was monitored.

5.2 Results and discussion

For indicating glucose concentration, the charging/discharging frequency of the 0.1 μF capacitor can be controlled by the performance of the glucose biofuel cell used to charge the capacitor via the charge pump IC. Once the capacitor is fully charged, the charge pump IC discharges the capacitor until the potential reaches 1.2 V. This charging/discharging of the capacitor continues as long as the glucose biofuel cell continues to produce power and is observed to be directly proportional to the biocatalytic reaction at the bioanode. Thus, by monitoring the charging frequency of the capacitor, the glucose analyte concentration can be determined. Triplicate testing

of the charging frequency to various glucose concentrations yielded a dynamic linear range of 0.1–35 mM glucose with the following regression equation (n = 14, $r^2 = 0.995$):

$$Cell\ response\ \left(\mu\frac{W}{cm^2}\right) = 1.3128\ (glucose)[mM] + 8.4841\ (\mu\frac{W}{cm^2}) \quad \text{..... (17)}$$

Figure 21A shows that the average frequency increased linearly with increasing glucose concentration. This indicates that the present SPGS system can sense the changes in glucose levels from hypoglycemic (0.5 mM) to hyperglycemic (20 mM) conditions. A wider linear dynamic range was achieved with this SPGS system and was found to exceed those previously reported [69]. The frequency of charging the capacitor was stable for 1 week, following which the power density dropped by 3% after a week of operation separately in both 10 mM and 20 mM glucose. The overall drop in the frequency was 15.38% and 11.76% over a period of 63 days of operation in 10 mM and 20 mM glucose, respectively (Figure 21B). The stability observed here supersedes the stability of the biofuel cell powering contact lens [114], which was reduced by 80% within the initial 4 h of operation.

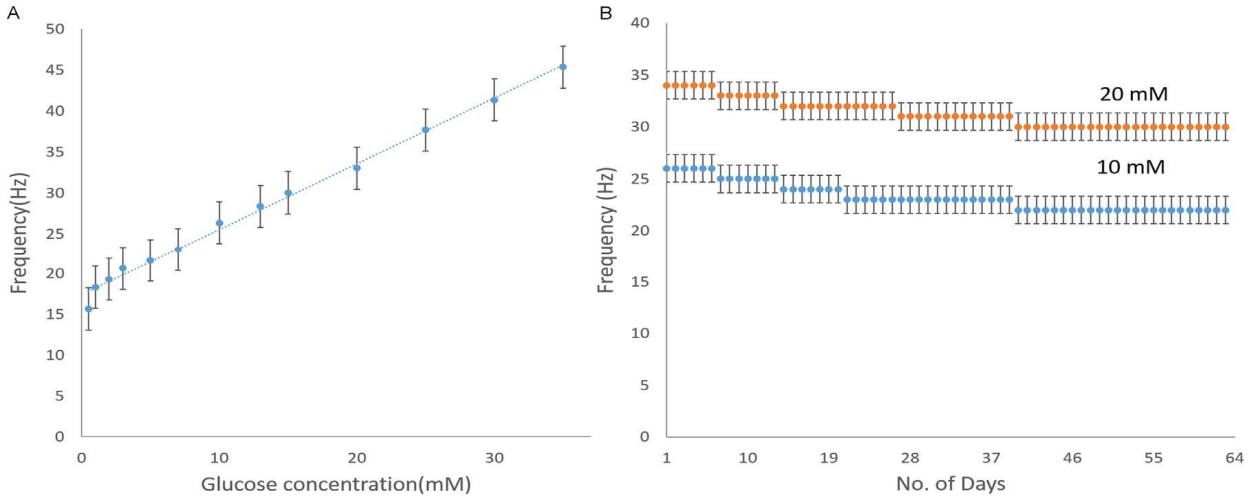

Figure 21. A) Calibration curve of SPGS response to glucose analyte and (B) 63-day stability profile in the presence of 10 mM and 20 mM glucose (37 °C, pH 7; error bars indicated the RSD).

The SPGS system was also characterized under various pH and temperature conditions in the presence of 10 mM glucose and 20 mM glucose solution. The temperature-dependent profile in response to 10 mM and 20 mM glucose for the present SPGS is seen in Figure 22A with a stable working temperature range of 35 – 40 °C. The pH dependent profile in response to 10 mM and 20 mM glucose for the present SPGS are seen in Figure 22B with a stable optimal working pH of 7.

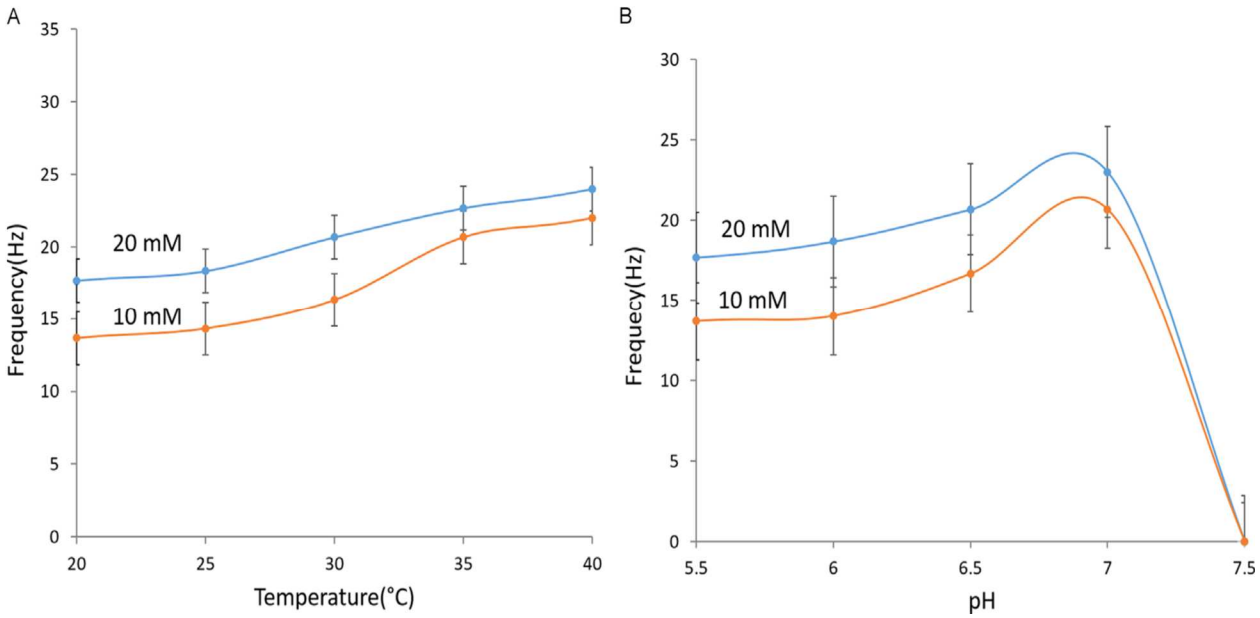

Figure 22. (A) Temperature and (B) pH response of the present SPGS in response to 10 mM glucose (orange dots) and 20 mM glucose (blue dots).

The charging/discharging frequency of capacitor steadily improved with increasing pH and peaked at pH 7 at which both PQQ-GDH and laccase enzymes are still active. Importantly, laccase from Trametes versicolor exhibits optimum biocatalytic activity at pH 5.5–6.0, and its activity is reduced at neutral pH. Therefore, beyond pH 7, laccase becomes inactive and as a result little or no power is generated to supply the present SPGS system. Overall, the activity of the present SPGS system in the presence of 20 mM glucose solution retains greater than 91% activity over the entire 63 days of investigation when compared to the SPGS system operating in 10 mM glucose solution, which retained 88.5% of its activity over the 63-day period. The overall system was active over a period of 96 days in 20mM glucose solution and 74 days in 10mM glucose solution respectively, as seen in Figure 23.

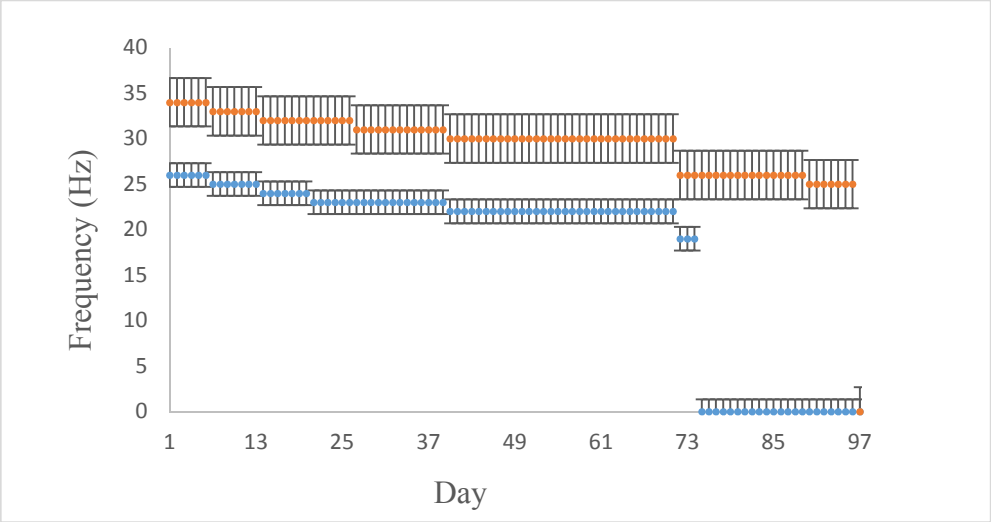

Figure 23. 96-day stability profile in the presence of 180 mg/dL (blue) and 360 mg/dL (orange) Glucose (37 °C, pH 7; error bars indicated the RSD).

The SPGS system exhibited an extended stability in 20 mM glucose concentration when compared to operating in10 mM glucose concentration. Once the voltage dropped below 300 mV, which was the lower limit for charge pump to operate, it no longer amplified the voltage and, subsequently, failed to charge the capacitor. We have successfully demonstrated a self-powered biosensing microsystem comprising of a glucose biofuel cell powering unit and a sensing unit consisting of a charge pump circuit and a capacitor functioning as transducing element. The system operated stably over a period of over 3 months in neutral pH at 37 °C.

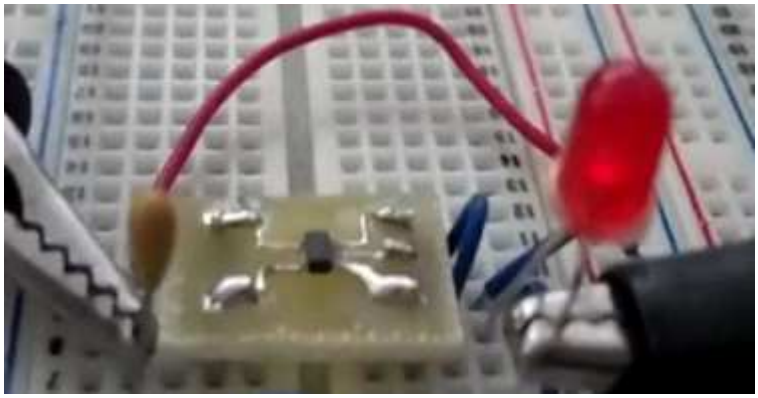

Figure 24. A charge pump circuit used to light LED

Additionally, the biofuel cell produced sufficient burst of power to drive the charge pump circuit to amplify the voltage and powered an LED. The charge pump produced a voltage of 1.8 V which was sufficient to power a LED with input voltage requirement of 1.5 V. Thus, we successfully demonstrated powering of a microelectronic device using a charge pump circuit.

Chapter 6: Biofuel cell prototype

Since enzymatic glucose biofuel cells are currently incapable of producing electrical power sufficient to power a device, various attempts were made to improve their performance. One such attempt involved connecting multiple biofuel cells in series that improved the voltage produced by the biofuel cell assembly. However, such arrangements make the assembly bulky and more complex. Moreover, if this assembly fails while operating in vivo, a surgery to replace the faulty stage is required imminently. Hence, instead of connecting multiple stages of biofuel cells, we focused on using various amplification circuits to improve the performance of our biofuel cell system along with making our single biofuel cell more robust.

Although the enzymatic glucose biofuel cell utilizes naturally-occurring enzymes which make it economical, easily renewable and clean; immobilization of enzymes on the substrate depends on various factors, such as the choice of electrodes with with high surface area, choice of enzymes to completely oxidize the fuel, electrode design and finally efficient charge transfer by the anode. Since different research groups design bioanode of different dimensions, it is difficult to compare their performance. Hence, the convention for reporting the electrical parameters of a biofuel cell is to calculate the current and power generated as density values in order to enable comparison of biofuel cells. Buckypaper electrode has been commonly used as the electrode material to immobilize enzymes. Buckypaper consist of mesh network of multi-walled carbon nanotubes, which improves the active surface area for enzyme immobilization. Carbon nanotubes (CNTs) are broadly classified into single walled and multi-walled carbon nanotubes. A single walled CNT consist of a single graphite sheet wrapped into a cylindrical sheet, whereas a multi-walled CNT comprises of array of single walled CNT concentrically nested like rings. CNTs can be further classified into metallic or semiconducting CNT based on the sheet direction about which the

graphite sheet is rolled to form a nanotube cylinder [115]. These graphene sheet wrapping is represented by a pair of indices (n, m) [116]. Indices (n, m) represent unit vectors along two directions in honeycomb lattice structure of graphene. If n = m, the nanotube is armchair type. However, if n – m = 3K (K being a non-negative integer), the nanotube is zig-zag type and rest all are chiral type. Armchair type nanotubes are always metallic, zig-zag type nanotubes that satisfy the above criteria are semiconductor with tiny band gap. Semiconductor CNTs band gap is inversely proportional to the diameter of the nanotube. The electronic properties of MWCNTs are similar to SWCNTs due to a weak coupling between the cylinders. Electronic transport between the MWCNTs occur without scattering over long lengths, which enables them to carry higher current densities without heat loss. Thus, buckypaper comprising of MWCNTs exhibits excellent electrical conductivity and thermal stability as high as 105.82 $(mho.cm)^{-1}$ and 331 $W.m^{-1}. K^{-1}$ along with biocompatibility [117]. The two proposed models to describe the structure of MWCNTs are the 'Russian Doll model' and the 'Parchment model'. In Russian model, the sheets of graphene are arranged in concentric cylinders, while in the Parchment model, a single sheet of graphene is rolled around itself. The Russian doll structure is observed more commonly. Due to the advantages of buckypaper over other metallic and non-metallic substrates, it has been commonly used to immobilize enzymes. In our research, we use buckypaper material with metallic bulk property. Buckypaper is fragile and tears easily if not handled properly and its probability to tear increases since the bioelectrodes are stored moist environment for most of the time. Hence, a novel design was implemented for the Buckypaper electrodes which improves its rigidity and provides a means for better handling mechanism.

6.1 Electrode preparation

Two 5 mm x 5 mm Buckypaper squares were carefully cut, followed by another Buckypaper strip which was 1 mm x 5 mm. A 2-cm long tungsten wire was cut and then sandwiched between the Buckypaper squares and strip and glued using Polyimide (PI) 2611. Also, all but the bottom edge of the Buckypaper was coated with PI 2611 to give it rigidity. It was then cured in a convection oven at 150 °C for 1 hour. Following which, PI 2611 was used to coat all the edges except the bottom edge on the back of the Buckypaper electrode and cured again at 150 °C for 1 hour in a convection oven.

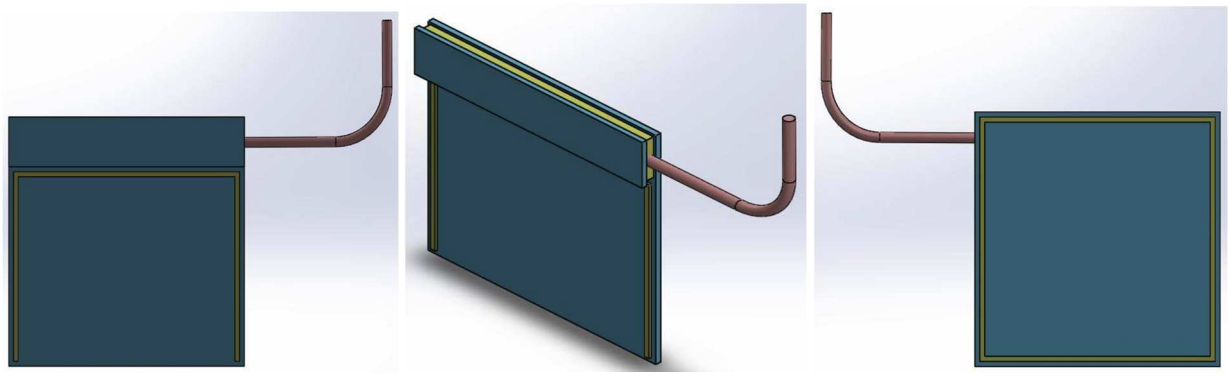

Figure 25. Buckypaper electrodes designed in SolidWorks. A) Front view B) Top View C) Back view.

Figure 25 shows three-dimensional views of the Buckypaper electrodes drawn using SolidWorks. The electrode designed in the above procedure yielded an active surface area of 0.04 cm^2 for the immobilization of enzymes.

6.2 Surface immobilization

Our previous work involving enzymatic glucose biofuel cell with PQQ-GDH modified bioanode and laccase modified biocathode allowed us to characterize and demonstrate a self-powering biosensing system at a pH 7 and 37 °C temperature. However, such a system involving laccase biocathode fails to operate in vivo as the optimal working pH of laccase biocathode is 5.5 – 6.

Hence, to enable our system to operate at physiological conditions (pH 7.4 and 37 °C), bilirubin oxidase enzyme was chosen at the biocathode. Both laccase and bilirubin oxidase enzymes are multi-copper enzymes with multiple active centers. However, the type II Cu center which is active in bilirubin oxidase allows for its optimal pH to be 7.4. Laccase does not have an active type II Cu center, which significantly causes its optimal pH to be at a low value. These electrodes were modified with respective enzyme solutions to form the bioelectrodes. The stepwise procedure to immobilize enzymes is explained elsewhere [113]. Instead of laccase as biocathode enzyme, buckypaper was modified with bilirubin oxidase to form biocathode as shown in Figure 26.

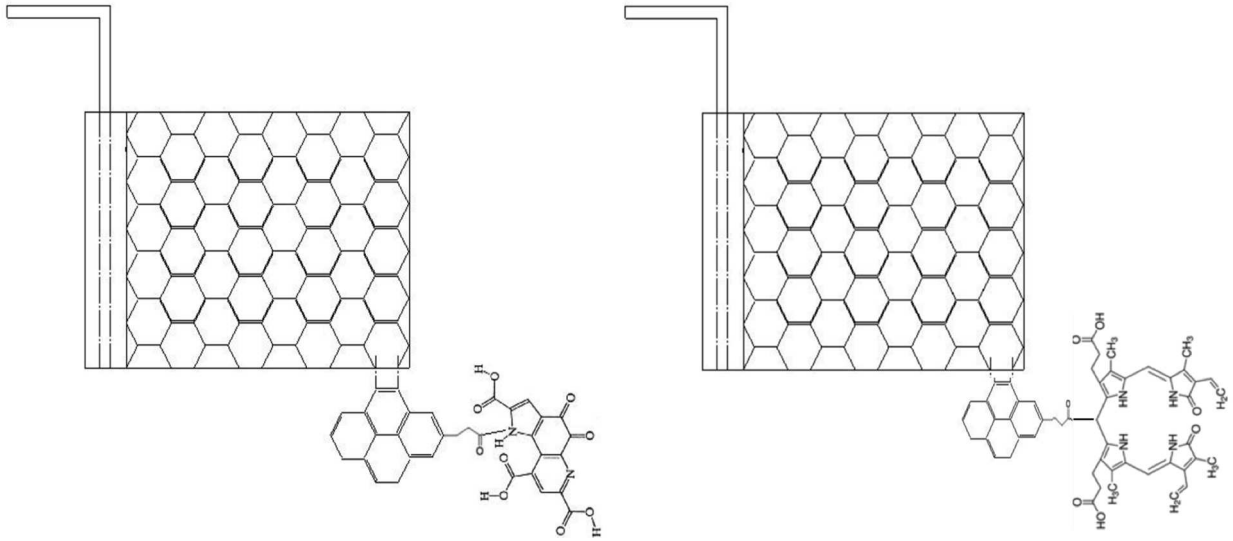

Figure 26. Surface modification of Buckypaper with A) PQQ-GDH B) BODx using Solid Works.

Since the enzymes cannot directly attach to the Buckypaper, PBSE crosslinker was used to link the amino group from the enzymes to the Buckypaper via a substitution reaction. The bioelectrodes were further coated with 2 µL Nafion® to avoid any leeching of the enzymes.

6.3 Prototype

The total area of the biofuel assembly using the above bioelectrodes was 0.5 cm^2, which was twice that of the unmodified Buckypaper squares. To reduce the overall dimensions, a filter paper was sandwiched between the bioelectrodes to serve as an insulator. Silicon epoxy, an insulating glue, was applied to the back end edges of the Buckypaper, except the bottom edge. A 5 mm x 5 mm filter paper was then placed on the epoxy end of the anode and was let to dry at room temperature. Once the bond between the filter paper and the anode was established, silicon epoxy was applied on the edges of the filter paper and the back end of the biocathode was placed on top of the filter paper and we again let it sit at room temperature to dry. This procedure resulted in the biofuel cell prototype as shown in Figure 27.

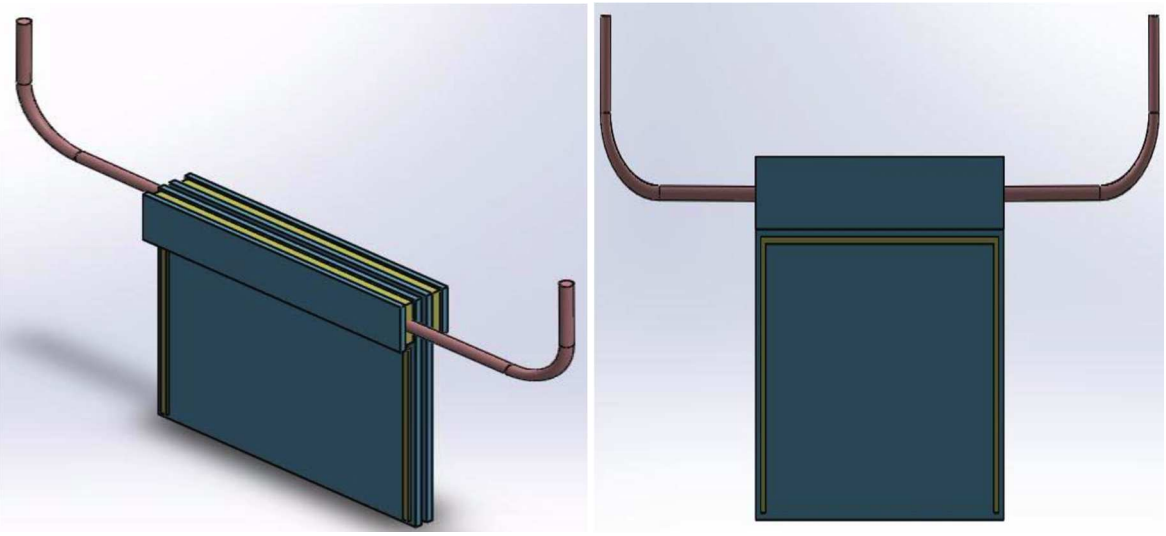

Figure 27. Solid Works schematic of the buckypaper prototype with bioelectrodes separated by a filter paper. A) Top view B) Front view.

The overall dimension of the above Buckypaper prototype sample was 0.5 cm x 0.5 cm, whereas the active surface region was 0.04 cm^2. The separation between the bioelectrodes is a tradeoff between the minimum separation to avoid short circuit and the bulkiness of the overall device. The

separation between the bioelectrodes was optimized at 0.8 mm. The biofuel cell prototype was then used to characterize the biofuel cell assembly in various glucose concentration solutions.

6.4 Results and discussion

6.4.1 Biofuel cell polarization characteristics

The novel electrode design allowed for better handling of the Buckypaper electrode and protected it from tearing during experiments. The conductive Buckypaper material comprising of a mesh network of multi-walled carbon nanotubes provided a large surface area for the enzyme immobilization. The biofuel cell comprising PQQ-GDH and bilirubin oxidase (BOD_X) enzymes at anode and cathode, respectively allowed their characterization at physiological conditions (pH 7.4 and 37 °C). The biofuel cell was characterized in various glucose concentrations, and the open circuit voltage along with short circuit current density and peak power density were calculated in their respective glucose solutions. All the experiments were performed in triplicate in standard glucose concentration solutions in a dynamic environment where a fresh supply of glucose was continuously provided.

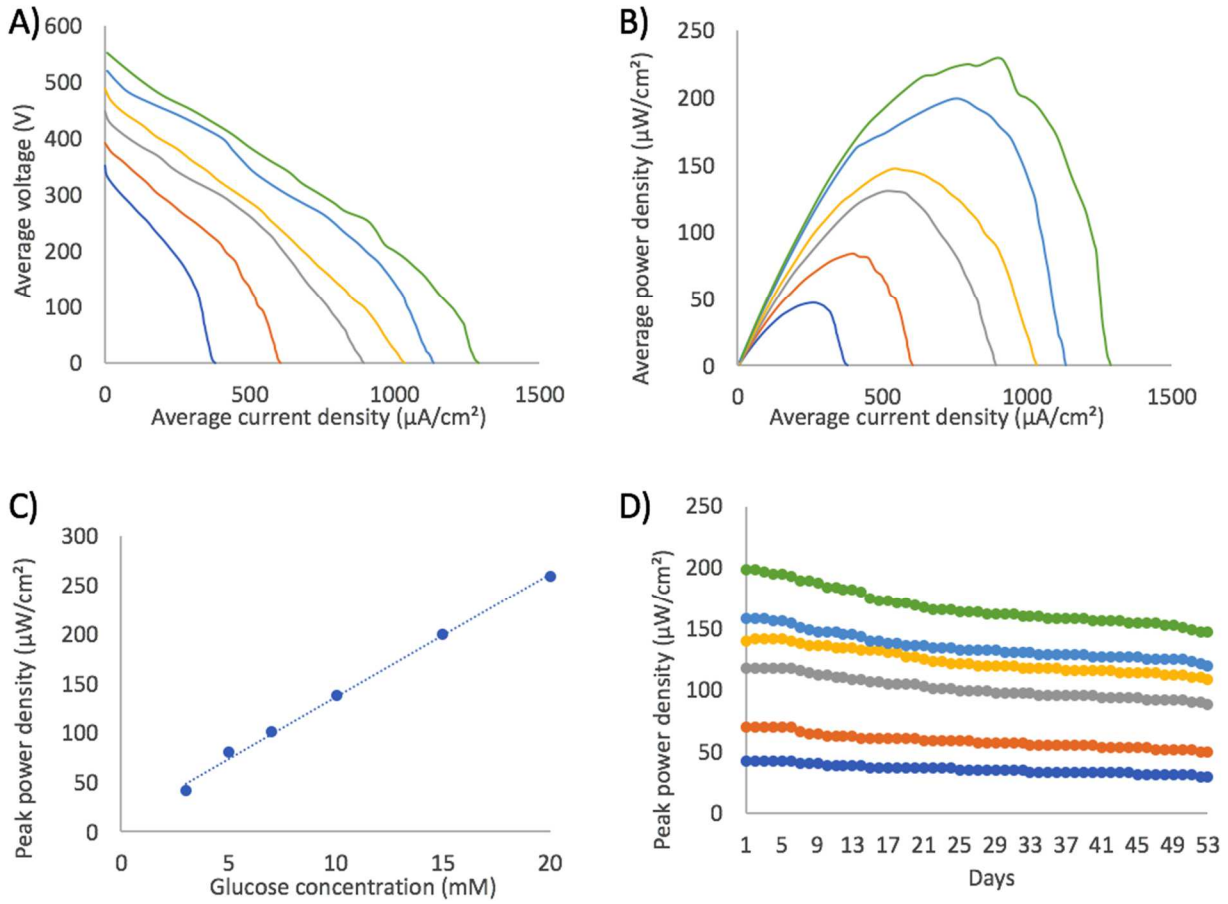

Figure 28. Glucose biofuel cell characterization. A) Polarization curves B) Corresponding power curves of glucose biofuel cell at varying glucose concentrations prepared in 100 mM PBS (37 °C and pH 7.4). C) Calibration curve of glucose biofuel cell response to glucose analytes. D) 53-day stability profile in the presence of various glucose concentration analytes (37 °C and pH 7.4).

The characterization of glucose biofuel cell was performed under physiological conditions in various glucose concentrations by measuring the current and voltage across variable load resistor. Further, the current density and the power density was calculated using the geometrical surface area of the active region of the anode (0.04 cm^2). Figure 28A shows the polarization curves of the biofuel cell, wherein both the open-circuit voltage and the short-circuit current density were observed to be increasing with an increase in glucose concentration due to the presence of more glucose molecules at higher concentration. The peak electrical parameters were obtained in the

presence of air-saturated 20 mM glucose solution (37 °C and pH 7.4) with an open circuit voltage and short circuit current density along with a peak power density of 552.37 mV, 1.285 mA/cm^2 and 0.225 mW/cm^2 at a cell voltage of 285.46 mV, respectively in the dynamic environment. These results are comparable or superior to those previously reported [96 – 98, 111]. At physiological concentrations (5 mM glucose at pH 7.4 and 37 °C), the glucose biofuel cell revealed an open circuit voltage of 391.36 mV and a peak power density of 84.64 μW/cm^2 at a cell voltage of 214.3 mV as shown in Figure 28B. Triplicate testing in a dynamic environment yielded a linear dynamic range from 3 – 20 mM glucose as shown in Figure 28C with the flowing regression equation (R^2 = 0.997):

$$\text{Cell response } \left(\frac{\mu W}{cm^2}\right) = 12.47\ [\text{glucose}](\text{mM}) + 12.38\ \left(\frac{\mu W}{cm^2}\right) \quad \text{(17)}$$

As observed from Figure 28C, the peak power density of the biofuel cell increased with an increase in glucose concentration from 3 – 20 mM glucose. The biofuel cell stability was further investigated by monitoring its electrical parameters in various glucose concentrations at their respective load resistance over a period of 53 days. Figure 28D shows a constant discharge curve acquired over 53 days. An initial maximum drop in peak power density was observed in the presence of 3 mM glucose solution, which was 5.25%, whereas a minimal drop of 0.56% was observed in the presence of 10 mM glucose solution at the end of first week. Thereupon, a constant decrease in electrical parameters was observed for subsequent days due to a slow degradation of the enzymes with regular testing of the biofuel cell. At the end of the 53rd day, peak drop in the performance of the glucose biofuel cell was observed in the presence of 3 mM, which was 31.75% while a minimum drop was observed in the presence of 10 mM which was 21.92%. The other

glucose concentration also recorded drops in the power density performance, which was 26 ± 6%. Although the electrical parameters decreased with time, the sheer ability of the biofuel cell to perform continuously over 53-day period was attributed to the use of Nafion coating which prevented the enzymes from leeching out, thus improving the life of the glucose biofuel cell. The above recorded stability is better than those previously reported [77, 107]. The above results were then compared to our previous work involving biofuel cell characterized in a static environment [118]. The electrical density values observed in a dynamic environment were higher than those observed in static environment due to the continuous fresh supply of glucose in the former case. The open circuit voltage was comparable; the peak current density in 20 mM glucose solution dynamic environment at physiological conditions was more than twice than observed in a static environment in 20 mM glucose solution at physiological conditions. At the same time, there was a 150% increase in peak power density in a dynamic environment at physiological conditions in 20 mM glucose solution compared to the static environment at same conditions. The huge boost in the electrical parameters was attributed to continuous fresh glucose supply. At physiological conditions (5 mM glucose at pH 7.4 and 37 °C), the open circuit voltage and the short circuit current density in a dynamic environment was observed to increase 24.52% and 78.63% respectively, compared to the static environment. Also, the peak power density increased 131% going from static to dynamic environment. Thus, the performance of the glucose biofuel cell improved tremendously in a dynamic environment at physiological conditions.

6.4.2 Self-powered biosensing system characterization

A single glucose biofuel cell has the potential to replace batteries as a power source, but to fulfill this primary goal, the electrical parameters from a single biofuel cell need to be amplified, as it is neither sufficient to sense glucose nor power any microelectronic devices. Past research has shown that the electrical parameters can be improved by stacking multiple biofuel cells in series or parallel, depending on the applications. However, it makes the overall design bulky and increases the circuit complexity [111] and due to the implantation constraints, several research groups have started using charge pump to amplify the electrical parameters from a single biofuel cell. In this work, we demonstrate the amplification of the electrical parameters of a single glucose biofuel cell by using the charge pump IC to enable simultaneous power amplification and glucose sensing.

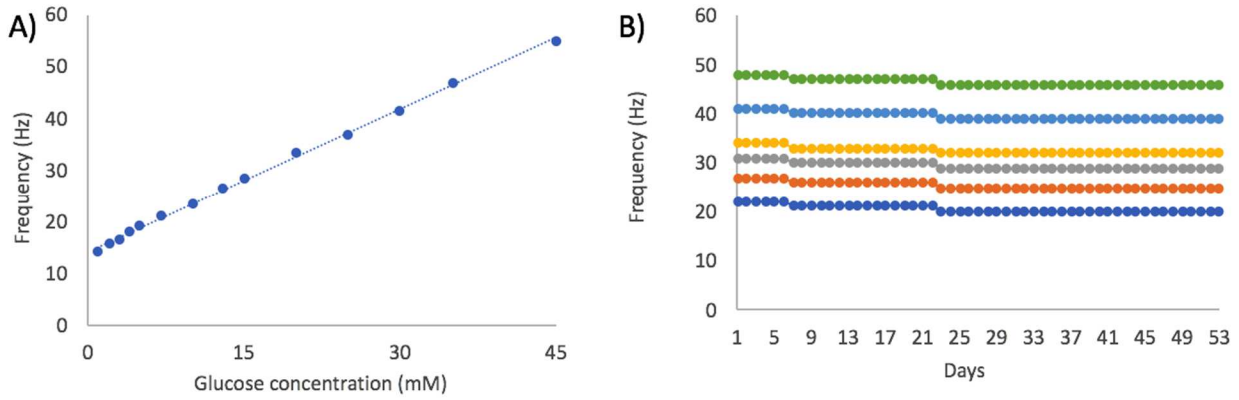

Figure 29. A) Calibration curve of glucose sensing system in various glucose concentration at physiological conditions across 0.1 µF capacitor in dynamic environment. B) Stability profile of glucose sensing system over a 53-day period at physiological conditions in dynamic environment.

The charge pump takes in an input voltage from the biofuel cell and amplifies it to 1.8 V per the mechanism explained in Figure 1. The burst of power generated by the charge pump was supplied to power a portable electronic device. The bioelectricity produced by the biofuel cell to be specific anode increased with increase in glucose concentration, which resulted in an increase in charge

and discharge across the capacitor. Thus, the varying charge cycles were a measure of the glucose sensed by the circuit. The triplicate testing of the charge cycle at various glucose concentration solutions (pH 7.4 and 37 °C) in dynamic environment yielded a dynamic range from 1 – 45 mM with a flowing regression equation ($R^2 = 0.9981$):

$$\text{Frequency response (Hz)} = 0.9252\ [\text{glucose}](\text{mM}) + 14.113\ (\text{Hz}) \quad (18)$$

The above range covers both the hyperglycemic (20 mM) and hypoglycemic (1 mM) states, including the normal glucose levels, and would be useful in detecting blood glucose levels. The extended linear dynamic range was found to be more than previously reported [79] and as shown in Figure 29Athe sensitivity was calculated to be 23.13 Hz/cm^2.mM., which was more than our previously reported work. The stability profile of the charge cycle frequency was monitored over 53 days as shown in Figure 29B. At the end of first week, a peak drop in the frequency response was observed in the presence of 3 mM, which was 4.54%, corresponding to the peak drop in peak power density. The least drop was observed in 20 mM glucose solution which was 2.08%. Further, the 53-day profile retained an over 90% response with both peak and minimum drop observed in 3 mM (9.09%) and 20 mM (4.17%) respectively. The drop in the performance was due to the drop in electrical parameters produced by the biofuel cell due to the degradation in the enzymes over a period.

6.4.3 pH and temperature stability profile

The above system was also characterized under various pH and temperature conditions in the presence of the 20 mM glucose solution, and the corresponding profile was determined. It is essential to determine the performance of our system under various pH and temperature conditions.

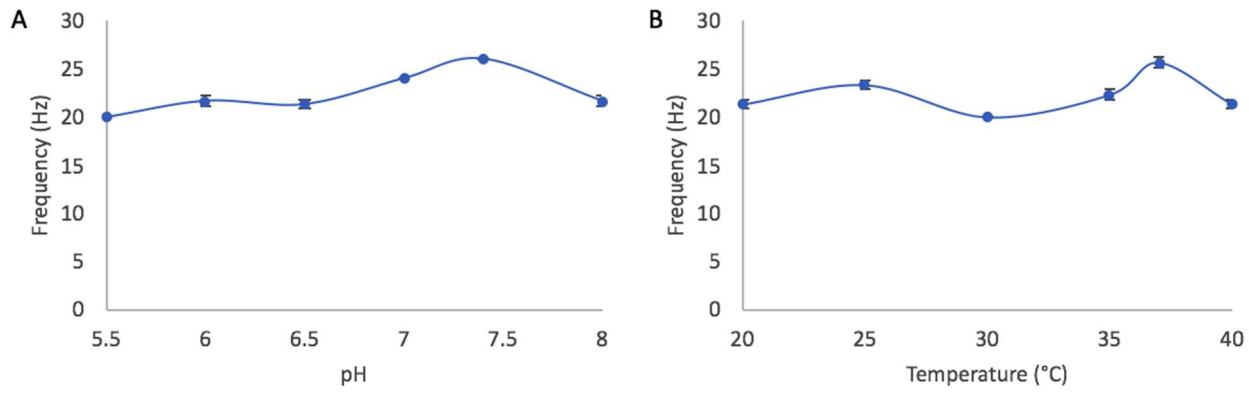

Figure 30. A) pH B) Temperature profile of the self-powering system in response to 20 mM glucose solution.

The pH-dependent profile of the system is shown in Figure 30A, where the response of the system was recorded under various pH levels and compared to the system's original performance shown in Figure 30A. It was observed that the system functions optimally at physiological pH of 7.4. Moreover, the biofuel cell comprising bilirubin oxidase cathodic enzyme performs better than the biofuel cell system with laccase cathodic enzyme, which fails to operate at physiological pH. This is very important from an in vivo systems point of view. Figure 30B shows a temperature profile of our system at variable temperatures. Our system performs optimally at 37 °C, which is the in vivo optimal temperature. Overall, our system performs optimally well at physiological conditions (pH 7.4 at 37 °C) and retains over 90% of the activity at the end of the 53rd day.

6.4.4 Interference testing

One of the essential qualities of a glucose sensing system is that it needs to be highly selective. When implanted in vivo, it is subjected to interference by various interfering species such as ascorbic acid, uric acid and acetaminophen and various competing species such as fructose, maltose and galactose [119 - 121]. The physiological glucose concentration in serum is ~3-8 mM, whereas the physiological concentration of these interfering and competing species is no more than 0.2 mM [122]. We monitored the charging and discharging across the capacitor for these interfering and competing species and compared the charge cycle with the unadulterated glucose solution. To confirm the results, we performed two sets of experiments to measure the effect of these species on the overall performance of the system at their physiological concentrations. Figure 31A & 31C shows the frequency of charge cycle when glucose was mixed with interfering and competing species. For this set of experiments, a fresh 5 mM glucose solution was used every time to mix corresponding species. Figure 31B & 31D shows the effect of the competing species and interfering species on the overall performance of the system individually. After every set of experiments, a fresh glucose solution was used to test the performance of the system.

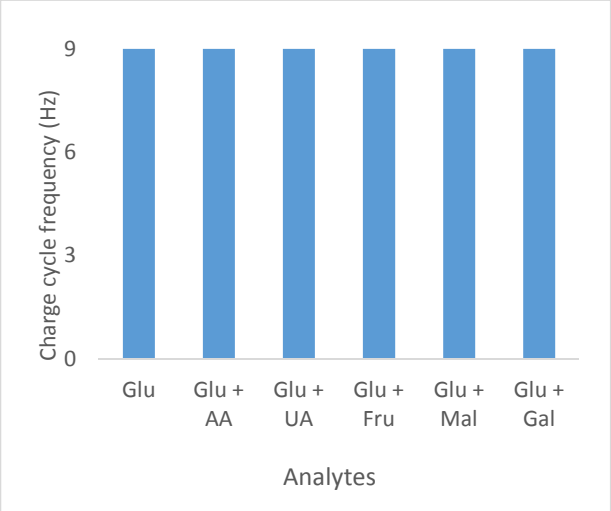

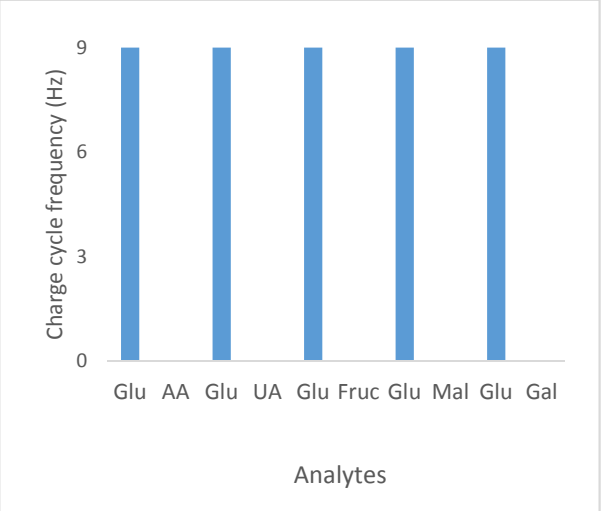

Species (5mM Glucose +)	Frequency (Hz)	Error % w.r.t 5mM glucose
-	9	0
0.2 mM ascorbic acid	9	0
0.2 mM Uric acid	9	0
0.2 mM Fructose	9	0
0.1 mM Maltose	9	0
0.1 mM Galactose	9	0

Analyte	Frequency (Hz)	Error %
5 mM Glucose	9	-
0.2 mM Ascorbic acid	0	0
5 mM Glucose	9	-
0.2 mM Uric acid	0	0
5 mM Glucose	9	-
0.2 mM Fructose	9	0
5 mM Glucose	9	-
0.1 mM Maltose	9	0
5 mM Glucose	9	-
0.1 mM Galactose	9	0

Figure 31. Interference testing. A) 5 mM glucose adulterated with 0.2 mM interfering analyte. B) 5 mM glucose tested between each 0.2 mM analyte by itself. C, D) Corresponding tabular values.

From the above figure, there was no charge/discharge response introduced by the interfering species, such as ascorbic acid and uric acid. This was because it interferes only at +700 mV, at which hydrogen peroxide breaks down. Since a single biofuel cell is incapable of producing such high potential, these interfering species fail to have any impact on the overall system performance. Competing species on the other hand such as maltose, fructose and galactose failed to produce

sufficient voltage to drive the charge pump circuit. Thus, there is no charge cycle observed across the capacitor. Thus, both competing and interfering species at their physiological concentration have no effect on the performance of the system, thus, our system exhibits excellent selectivity.

6.5 Simultaneous glucose sensing and powering of glucometer device

Although a charge pump circuit amplifies electrical parameters from a single biofuel cell, it supplies a burst of power which is inconvenient to power any micro-electronic devices. Also, since the output from the charge pump circuit ranges between 1.2 V and 1.8 V, finding a microelectronic device that can transmit data wirelessly with a burst supply of power is very difficult. Therefore, there is a need for a steady DC supply, thus, a step-up DC converter circuit was used, as shown in Figure 32

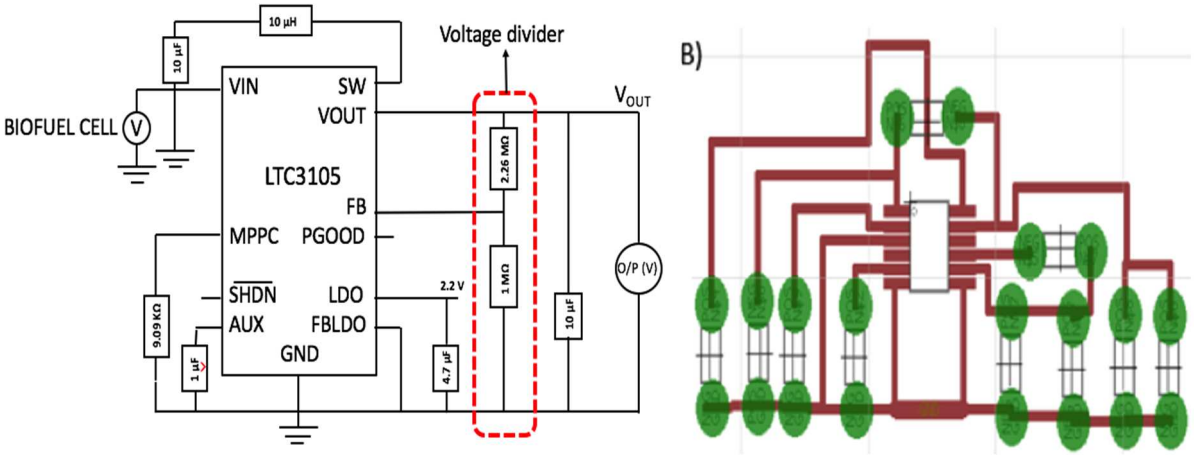

Figure 32. A) Step-up DC converter circuit configuration consisting of voltage divider circuit. B) Board schematic of step-up DC converter circuit implemented in eagle PCB software.

This device needed an initial trigger of 1.4 V, which was easily supplied by the charge pump circuit. Following which, step up DC convertor circuit could operate at a voltage as low as 225 mV which was easily fulfilled by a single glucose biofuel cell thereby, conserving the energy. The

output of the step-up DC convertor circuit was a steady DC voltage which was then applied to various digital devices, such as a digital thermometer and a digital glucometer device.

This circuit consists of a 3 mm x 3 mm x 0.75 mm IC and an output capacitor to store the charge developed by the IC. It also consists of a voltage divider circuit which is used to amplify the output voltage based on the requirement as shown in the Figure 32A. Theoretically, output DC voltage was calculated using the equation below:

$$V_{OUT} = 1.004 * ((\frac{R_2}{R_1}) + 1) \quad \text{.....(19)}$$

PSpice software was used to optimize the resistor value such that the output DC voltage obtained was 3.3 V. Under ideal conditions and disregarding the triggering voltage, the minimum input voltage required to achieve an output voltage of 3.3 V was observed to be 0.52 V. Further, different resistors were connected in the voltage divider circuit to observe the change in output voltages.

Table II. Percentage error in theoretical and measured DC output voltage produced by step-up convertor

Ω Ratio	Theoretical (V)	Measured (V)	Percentage error (%)
1.39	2.399	1.951	18.674
1.632	2.643	2.066	21.831
2.26	3.3	3.2	3.03

Table II shows some variation between the theoretical and practical output DC voltage values, which could be attributed to the energy loss in the form of heat at the orthogonal turns in the original PCB designs copper traces losses in the circuits. Moreover, signal losses could emerge

due to long distance connection between the IC and the output measuring pins. Various output voltages such as 1.951 V and 3.259 V observed by varying the voltage divider resistances were sufficient to drive digital thermometer and digital glucometer respectively.

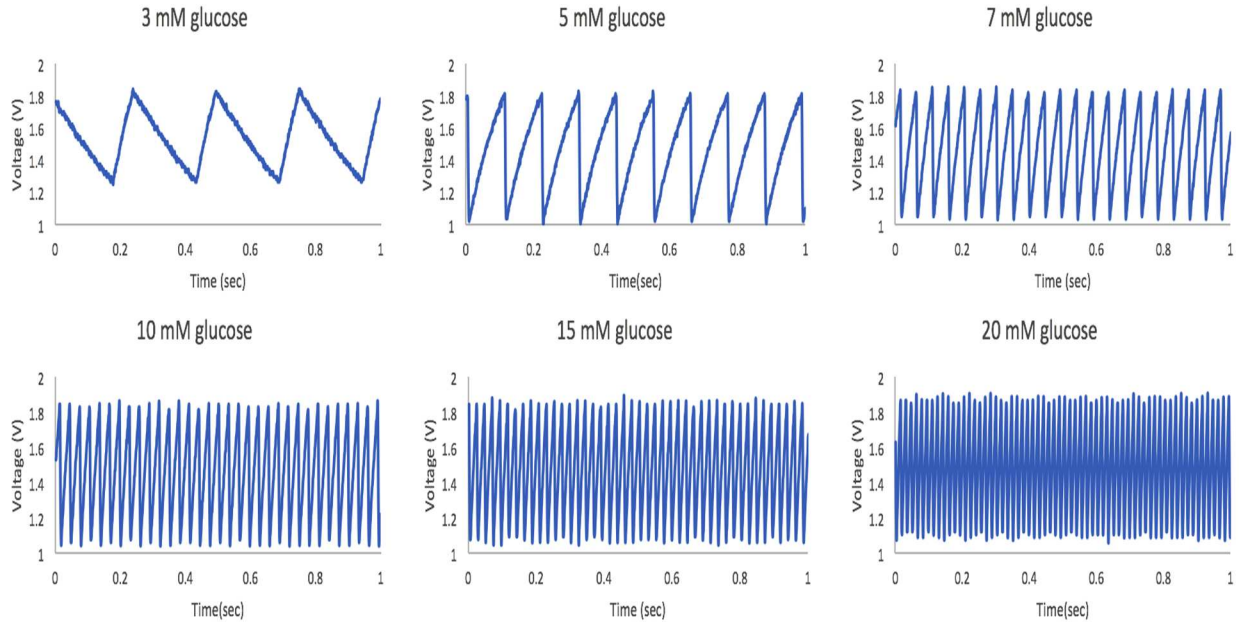

Concentration (mM)	Frequency (Hz)
3	3
5	9
7	20
10	29
15	43
20	63

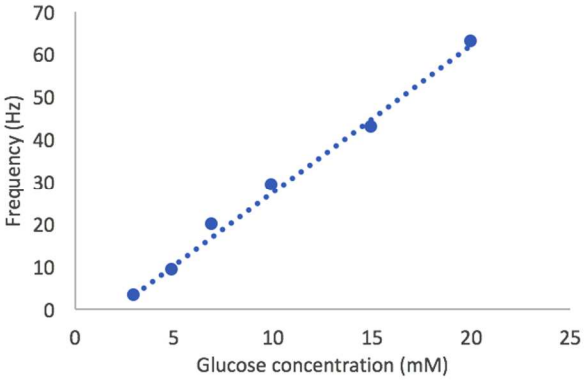

Figure 33. A) Charge cycle frequency of 0.1 µF capacitor in various glucose concentration (3 – 20 mM) at pH 7.4 and 37 ℃. B) Tabular representation of the charge cycle frequencies corresponding to respective glucose concentration. C) A calibration curve of the entire system operating at physiological conditions (pH 7.4 and 37 °C) when simultaneously sensing glucose and powering a glucometer device.

Figure 33A shows the frequency of the charge cycle corresponding to various glucose concentration while the system is simultaneously powering a digital glucometer. This system operates over a wide range of glucose concentration from 3 – 20 mM with a following regression equation ($R^2 = 0.9938$):

$$Frequency\ response\ (Hz) = 3.4567\ [glucose]\ (mM) + (-6.734)(Hz) \quad \text{(20)}$$

The calibration curve shown in Figure 33C yielded a sensitivity of 86.42 Hz/cm^2. mM., which was better than our previously published work [113, 118]. Therefore, this novel system is designed such that it can simultaneously sense glucose using a transducing element capacitor connected at the output of the charge pump circuit and power a digital device such as a digital thermometer and digital glucometer. The schematic of such a novel device is shown in Figure 34.

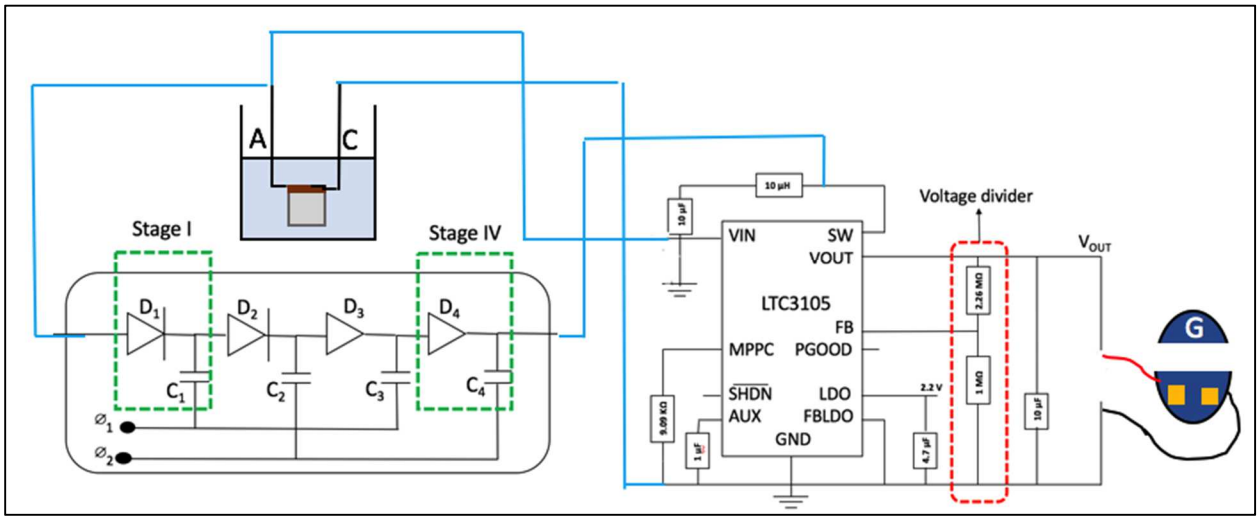

Figure 34. Simultaneous glucose sensing and powering of glucometer device.

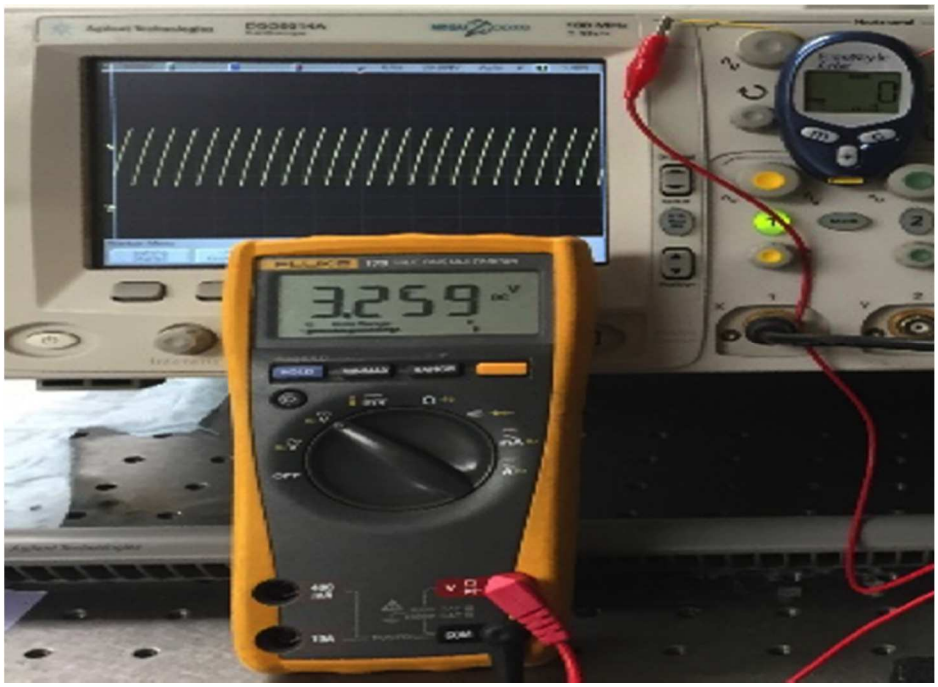

Figure 35. System showing simultaneous glucose sensing (oscilloscope reading) and powering of a glucometer in the presence of 7 mM glucose solution.

Figure 35. shows the simultaneous operation, in which the oscilloscope reading signifies the frequency of charge and discharge cycle that increases with increase in glucose concentration solution. Also, the figure shows a digital glucometer indicating a '0' on the display, which is powered by the voltage that is produced at the output of step-up DC converter circuit and is displayed on the multimeter screen. We observed that the overall system's performance improves when the system is fully functional with a microelectronic device being powered. Since the glucose-sensing was dependent on the power produced by the single glucose biofuel cell, we designed an experiment to determine whether the powering of microelectronic device has any effect on the sensing performance of the system. The device under test (DUT) was a digital glucometer manufactured by freeStyle Lite which requires a minimum voltage supply of 3 V. The

experiment was performed in various glucose concentrations ranging from 3 – 20 mM at physiological conditions in dynamic environment.

Glucose concentration (mM)	Glucometer device present (Hz)	Glucometer device absent (Hz)	Percentage error (%)
3	3	3	-
5	9	9	-
7	20	19	5
10	29	28	3.45
15	42	42	-
20	61	61	-

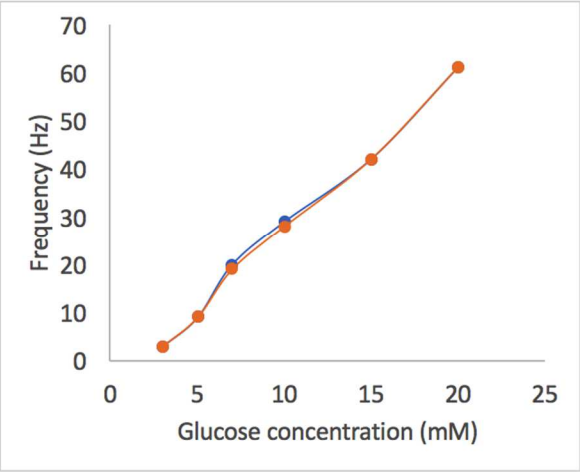

Figure 36. Frequency response of the device in the presence of glucometer device being powered (blue) and in the absence of glucometer device (orange) at physiological conditions in dynamic environment in various glucose concentrations.

Figure 36 shows the charge cycle frequency in various glucose concentrations at physiological conditions in the presence of the glucometer device being powered and in the absence of glucometer device being powered. Except for 7 mM and 10 mM glucose solutions, other concentrations exhibit an ideal response irrespective of the device being powered. Moreover, the slight variation observed in the presence of 7 mM and 10 mM can be rectified using a more robust algorithm and by running multiple test runs and averaging the observed frequencies. Overall, the performance of the system is not significantly affected by the simultaneous glucose sensing and powering of a digital glucometer device. This is a novel system and such simultaneous glucose sensing and powering has never been implemented before, to the best of our knowledge.

6.6 Biofuel cell operating in serum glucose

Further, in vivo implantations of such system is desired and highly important. However, blood consists of species other than glucose such as uric acid, ascorbic acid, fructose, maltose and galactose along with some minerals. Thus, it is of immense importance to test the performance of our glucose sensing system in the presence of these species. Researchers have demonstrated the functional biofuel cell as a power source in the presence of serum solution [123 - 126]. Here, we demonstrate the glucose sensor performance in serum.

We characterize the biofuel cell system in various serum solutions by performing the cyclic voltammetry that ascertains the presence of enzymes on the electrode surface. We further address the various losses occurring in the biofuel cell system by performing linear scan voltammetry (LSV) and calculate the percentage losses at various glucose concentrations. Polarization characteristics of the biofuel cells were determined as previously discussed and we demonstrate glucose sensing in serum by monitoring the charge/discharge frequency of the capacitor.

6.6.1 Results and Discussions

The presence of enzyme on the surface of the bioelectrodes was confirmed by performing cyclic voltammetry (CV) scans in the presence of standard buffered solution as well as serum at physiological conditions (pH 7.4 and 37 ºC). The direct electron transfer between the active sites of the enzyme and the buckypaper electrode was ascertained from the CV scans. The scans were monitored over a voltage range from -0.8 V to +0.8 V and back at a scan rate of 20 $mV.s^{-1}$.

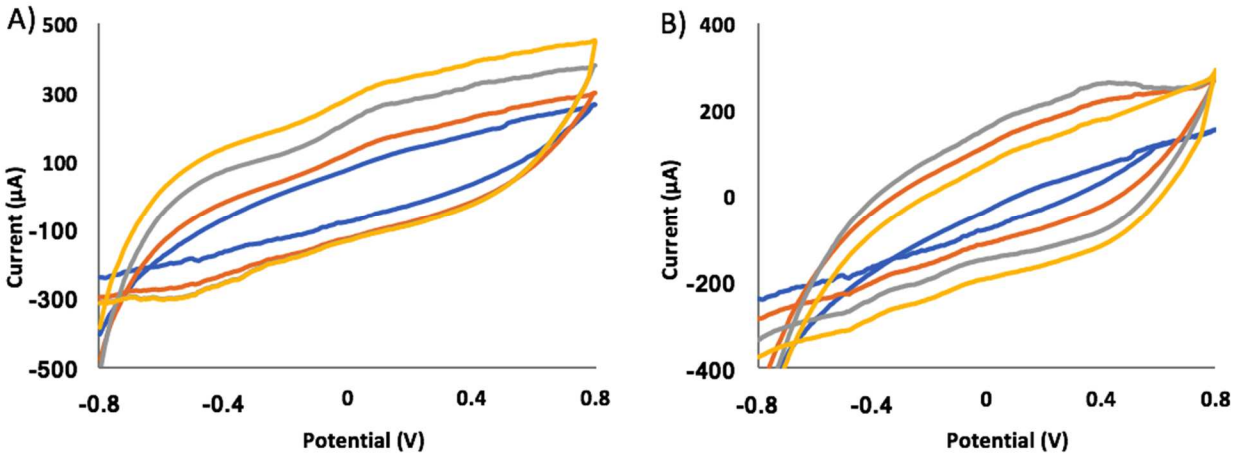

Figure 37. Cyclic voltammetry of A) bioanode B) biocathode performed at physiological conditions (pH 7.4 and 37 ºC) in the absence of glucose (blue) and in the presence of various serum glucose solution at 2.78 mM (orange), 5 mM serum glucose solution (gray) and 10 mM glucose solution (yellow) in air saturated environment.

Glucose oxidation by PQQ-GDH enzyme at the surface of the bioanode in the presence of serum is shown in Figure 37A. The bioanode does not show any peak in the presence of 100 mM PBS (pH 7.4) indicating the bioanode is non-responsive to the buffer. However, when the serum concentration was increased, a significant increase in peak current corresponding to glucose oxidation was observed at negative potential. The onset of the oxidation potential became more negative with an increase in glucose serum solution. The electro-oxidation potential of glucose fuel in the presence of 10 mM glucose serum solution was detected at an onset potential of -0.199 V vs Ag/AgCl. The more negative onset potential is desirable for better biofuel cell performance. Figure 37B. shows the CV scan for biocathode, where oxygen reduction occurs at the surface of the biocathode by bilirubin oxidase enzyme. With an increase in glucose concentration, more glucose molecules were present for redox reaction. As a result, the onset potential for oxygen reduction becomes more positive. The electro-reduction potential of oxygen in the presence of 10

mM serum glucose solution was detected at +0.399 V vs Ag/AgCl. The overall cell voltage of the biofuel cell is governed by the Nernst equation given by,

$$V_{CELL} = V_{CATHODE} - V_{ANODE} \quad \text{.....(21)}$$

According to the Nernst equation, the theoretical biofuel cell voltage was calculated to 0.598 V from the cyclic voltammetry scan in the presence of 10 mM glucose serum solution at physiological conditions. However, the experimentally calculated biofuel cell voltage was observed to be 0.479 V. The difference in the cell voltage was attributed to various losses occurring in the biofuel cell system which was further studied by performing linear scan voltammetry (LSV).

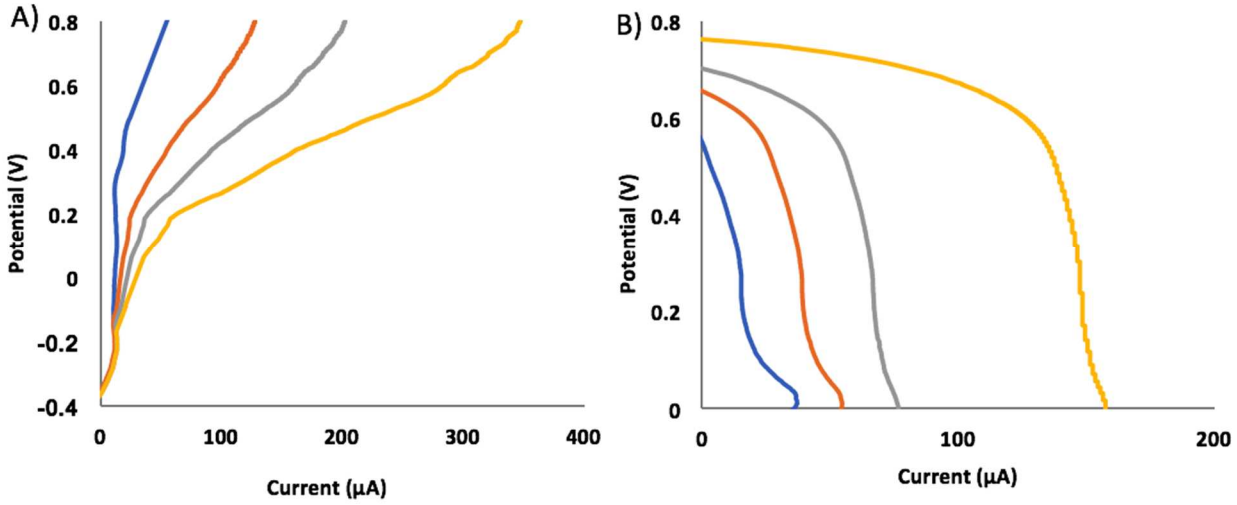

Figure 38. Linear scan voltammetry. A) Bioanode B) Biocathode performed at physiological conditions (pH 7.4 and 37 ºC) in the absence of glucose (blue) and in the presence of various serum glucose solution at 2.78 mM (orange), 5 mM serum glucose solution (gray) and 10 mM glucose solution (yellow) in air saturated environment.

Figure 38A shows LSV for bioanode in which, the ohmic losses become dominant beyond -0.2 V due to the resistance offered by the solution to the flow of electrons. Upon oxidation of glucose fuel, electrons are generated which flow towards the current collector. At higher glucose concentration, the solution becomes more conductive. The resistance offered to the electrons

decreases as the solution becomes more conductive. Thus, the biofuel cell overcomes the ohmic losses by producing more current at higher glucose concentration as seen from Figure 38A. Table 3 shows ohmic loss percentage in various serum solutions.

Table III. Percentage ohmic loss in biofuel cell at different glucose serum concentration

Serum glucose concentration (mM)	Theoretical voltage (mV)	Experimental Voltage (mV)	Ohmic loss percentage (%)
2.78	463	325.7	29.65
5	524	387.9	25.97
10	598	479.7	19.78

The increase in glucose concentration makes the solution more conductive and reduces ohmic losses as observed from Table 3. Oxygen reduction occurs at the surface of biocathode at +0.6 V. At such higher potentials, concentration losses become dominant and are caused due to saturation of oxygen gas molecules at the bioelectrodes surface. Due to the concentration losses, fresh oxygen molecules cease to reach the active region of the bioelectrode. By increasing the glucose concentration, more fuel is available for redox reaction. Figure 38B shows that the biocathode overcomes the concentration losses at higher glucose concentration and the onset of the reduction potential becomes more positive. The performance of glucose biofuel cell improves at higher glucose concentration by overcoming various losses occurring within the assembly.

The glucose biofuel cell was then characterized in vitro by measuring the voltage and the current values at varying the load. The current and power densities were calculated using the geometrical surface area of the bioanode which was 0.01 cm^2.

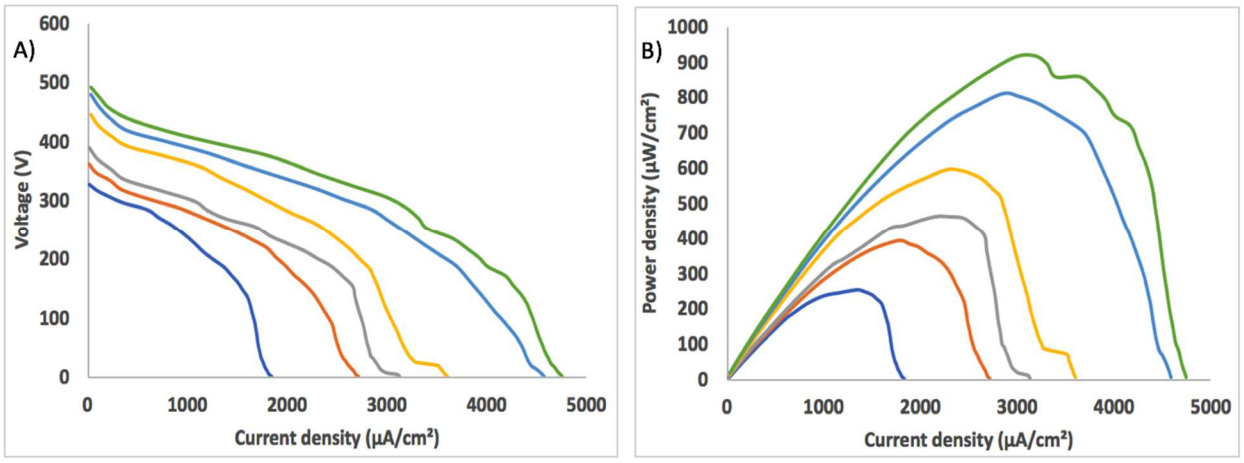

Figure 39. Glucose biofuel cell characterization. (A) Polarization curve and (B) corresponding power curves of glucose biofuel cell at varying serum glucose concentration from 2.78 mM to 11.11 mM (37 °C, pH 7).

Fig. 39A shows the polarization curve of the cell, wherein the electrical parameters produced by a single glucose biofuel cell such as open circuit voltage and the short circuit current increased with increasing glucose concentrations due to the presence of more glucose molecules at higher glucose serum concentration. The maximum cell parameters were obtained in the presence of 11.11 mM glucose with an open circuit voltage, short circuit current density and power density of 491.5 mV, 4.75 mA/cm^2, and 0.917 mW/cm^2 at a cell voltage of 288.4 mV, respectively as seen from Figure 39B. These results compared well to those previously reported [73, 79, 127 - 129]. At physiological serum glucose concentration (5 mM glucose at 37 °C, pH 7), the cell exhibits an open circuit voltage of 387.9 mV, a maximum power density of 0.462 mW/cm^2 at a cell voltage of 212.9 mV. The power generated by the biofuel cell assembly over the wide range from 2.78 mM – 11.11 mM in the serum glucose solution covers both hypoglycemic state as well as hyperglycemic state. Moreover, the biofuel cell produced sufficient power to drive the charge pump circuit comprising the capacitor for which, the charge/discharge frequency was monitored. The charge/discharge

frequency across the capacitor was monitored over a wide concentration range 2.78 mM – 11.11 mM at physiological conditions.

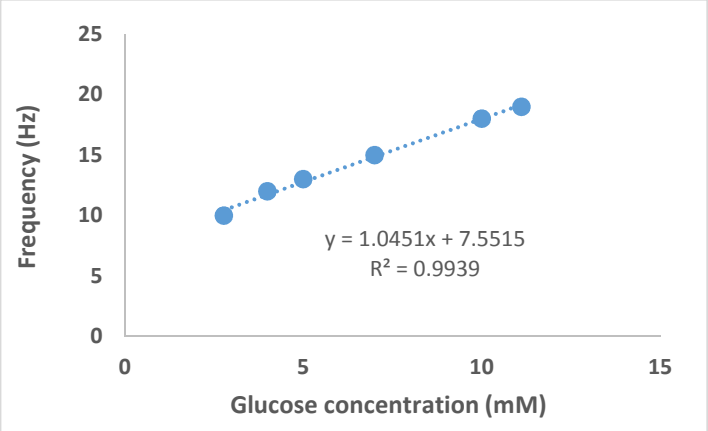

Figure 40. Calibration curve of glucose sensing system's response to glucose analyte at physiological conditions.

Figure 40 shows a calibration curve of sensed glucose over a dynamic range between 2.78 mM – 11.11 mM. Sensitivity of glucose sensor was calculated to be 104.51 Hz/cm^2.mM in the presence of serum glucose solution. We observed an increase in the sensitivity of our glucose sensor in the presence of serum solution. A 13% increase in the sensitivity was observed in comparison to the standard glucose solution. The limit of detection was calculated to be 2.31 mM in the presence of serum solution, which is below the dynamic operating range. This limit of detection was also lower than the standard glucose solution, where it was calculated to be 4.84 mM. Our system can sense glucose in blood serum covering the hypoglycemic and hyperglycemic region.

Chapter 8: Conclusion

8.1 Summary

We have successfully fabricated a novel self-powered glucose biosensing system, which is capable of simultaneously sensing glucose and powering an electronic device such as a glucometer. This novel device relies on a single glucose biofuel as its power source, unlike, existing glucose sensors, which rely on batteries. The glucose biofuel cell comprised two 5 mm x 5 mm buckypaper bioelectrodes, one of which was modified with pyrolloquinoline quinone glucose dehydrogenase (PQQ-GDH), a glucose selective enzyme and the other with bilirubin oxidase, an oxygen reducing enzyme to create the bioanode and biocathode, repectively. The glucose fuel is oxidized at the bioanode to form gluconolactone along with the release of electrons and protons. These electrons and protons migrate towards the biocathode, where oxygen is reduced to form water. The flow of electrons lead to current and hence, power being generated. Upon biofuel cell characterization in the presence of various glucose concentration solutions, this assembly produced a peak open circuit voltage and a peak power density of 552.37 mV and 0.225 mW/cm^2, respectively and a peak current density of 1.285 mA/cm^2 in the presence of 20 mM standard glucose solution. These results showed that glucose biofuel cells can be further investigated in the development of a self-powered glucose biosensor. Since, the glucose biofuel cell by itself can neither sense glucose nor power any device, a charge pump circuit was incorporated. The transducer element capacitor connected at the output of charge pump was used to sense glucose by monitoring the charge cycle frequency. The glucose sensor exhibited a dynamic range between 1 – 45 mM with the sensitivity calculated to be 23.13 Hz/cm^2.mM at the correlation coefficient of 0.9981.

The charge pump circuit supplied a burst of power, which is undesirable to power any electronic device. We then use a step-up DC convertor circuit to produce a steady DC voltage. The output of

the step-up DC convertor was measured to be 3.259 V, which was sufficient to power a glucometer device. We also studied the pH and temperature profile of the system and observed that the system performs optimally at physiological conditions (pH 7.4 and 37 ºC). Further, the system was observed to possess excellent selectivity in the presence of various interfering and competing species such as ascorbic acid, uric acid, maltose, fructose and galactose. The operational stability of the system was observed to be 53-days with over 90 % of the original activity being retained. A single glucose biofuel cell along with various power amplification circuits enabled the simultaneous glucose sensing and powering of a glucometer, thus eliminating the need for a battery.

To conclude, we have successfully fabricated a novel prototype design that allows us to achieve higher electrical power density at physiological conditions (pH 7.4 and 37 ºC). The electrical parameters produced by a single glucose biofuel cell were amplified using a charge pump circuit. A capacitor connected to the output of the charge pump sensed changes in glucose concentration. The charge/discharge frequency increased proportionally with glucose concentration over a wide dynamic range from 1 – 45 mM glucose solution, which includes hypoglycemia to hyperglycemia. The charge pump circuit interfaced with the step-up convertor circuit enabled glucose sensing and powering of a glucometer, all at the same time. The system shows excellent selectivity in the presence of various competing and interfering species at their physiological concentration. This system retained over 90% of the glucose sensing activity over a 53-day period. Hence, our system overcomes the drawbacks of glucose monitoring devices such as a glucometer and a CGM device, which are battery operated.

8.2 Future work

8.2.1 Design and fabrication of microfluidic chamber

The future work in this area may involve the design and development of a microfluidic system to allow for characterization of the entire system in a dynamic environment, wherein the biofuel cell is subjected to a continuous supply of fresh glucose fuel. The microfluidic chamber may be constructed with polydimethoxysilane (PDMS) via soft-lithography will not only serve as dynamic environment but also serve as a flexible protective chamber for the biofuel cell from the external conditions.

8.2.2 Operational stability of biofuel cell

To truly replace batteries, biofuel cell's operational stability must be further improved. In this system, the operational stability refers to the drop in the performance of the biofuel cell or a glucose sensor over a period of time due to the slow denaturing of the enzymes. To improve the operational stability, the enzymes could be coated with permeselective membranes such as hydrogels, chitosan, which are biocompatible membranes that prolong the life of the immobilized enzymes on the bioelectrodes surface.

8.2.3 Wireless transmission of sensed data

We have demonstrated that our single enzymatic glucose biofuel cell can simultaneously sense glucose and power an electronic device. To make this system a smart healthcare system, it is important to transfer the sensed glucose data wirelessly to the user end device such as a mobile phone or a laptop. The DC voltage produced by the step-up convertor circuit, can be utilized to drive the microcontroller circuit. The inbuilt A/D convertor inside microcontroller will convert the analog glucose sensed data to digital signal and transmit it wirelessly to the user end device. The

data interpretation algorithm stored at the user end will convert the digital data and display it on the user end device screen. This will enable the development of a smart glucose sensor that can sense glucose continuously and transmit the data to the user end.

8.2.4 Optimization of the overall system's performance using COMSOL simulation

The optimization of the system can be further performed in COMSOL simulation software to improve its performance. The computer simulation of the performance of the electrodes under varying external conditions such as temperature, pressure, humidity and internal conditions such as various losses can be studied. The system's performance can vary tremendously even by altering a single parameter. For instance, the size of the bioelectrodes and the concentration of the enzymes could be altered to find the optimal value. The experimental data can be compared with the simulated data to enable the experimental conditions to be change to enhance the performance of the system. After exhaustive device testing under both standard glucose solution as well as plasma, the device would be ready to be implanted inside a laboratory specimen to study its performance as well as its viability to serve in vivo.

References

1. Centers for Disease Control and Prevention. "National diabetes statistics report: estimates of diabetes and its burden in the United States, 2014."*Atlanta, GA: US Department of Health and Human Services* (2014).
2. Forbes, Josephine M., and Mark E. Cooper. "Mechanisms of diabetic complications." *Physiological reviews* 93, no. 1 (2013): 137-188.
3. Koschinsky, T., and L. Heinemann. "Sensors for glucose monitoring: technical and clinical aspects." *Diabetes/metabolism research and reviews*17, no. 2 (2001): 113-123.
4. Newman, Jeffrey D., and Anthony PF Turner. "Home blood glucose biosensors: a commercial perspective." *Biosensors and Bioelectronics* 20, no. 12 (2005): 2435-2453.
5. Pikov, Victor, and Peter H. Siegel. "Methods and systems for non-invasive measurement of blood glucose concentration by transmission of millimeter waves through human skin." U.S. Patent Application No. 14/835,253.
6. "Enzyme Substrate Electrode." *Gold Book IUPAC Compendium of Chemical Terminology*.
7. Hiratsuka, Atsunori, Kohta Fujisawa, and Hitoshi Muguruma. "Amperometric Biosensor Based on Glucose Dehydrogenase and Plasma-polymerized Thin Films." *Analytical Sciences Anal. Sci.* 24, no. 4 (2008): 483-86.
8. Chambers, James P., Bernard P. Arulanandam, Leann L. Matta, Alex Weis, and James J. Valdes. *Biosensor recognition elements*. Texas Univ at San Antonio Dept of Biology, 2008.

9. Iqbal, Shahzi S., Michael W. Mayo, John G. Bruno, Burt V. Bronk, Carl A. Batt, and James P. Chambers. "A review of molecular recognition technologies for detection of biological threat agents." *Biosensors and Bioelectronics* 15, no. 11 (2000): 549-578.

10. Habermüller, Katja, Marcus Mosbach, and Wolfgang Schuhmann. "Electron-transfer mechanisms in amperometric biosensors." *Fresenius' journal of analytical chemistry* 366, no. 6-7 (2000): 560-568.

11. Pearson, J. E., A. Gill, and P. Vadgama. "Analytical aspects of biosensors."*Annals of clinical biochemistry* 37, no. 2 (2000): 119-145.

12. Thevenot, Daniel R., Klara Toth, Richard A. Durst, and George S. Wilson. "Electrochemical biosensors: recommended definitions and classification."*Pure and Applied Chemistry* 71, no. 12 (1999): 2333-2348.

13. Turner, Anthony PF, Beining Chen, and Sergey A. Piletsky. "In vitro diagnostics in diabetes: meeting the challenge." *Clinical chemistry* 45, no. 9 (1999): 1596-1601.

14. Heller, Adam. "Amperometric biosensors." *Current opinion in biotechnology*7, no. 1 (1996): 50-54.

15. Price, Christopher P. "Point-of-care testing in diabetes mellitus." *Clinical chemistry and laboratory medicine* 41, no. 9 (2003): 1213-1219.

16. D'costa, E. J., I. J. Higgins, and A. P. F. Turner. "Quinoprotein glucose dehydrogenase and its application in an amperometric glucose sensor."*Biosensors* 2, no. 2 (1986): 71-87.

17. Slein, M. W. "D-glucose determination with hexokinase and glucose-6-phosphate dehydrogenase." *Methods of enzymatic analysis* 177 (1963): 177.

18. Heller, Adam, and Ben Feldman. "Electrochemical glucose sensors and their applications in diabetes management." *Chemical reviews* 108, no. 7 (2008): 2482-2505.

19. Bankar, Sandip B., Mahesh V. Bule, Rekha S. Singhal, and Laxmi Ananthanarayan. "Glucose oxidase—an overview." *Biotechnology advances*27, no. 4 (2009): 489-501.

20. Drury, M. I., F. J. Timoney, and P. Delaney. "Dextrostix--A Rapid Method of Estimating Blood Glucose Levels." *Journal of the Irish Medical Association* 56 (1965): 52-53.

21. Liu, Jie, and Joseph Wang. "A novel improved design for the first-generation glucose biosensor." *Food technology and biotechnology* 39, no. 1 (2001): 55-58.

22. Cass, Anthony EG, Graham Davis, Graeme D. Francis, H. Allen O. Hill, William J. Aston, I. John Higgins, Elliot V. Plotkin, Lesley DL Scott, and Anthony PF Turner. "Ferrocene-mediated enzyme electrode for amperometric determination of glucose." *Analytical chemistry* 56, no. 4 (1984): 667-671.

23. Frew, Jane E., and H. Allen O. Hill. "Electrochemical biosensors." *Analytical chemistry* 59, no. 15 (1987): 933A-944A.

24. Shichiri, Motoaki, Yoshimitsu Yamasaki, Ryuzo Kawamori, Nobuyoshi Hakui, and Hiroshi Abe. "Wearable artificial endocrine pancreas with needle-type glucose sensor." *The Lancet* 320, no. 8308 (1982): 1129-1131.

25. Chaubey, Asha, and B. D. Malhotra. "Mediated biosensors." *Biosensors and bioelectronics* 17, no. 6 (2002): 441-456.

26. Frew, J. E., H. A. O. Hill, and J. D. R. Thomas. "Electron-Transfer Biosensors [and Discussion]." *Philosophical Transactions of the Royal Society of London B: Biological Sciences* 316, no. 1176 (1987): 95-106.

27. Ballarin, Barbara, Maria Cristina Cassani, Rita Mazzoni, Erika Scavetta, and Domenica Tonelli. "Enzyme electrodes based on sono-gel containing ferrocenyl compounds." *Biosensors and Bioelectronics* 22, no. 7 (2007): 1317-1322.

28. Di Gleria, Katalin, Monika J. Green, H. Allen O. Hill, and Calum J. McNeil. "Homogeneous ferrocene-mediated amperometric immunoassay." *Analytical chemistry* 58, no. 6 (1986): 1203-1205.

29. Hilditch, Paul I., and Monika J. Green. "Disposable electrochemical biosensors." *Analyst* 116, no. 12 (1991): 1217-1220.

30. Matthews, D. R., E. Bown, A. Watson, R. R. Holman, J. Steemson, S. Hughes, and D. Scott. "Pen-sized digital 30-second blood glucose meter."*The Lancet* 329, no. 8536 (1987): 778-779.

31. Murray, Royce W., Andrew G. Ewing, and Richard A. Durst. "Chemically modified electrodes molecular design for electroanalysis." *Analytical Chemistry* 59, no. 5 (1987): 379A-390A.

32. Zhang, Wenjun, and Genxi Li. "Third-generation biosensors based on the direct electron transfer of proteins." *Analytical sciences* 20, no. 4 (2004): 603-609.

33. Wang, Joseph. "Electrochemical glucose biosensors." *Chemical reviews*108, no. 2 (2008): 814-825.

34. Gregg, Brian A., and Adam Heller. "Cross-linked redox gels containing glucose oxidase for amperometric biosensor applications." *Analytical Chemistry* 62, no. 3 (1990): 258-263.

35. Lin, Yuehe, Wassana Yantasee, and Joseph Wang. "Carbon nanotubes (CNTs) for the development of electrochemical biosensors." *Front. Biosci* 10, no. 492-505 (2005): 582.

36. Riklin, Azalla, Eugenii Katz, I. Willner, Achim Stocker, and Andreas F. Bückmann. "Improving enzyme-electrode contacts by redox modification of cofactors." *Nature* 376, no. 6542 (1995): 672-675.

37. Albisser, A. Ml, B. S. Leibel, T. G. Ewart, Z. Davidovac, C. K. Botz, W. Zingg, H. Schipper, and R. Gander. "Clinical control of diabetes by the artificial pancreas." *Diabetes* 23, no. 5 (1974): 397-404.

38. Bindra, Dilbir S., Yanan Zhang, George S. Wilson, Robert Sternberg, Daniel R. Thevenot, Dinah Moatti, and Gerard Reach. "Design and in vitro studies of a needle-type glucose sensor for subcutaneous monitoring." *Analytical Chemistry* 63, no. 17 (1991): 1692-1696.

39. Albery, W. John, Philip N. Bartlett, and Derek H. Craston. "Amperometric enzyme electrodes: Part II. Conducting salts as electrode materials for the oxidation of glucose oxidase." *Journal of Electroanalytical Chemistry and Interfacial Electrochemistry* 194, no. 2 (1985): 223-235.

40. Palmisano, Francesco, Pier Giorgio Zambonin, Diego Centonze, and Maurizio Quinto. "A disposable, reagentless, third-generation glucose biosensor based on overoxidized poly (pyrrole)/tetrathiafulvalene-tetracyanoquinodimethane composite." *Analytical chemistry* 74, no. 23 (2002): 5913-5918.

41. Csoeregi, Elisabeth, David W. Schmidtke, and Adam Heller. "Design and optimization of a selective subcutaneously implantable glucose electrode based on" wired" glucose oxidase." *Analytical Chemistry* 67, no. 7 (1995): 1240-1244.

42. Henry, Celia. "Getting under the skin: implantable glucose sensors."*Analytical chemistry* 70, no. 17 (1998): 594A-598A.

43. Schmidtke, David W., Angela C. Freeland, Adam Heller, and Roger T. Bonnecaze. "Measurement and modeling of the transient difference between blood and subcutaneous glucose concentrations in the rat after injection of insulin." *Proceedings of the National Academy of Sciences* 95, no. 1 (1998): 294-299.

44. Rebrin, Kerstin, and Garry M. Steil. "Can interstitial glucose assessment replace blood glucose measurements?." *Diabetes technology & therapeutics*2, no. 3 (2000): 461-472.

45. Gross, Todd M., Bruce W. Bode, Daniel Einhorn, David M. Kayne, John H. Reed, Neil H. White, and John J. Mastrototaro. "Performance evaluation of the MiniMed® continuous glucose monitoring system during patient home use." *Diabetes technology & therapeutics* 2, no. 1 (2000): 49-56.

46. Cox, Marilyn. "An overview of continuous glucose monitoring systems."*Journal of Pediatric Health Care* 23, no. 5 (2009): 344-347.

47. Hashiguchi, Yasuhiro, Michiharu Sakakida, Kenro Nishida, Takero Uemura, Ken-Ichiro Kajiwara, and Motoaki Shichiri. "Development of a miniaturized glucose monitoring system by combining a needle-type glucose sensor with microdialysis sampling method: long-term subcutaneous tissue glucose monitoring in ambulatory diabetic patients." *Diabetes care* 17, no. 5 (1994): 387-396.

48. Poscia, A., M. Mascini, D. Moscone, M. Luzzana, G. Caramenti, P. Cremonesi, F. Valgimigli, C. Bongiovanni, and M. Varalli. "A microdialysis technique for continuous subcutaneous glucose monitoring in diabetic patients (part 1)." *Biosensors and bioelectronics* 18, no. 7 (2003): 891-898.

49. Wentholt, Iris M., Marit A. Vollebregt, Augustus A. Hart, Joost B. Hoekstra, and J. Hans DeVries. "Comparison of a needle-type and a microdialysis continuous glucose monitor in type 1 diabetic patients." *Diabetes Care* 28, no. 12 (2005): 2871-2876.

50. Nielsen, Jannik Kruse, G. Freckmann, C. Kapitza, G. Ocvirk, K. H. Koelker, U. Kamecke, R. Gillen, Amann-Zalan, I., Jendrike, N., Christiansen, J.S. and Koschinsky, T. "Glucose monitoring by microdialysis: performance in a multicentre study." *Diabetic Medicine* 26, no. 7 (2009): 714-721.

51. Klonoff, David C. "Noninvasive blood glucose monitoring." *Diabetes Care* 20, no. 3 (1997): 433-437.

52. Oliver, N. S., C. Toumazou, A. E. G. Cass, and D. G. Johnston. "Glucose sensors: a review of current and emerging technology." *Diabetic Medicine*26, no. 3 (2009): 197-210.

53. Rabinovitch, B., W. F. March, and Robert L. Adams. "Noninvasive glucose monitoring of the aqueous humor of the eye: Part I. Measurement of very small optical rotations." *Diabetes Care* 5, no. 3 (1982): 254-258.

54. Cote, G. L., R. Erckens, W. March, and Mohammad Motamedi. "Application of a multivariate technique to Raman spectra for quantification of body chemicals." *Biomedical Engineering, IEEE Transactions on* 42, no. 7 (1995): 728-731.

55. Gabriely, Ilan, Robert Wozniak, Michele Mevorach, Jonathan Kaplan, Y. I. G. A. L. Aharon, and H. A. R. R. Y. Shamoon. "Transcutaneous glucose measurement using near-infrared spectroscopy during hypoglycemia."*Diabetes Care* 22, no. 12 (1999): 2026-2032.

56. MacKenzie, Hugh A., Helen S. Ashton, Stephen Spiers, Yaochun Shen, Scott S. Freeborn, John Hannigan, John Lindberg, and Peter Rae. "Advances in photoacoustic noninvasive glucose testing." *Clinical Chemistry*45, no. 9 (1999): 1587-1595.

57. Larin, Kirill V., Mohsen S. Eledrisi, Massoud Motamedi, and Rinat O. Esenaliev. "Noninvasive blood glucose monitoring with optical coherence tomography a pilot study in human subjects." *Diabetes care* 25, no. 12 (2002): 2263-2267.

58. D'Orazio, P., R. W. Burnett, N. Fogh-Andersen, E. Jacobs, K. Kuwa, W. R. Külpmann, L. Larsson et al. "International Federation of Clinical Chemistry Scientific Division Working Group on Selective Electrodes and Point of Care Testing. Approved IFCC recommendation on reporting results for blood glucose (abbreviated)." *Clin Chem* 51, no. 9 (2005): 1573-6.

59. Grove, William R. "XXIV. On voltaic series and the combination of gases by platinum." *The London and Edinburgh philosophical magazine and journal of science* 14, no. 86 (1839): 127-130.

60. Andújar, J. M., and F. Segura. "Fuel cells: History and updating. A walk along two centuries." *Renewable and sustainable energy reviews* 13, no. 9 (2009): 2309-2322.

61. Hoff, Arnold J., and Johann Deisenhofer. "Photophysics of photosynthesis. Structure and spectroscopy of reaction centers of purple bacteria." *Physics reports* 287, no. 1 (1997): 1-247.

62. Linden, David, and Thomas B. Reddy. "Handbook of Batteries. 3rd." (2002).

63. Sue, Chung-Yang, and Nan-Chyuan Tsai. "Human powered MEMS-based energy harvest devices." *Applied Energy* 93 (2012): 390-403.

64. Szczupak, Alon, Jan Halámek, Lenka Halámková, Vera Bocharova, Lital Alfonta, and Evgeny Katz. "Living battery–biofuel cells operating in vivo in clams." *Energy & Environmental Science* 5, no. 10 (2012): 8891-8895.

65. Hayes, David L., and Paul A. Friedman. *Cardiac pacing, defibrillation and resynchronization: a clinical approach*. John Wiley & Sons, 2011.

66. Zebda, Abdelkader, Chantal Gondran, Alan Le Goff, Michael Holzinger, Philippe Cinquin, and Serge Cosnier. "Mediatorless high-power glucose biofuel cells based on compressed carbon nanotube-enzyme electrodes."*Nature communications* 2 (2011): 370.

67. Reuillard, Bertrand, Alan Le Goff, Charles Agnes, Michael Holzinger, Abdelkader Zebda, Chantal Gondran, Kamal Elouarzaki, and Serge Cosnier. "High power enzymatic biofuel cell based on naphthoquinone-mediated oxidation of glucose by glucose oxidase in a carbon nanotube 3D matrix."*Physical Chemistry Chemical Physics* 15, no. 14 (2013): 4892-4896.

68. Zebda, Abdelkader, Serge Cosnier, J-P. Alcaraz, Michael Holzinger, Alan Le Goff, Chantal Gondran, François Boucher et al. "Single glucose biofuel cells implanted in rats power electronic devices." *Scientific reports* 3 (2013).

69. Liu, Zenghe, Brian Cho, Tianmei Ouyang, and Ben Feldman. "Miniature amperometric self-powered continuous glucose sensor with linear response." *Analytical chemistry* 84, no. 7 (2012): 3403-3409.

70. Castorena-Gonzalez, Jorge A., Christopher Foote, Kevin MacVittie, Jan Halámek, Lenka Halámková, Luis A. Martinez-Lemus, and Evgeny Katz. "Biofuel cell operating in vivo in rat." *Electroanalysis* 25, no. 7 (2013): 1579-1584.

71. MacVittie, Kevin, Jan Halámek, Lenka Halámková, Mark Southcott, William D. Jemison, Robert Lobel, and Evgeny Katz. "From “cyborg” lobsters to a pacemaker powered by implantable biofuel cells." *Energy & Environmental Science* 6, no. 1 (2013): 81-86.

72. Schröder, Uwe. "From in vitro to in vivo—biofuel cells are maturing."*Angewandte Chemie International Edition* 51, no. 30 (2012): 7370-7372.

73. Southcott, Mark, Kevin MacVittie, Jan Halámek, Lenka Halámková, William D. Jemison, Robert Lobel, and Evgeny Katz. "A pacemaker powered by an implantable biofuel cell operating under conditions mimicking the human blood circulatory system–battery not included." *Physical chemistry chemical physics* 15, no. 17 (2013): 6278-6283.

74. Katz, Evgeny, and Kevin MacVittie. "Implanted biofuel cells operating in vivo–methods, applications and perspectives–feature article." *Energy & Environmental Science* 6, no. 10 (2013): 2791-2803.

75. Vaddiraju, Santhisagar, Ioannis Tomazos, Diane J. Burgess, Faquir C. Jain, and Fotios Papadimitrakopoulos. "Emerging synergy between nanotechnology and implantable biosensors: a review." *Biosensors and Bioelectronics* 25, no. 7 (2010): 1553-1565.

76. Calabrese Barton, Scott, Josh Gallaway, and Plamen Atanassov. "Enzymatic biofuel cells for implantable and microscale devices." *Chemical reviews* 104, no. 10 (2004): 4867-4886.

77. Desmaële, Denis, Louis Renaud, and Sophie Tingry. "A wireless sensor powered by a flexible stack of membraneless enzymatic biofuel cells."*Sensors and Actuators B: Chemical* 220 (2015): 583-589.

78. Liu Z, Cho B, Ouyang T, Feldman B (2012) Miniature amperometric selfpowered continuous glucose sensor with linear response. Analytical chemistry 84: 3403-3409.

79. Pinyou, Piyanut, Felipe Conzuelo, Kirill Sliozberg, Jeevanthi Vivekananthan, Andrea Contin, Sascha Pöller, Nicolas Plumeré, and Wolfgang Schuhmann. "Coupling of an Enzymatic Biofuel Cell to an Electrochemical Cell for Self-powered Glucose Sensing with Optical Readout." *Bioelectrochemistry* 106 (2015): 22-27.

80. Yoshino S, Miyake T, Yamada T, Hata K, Nishizawa M (2013) Molecularly ordered bioelectrocatalytic composite inside a film of aligned carbon nanotubes. Advanced Energy Materials 3: 60-64.

81. Andoralov V, Falk M, Suyatin DB, Granmo M, Sotres J, et al. (2013) Biofuel cell based on microscale nanostructured electrodes with inductive coupling to rat brain neurons. Scientific reports 3: 3270.

82. Falk M, Andoralov V, Silow M, Toscano MD, Shleev S, et al. (2013) Miniature biofuel cell as a potential power source for glucose-sensing contact lenses. Analytical chemistry 85: 6342-6348.

83. Kulkarni, Tanmay, Deepa Gupta, and Gymama Slaughter. "An enzymatic glucose biofuel cell based on Au nano-electrode array." In *SENSORS, 2015 IEEE*, pp. 1-4. IEEE, 2015.

84. Cai, Zhi-xiong, Cong-cong Liu, Geng-huang Wu, Xiao-mei Chen, and Xi Chen. "Palladium nanoparticles deposit on multi-walled carbon nanotubes and their catalytic applications for electrooxidation of ethanol and glucose."*Electrochimica Acta* 112 (2013): 756-762.

85. Sun, Zhihong, Faliang Cheng, and Xiangcheng Dai. "Highly ordered Pd nanowire array by template fabrication for propanol electrooxidation." *Journal of Analytical Methods in Chemistry* 2009 (2009).

86. Taşaltın, Nevin, Sadullah Öztürk, Necmettin Kılınç, Hayrettin Yüzer, and Zafer Ziya Öztürk. "Fabrication of vertically aligned Pd nanowire array in AAO template by electrodeposition using neutral electrolyte." *Nanoscale research letters* 5, no. 7 (2010): 1137-1143.

87. Guiseppi-Elie, Anthony, Sean Brahim, Gymama Slaughter, and Kevin R. Ward. "Design of a subcutaneous implantable biochip for monitoring of glucose and lactate." *Sensors journal, IEEE* 5, no. 3 (2005): 345-355.

88. Calabrese Barton, Scott, Josh Gallaway, and Plamen Atanassov. "Enzymatic biofuel cells for implantable and microscale devices." *Chemical reviews* 104, no. 10 (2004): 4867-4886.

89. Yehezkeli, Omer, Ran Tel-Vered, Sara Raichlin, and Itamar Willner. "Nano-engineered flavin-dependent glucose dehydrogenase/gold nanoparticle-modified electrodes for glucose sensing and biofuel cell applications." *ACS nano* 5, no. 3 (2011): 2385-2391.

90. Li, Liang, Bo Liang, Feng Li, Jianguo Shi, Marco Mascini, Qiaolin Lang, and Aihua Liu. "Co-immobilization of glucose oxidase and xylose dehydrogenase displayed whole cell on multiwalled carbon nanotube nanocomposite films modified electrode for simultaneous voltammetric detection of d-glucose and d-xylose." *Biosensors and Bioelectronics* 42 (2013): 156-162.

91. Lang, Qiaolin, Long Yin, Jianguo Shi, Liang Li, Lin Xia, and Aihua Liu. "Co-immobilization of glucoamylase and glucose oxidase for electrochemical sequential

enzyme electrode for starch biosensor and biofuel cell."*Biosensors and Bioelectronics* 51 (2014): 158-163.

92. Kangralkar, V. A., Shivraj D. Patil, and R. M. Bandivadekar. "Oxidative stress and diabetes: a review." *Int J Pharm Appl* 1, no. 1 (2010): 38-45.

93. Atanassov, Plamen, Carolin Lau, Claudia Narváez Villarrubia, Gustavo Ciniciato, Sergio O. Garcia, Rosalaba Rincon, Scott Sibbett et al. "Paper-Based Biofuel Cells." In *Meeting Abstracts*, no. 39, pp. 1452-1452. The Electrochemical Society, 2012.

94. Shin, Min Kyoon, Jiyoung Oh, Marcio Lima, Mikhail E. Kozlov, Seon Jeong Kim, and Ray H. Baughman. "Elastomeric conductive composites based on carbon nanotube forests." *Advanced Materials* 22, no. 24 (2010): 2663-2667.

95. Mirón, Jesús, M. P. González, Lorenzo Pastrana, and M. A. Murado. "Diauxic production of glucose oxidase by Aspergillus niger in submerged culture: A dynamic model." *Enzyme and Microbial Technology* 31, no. 5 (2002): 615-620.

96. Holzinger, Michael, Alan Le Goff, and Serge Cosnier. "Carbon nanotube/enzyme biofuel cells." *Electrochimica Acta* 82 (2012): 179-190.

97. Roman, T., W. A. Dino, H. Nakanishi, and H. Kasai. "Amino acid adsorption on single-walled carbon nanotubes." *The European Physical Journal D-Atomic, Molecular, Optical and Plasma Physics* 38, no. 1 (2006): 117-120.

98. Katz, Evgeny, José M. Pingarrón, Shay Mailloux, Nataliia Guz, Maria Gamella, Galina Melman, and Artem Melman. "Substance Release Triggered by Biomolecular Signals in Bioelectronic Systems." *The journal of physical chemistry letters* 6, no. 8 (2015): 1340-1347.

99. Miyake, Takeo, Syuhei Yoshino, Takeo Yamada, Kenji Hata, and Matsuhiko Nishizawa. "Self-Regulating Enzyme− Nanotube Ensemble Films and Their Application as Flexible Electrodes for Biofuel Cells." *Journal of the American Chemical Society* 133, no. 13 (2011): 5129-5134.

100. Katz, Evgeny, and Kevin MacVittie. "Implanted biofuel cells operating in vivo–methods, applications and perspectives–feature article." *Energy & Environmental Science* 6, no. 10 (2013): 2791-2803.

101. Sales, Fernanda C. P. F., Rodrigo M. Iost, Marccus V. A. Martins, Maria C. Almeida, and Frank N. Crespilho. "An Intravenous Implantable Glucose/dioxygen Biofuel Cell with Modified Flexible Carbon Fiber Electrodes." *Lab Chip* 13, no. 3 (2013): 468-74.

102. Rasmussen, Michelle, Roy E. Ritzmann, Irene Lee, Alan J. Pollack, and Daniel Scherson. "An Implantable Biofuel Cell for a Live Insect." *J. Am. Chem. Soc. Journal of the American Chemical Society* 134, no. 3 (2012): 1458-460.

103. Giroud, Fabien, Chantal Gondran, Karine Gorgy, Vincent Vivier, and Serge Cosnier. "An Enzymatic Biofuel Cell Based on Electrically Wired Polyphenol Oxidase and Glucose Oxidase Operating under Physiological Conditions." *Electrochimica Acta* 85 (2012): 278-82.

104. Cinquin, Philippe, Chantal Gondran, Fabien Giroud, Simon Mazabrard, Aymeric Pellissier, François Boucher, Jean-Pierre Alcaraz, Karine Gorgy, François Lenouvel, Stéphane Mathé, Paolo Porcu, and Serge Cosnier. "A Glucose BioFuel Cell Implanted in Rats." *PLoS ONE* 5, no. 5 (2010).

105. Barrière, Frédéric, Paul Kavanagh, and Dónal Leech. "A laccase–glucose Oxidase Biofuel Cell Prototype Operating in a Physiological Buffer." *Electrochimica Acta* 51, no. 24 (2006): 5187-192.

106. Yang C-Y, Tsai T-H, Chen S-M, Lou B-M, and Liu X. "Development of a Multiple Biosensor and Its Application of Biofuel Cell." *International Journal of Electrochemical Science* 10, no. 1 (2015): 579-88.

107. Falk, Magnus, Miguel Alcalde, Philip N. Bartlett, Antonio L. De Lacey, Lo Gorton, Cristina Gutierrez-Sanchez, Raoudha Haddad, Jeremy Kilburn, Dónal Leech, Roland Ludwig, Edmond Magner, Diana M. Mate, Peter Ó. Conghaile, Roberto Ortiz, Marcos Pita, Sascha Pöller, Tautgirdas Ruzgas, Urszula Salaj-Kosla, Wolfgang Schuhmann, Fredrik Sebelius, Minling Shao, Leonard Stoica, Cristoph Sygmund, Jonas Tilly, Miguel D. Toscano, Jeevanthi Vivekananthan, Emma Wright, and Sergey Shleev. "Self-Powered Wireless Carbohydrate/Oxygen Sensitive Biodevice Based on Radio Signal Transmission." *PLoS ONE* 9, no. 10 (2014).

108. Miyake, Takeo, Keigo Haneda, Nobuhiro Nagai, Yohei Yatagawa, Hideyuki Onami, Syuhei Yoshino, Toshiaki Abe, and Matsuhiko Nishizawa. "Enzymatic Biofuel Cells Designed for Direct Power Generation from Biofluids in Living Organisms." *Energy & Environmental Science Energy Environ. Sci.* 4, no. 12 (2011): 5008.

109. Pizzariello, A., M. Stred'ansky, and S. Miertuš. "A Glucose/hydrogen Peroxide Biofuel Cell That Uses Oxidase and Peroxidase as Catalysts by Composite Bulk-modified Bioelectrodes Based on a Solid Binding Matrix." *Bioelectrochemistry* 56, no. 1-2 (2002): 99-105.

110. Clark, Leland C., and Champ Lyons. "Electrode Systems for Continuous Monitoring In Cardiovascular Surgery." *Annals of the New York Academy of Sciences* 102, no. 1 (2006): 29-45.

111. Miyake, Takeo, Keigo Haneda, Syuhei Yoshino, and Matsuhiko Nishizawa. "Flexible, layered biofuel cells." *Biosensors and Bioelectronics* 40, no. 1 (2013): 45-49.

112. Palumbo, Gaetano, and Domenico Pappalardo. "Charge pump circuits: An overview on design strategies and topologies." *Circuits and Systems Magazine, IEEE* 10, no. 1 (2010): 31-45.

113. Slaughter, Gymama, and Tanmay Kulkarni. "A self-powered glucose biosensing system." *Biosensors and Bioelectronics* 78 (2016): 45-50.

114. Reid, Russell C., Shelley D. Minteer, and Bruce K. Gale. "Contact lens biofuel cell tested in a synthetic tear solution." *Biosensors and Bioelectronics* 68 (2015): 142-148.

115. Baughman, Ray H., Anvar A. Zakhidov, and Walt A. De Heer. "Carbon nanotubes--the route toward applications." *science* 297, no. 5582 (2002): 787-792.

116. Wilder, Jeroen WG, Liesbeth C. Venema, Andrew G. Rinzler, Richard E. Smalley, and Cees Dekker. "Electronic structure of atomically resolved carbon nanotubes." *Nature* 391, no. 6662 (1998): 59-62.

117. Wang, Ding, Pengcheng Song, Changhong Liu, Wei Wu, and Shoushan Fan. "Highly oriented carbon nanotube papers made of aligned carbon nanotubes." *Nanotechnology* 19, no. 7 (2008): 075609.

118. Kulkarni, Tanmay, and Gymama Slaughter. "Self-powered glucose biosensor operating under physiological conditions." *SENSORS, 2016 IEEE*. IEEE, 2016.

119. Morales, A., F. Céspedes, and S. Alegret. "Graphite–methacrylate biocomposite material with renewable sensing surface for reagentless amperometric biosensors based on glucose dehydrogenase." *Materials Science and Engineering: C* 7.2 (1999): 99-104.

120. Gerard, Manju, Asha Chaubey, and B. D. Malhotra. "Application of conducting polymers to biosensors." *Biosensors and Bioelectronics* 17.5 (2002): 345-359.

121. Kulkarni, Tanmay, and Gymama Slaughter. "Application of Semipermeable Membranes in Glucose Biosensing." *Membranes* 6.4 (2016): 55.

122. Lee, Seung Ho, Joo-Ho Chung, Hun-Kuk Park, and Gi-Ja Lee. "A Simple and Facile Glucose Biosensor Based on Prussian Blue Modified Graphite String." *Journal of Sensors* 2016 (2016).

123. Gao, Feng, Yiming Yan, Lei Su, Lun Wang, and Lanqun Mao. "An enzymatic glucose/O 2 biofuel cell: preparation, characterization and performance in serum." *Electrochemistry Communications* 9, no. 5 (2007): 989-996.

124. Holade, Yaovi, Kevin MacVittie, Tyler Conlon, Nataliia Guz, Karine Servat, Teko W. Napporn, K. Boniface Kokoh, and Evgeny Katz. "Pacemaker activated by an abiotic biofuel cell operated in human serum solution." *Electroanalysis* 26, no. 11 (2014): 2445-2457.

125. Lee, Jin Young, Hyun Yong Shin, Seong Woo Kang, Chulhwan Park, and Seung Wook Kim. "Application of an enzyme-based biofuel cell containing a bioelectrode modified with deoxyribonucleic acid-wrapped single-walled carbon nanotubes to serum." *Enzyme and microbial technology* 48, no. 1 (2011): 80-84.

126. Güven, Güray, Samet Şahin, Arcan Güven, and Eileen H. Yu. "Power harvesting from human serum in Buckypaper-Based enzymatic Biofuel cell." *Frontiers in Energy Research* 4 (2016): 4.

127. Milton, Ross D., Koun Lim, David P. Hickey, and Shelley D. Minteer. "Employing FAD-dependent glucose dehydrogenase within a glucose/oxygen enzymatic fuel cell operating in human serum." *Bioelectrochemistry* 106 (2015): 56-63.

128. Mano, Nicolas, Fei Mao, and Adam Heller. "A miniature biofuel cell operating in a physiological buffer." *Journal of the American Chemical Society* 124, no. 44 (2002): 12962-12963.

129. Falk, Magnus, Viktor Andoralov, Zoltan Blum, Javier Sotres, Dmitry B. Suyatin, Tautgirdas Ruzgas, Thomas Arnebrant, and Sergey Shleev. "Biofuel cell as a power source for electronic contact lenses." *Biosensors and Bioelectronics* 37, no. 1 (2012): 38-45.